Sudan University of Science and Technology

College of Graduate Studies

Derivation of A Conserved Linear Energy and Klein Gordon Equations to Describe Spin and Magic Numbers Using Generalized Special Relativity

استنباط معادلات حفظ خطية للطاقة وكلاين وقوردون لوصف المغزل والأرقام السحرية باستخدام النسبية الخاصة المعممة

A thesis Submitted in Partial Fulfillment for the Requirement for the Award of the Degree of Doctor of Philosophy in Physics

By

Hleima Faddal Ezaldein Rewais

Supervisor:

Professor: Mubarak Dirar Abd- Allah

Co - Supervisor

Dr. Ahmmed ALhassan Alfki

November2021

الآيـــــة

قَالَ تَعَالَىٰ:

﴿ يَٰٓأَيُّهَا ٱلَّذِينَ ءَامَنُوٓاْ إِذَا قِيلَ لَكُمۡ تَفَسَّحُواْ فِي ٱلۡمَجَٰلِسِ فَٱفۡسَحُواْ يَفۡسَحِ ٱللَّهُ لَكُمۡۖ وَإِذَا قِيلَ ٱنشُزُواْ فَٱنشُزُواْ يَرۡفَعِ ٱللَّهُ ٱلَّذِينَ ءَامَنُواْ مِنكُمۡ وَٱلَّذِينَ أُوتُواْ ٱلۡعِلۡمَ دَرَجَٰتٖۚ وَٱللَّهُ بِمَا تَعۡمَلُونَ خَبِيرٞ ١١ ﴾

صدق الله العظيم

المجادلة: الآيــة (١١)

Dedication

This research work is dedication to My Parents, Brother, and Sisters

My Teachers, My Friend and, All Those, Whom I Love.

Hleima

Acknowledgment

Thanks first to Allah; I would like to express my deep gratitude and especial thanks to my supervisor professor. Mubarak Dirar Abd-allh. For his kind supervision and invaluable**.** My thanks also extended to the Sudan University of Science and Technology, College of Graduate Studies, and my thanks to college of Science, department of physics.

Also my thanks to my Co-supervisor Dr. Ahmmed ALhassan Alfki. My gratitude goes also to my family for their patience and financial support, especially my mother.

At last, but not at least, thanks to every one that helped me to finish this work.

Abstract

The concept of energy in special relativity does not satisfy Newton limit. It does not also conforms to observations. The aim of this work is to use generalized special relativity to formulate a new expression for the linear energy. One also needs to construct a new quantum relativistic Klein Gordon equation, which can describe spin phenomena instead of using two different quantum equations to describe particles having integral and half-integral spin quantum numbers, one is the Klein- Gordon equation, while the other is the Dirac equation.

The energy conservation of the potential dependent special relativity has been developed. The energy expression can be simplified and the conservation can be secured when using vector four-dimensional representation with the fourth time component is imaginary and related to the momentum. Treating particles as strings an imaginary energy has been found to be quantized and proportional to the harmonic energy .This resembles the imaginary wave number reflecting the energy liberated by electromagnetic waves that interact with matter.

Potential dependent energy- momentum relativistic relation was utilized to derive new quantum Klein- Gordon equation. This equation reduces to the ordinary Klein-Gordon equation in the absence of potential. Treating nucleons as strings, a new energy-quantized expression was obtained. This energy resembles that of Schrödinger harmonic oscillator with additional term representing the rest mass. This model also predicts the magic numbers.

The conservation of energy in potential dependent special relativity has been found using 4- dimensional representation. In this version, the square of the momentum multiplied by the square of the free speed of light subtracted from the curved space energy is invariant and constant everywhere. The quantum equation derived from this equation in a weak field limit shows that the momentum is quantized and the energy is reduced to that of Schrodinger harmonic oscillator when neglecting the rest mass term.

In addition, the proposed model shows the possibility of using potential dependent Klein-Gordon equation to find the magic numbers. This shows that, this equation can describe fermions as well as bosons.

مستخلص البحث

لا يستوفي مفهوم الطاقة في النسبية الخاصة التقريب النيوتني . وهي لا تتفق أيضاً مع المشاهدات. يهدف هذا البحث لاستخدام النسبية الخاصة المعممة لصياغة صيغة جديدة للطاقة الخطية. وهناك رغبة أيضاً في صياغة معادلة كمية نسبية جديدة لكلاين وقوردون يمكن أن تصف ظاهرة المغزل بدلاً من استخدام معادلتين كميتين لوصف العدد الكمي المغزلي الصحيح والكسري ،أحداهما هي معادلة كلاين وقوردون الأخرى هي معادلة ديراك .

طُور حفظ الطاقة للنسبية الخاصة المعتمدة على الجهد. حيث بُسطت صيغة الطاقة واستخلصت صيغة الحفظ باستخدام التمثيل المتجهى الرباعي، باعتبار المركبة الرابعة الزمنية تخيلية وذات علاقة بالاندفاع. باعتبار الجسيمات أوتار وُجد أن الطاقة التخيلية مكممه وتتناسب مع طاقة المتذبذب. وهذا يشبه العدد الموجي التخيلي الذي يعكس الطاقة المتحررة بالموجات الكهرومغناطيسية التي تتفاعل مع المادة.

استخدمت علاقة الطاقة والاندفاع للنسبية المعتمدة على الجهد لاستنباط معادلة جديدة لكلاين وقوردون. هذه المعادلة تؤول لمعادلة كلاين وقوردون العادية في غياب الجهد. باعتبار النيوكلونات أوتار وجدت صيغة جديدة مكممه للطاقة. هذه الطاقة تشبه تلك التي لمعادلة شورد ينجر للمتذبذب التوافقي مع وجود حد إضافي يمثل كتلة السكون. هذا النموذج يتنبأ أيضا بالأرقام السحرية.

وُجدت صيغة حفظ الطاقة في النسبية الخاصة المعتمدة على الجهد باستخدام التمثيل الاحداثي الرباعي. في هذا المنحى يكون مربع الاندفاع مضروباً في مربع سرعة الضوء في الفراغ مطروحاً منه الطاقة في الفراغ المحدب مقدار لا متغير وثابت في أي مكان. وقد بينت المعادلة الكمية المشتقة من هذه المعادلة في تقريب المجال الضعيف أن الاندفاع مكمم وأن الطاقة تختزل لتلك التي للمتذبذب التوافقي لشورديتجر عند إهمال حد كتلة السكون.

بالإضافة إلى ذلك بين النموذج المقترح إمكانية استخدام معادلة كلاين وقوردون المعتمدة على الجهد لإيجاد الأرقام السحرية، وهذا يوضح أن هذه المعادلة تصف الفيرميونات بنفس القدر الذي تصف به البوزونات.

List of Contents

List of Table

List of Figures

Chapter One

Introduction

1.1 Quantum Mechanics and Relativity

Quantum mechanics describes, atoms, the building blocks of matter [1] .Quantum mechanics is been based mainly on the particle, wave dual nature of atomic particles. The first one who recognize the word quantum is Max Plank .He propose that light behaves as discrete quanta. Thus, light behaves sometimes as waves and sometimes as particles. The same holds for particles, which behaves sometimes as waves. This dual nature can be described by Schrödinger nun relativistic equations beside Klein Gordon and Dirac relativistic equations [2, 3, 4].

The law of quantum mechanics predicts energy quantization beside quantization of other physical quantities .these quantization's leads to explain a wide variety of matter and atoms physical phenomena. This leads to appearance of many technical applications in atomic spectroscopy, mineral exploration, electronic, medicine and industry [5, 6, 7].

The emergence of quantum mechanics is associated with emergence of special relativity theory, which makes radical modification in the concepts of space and time, beside the notion of energy [8, 9].

It leads to understand some atomic interaction like energy production from mass defects, pair production, a halation, photo electronic effect and nuclear radiation [10, 11].

Despite these remarkable successes, SR suffers from the lack of expression recognizing the field potential. Thus, its energy expression does not reduce to the Newtonian one far law speed particles [12].

This defect was to cured by some author to construct generalized SR version that accounts for the effect of potential of the fields and space, time and mass[13,14].

Physical system are been described by the equation of motion and conserved quantities, like energy and momentum.

The equation of motion describes the time evolution, while conserved quantities describe those constant physical quantities that does not change with space or time [15].

One of the most important one is the concept of energy. In Newtonian mechanics, the energy is the equal to the sum of kinetic and potential energy [16]. In Special Relativity (S R), the total energy is related to the rest mass energy and momentum, without recognizing the potential energy. This situation is in direct conflict with observations , beside Newton's laws and quantum laws .According to (SR) version two identical particle moving with same velocity ,one in vacuum and the other revolves around a nucleus have the name total energy . This is in direct conflict with observed atomic spectra of different atoms. The electron total energy was directly affected by its potential energy. This result does not conform to SR energy from which does not recognize potential energy [17, 18].

This situation encourages some scientists to cure this defect by constructing new models [19, 20, 21]. One of the most popular one is the one proposed by Mubarak Dirar, which recognize the effect of the potential. His original work was be based on the energy expression in a curved space-time [22]. Later on the utilized Lorentz transformation to incorporate potential energy in the total energy from [23, 24]. Those models succeeded in bridging the gap between relativity and quantum beside Newtonian mechanics. Even same models tries to study conservation laws for this potential dependent special relativity and quantum beside Newtonian mechanics. Even some models tries to study conservation laws for this potential dependent special relativity (psr) [25]. However, no ultimate regions version is been obtained.

Atoms are the building blocks of matter. The bulk matter were described by using classical laws like Newton laws and Maxwell's equations [26].the experiments done that they consist of small tiny particles revolving around the nucleus known as electrons. The nucleus consists of protons and neutrons of almost equal numbers. The excitation of these atoms by any energy source causes them to emit electromagnetic radiation. One of the important atomic radiations was called black body radiation, due to excitation by heat. The spectra of black body, is the first challenge that shows the failure of classical laws in describing the behavior of the atomic

world [27]. This encourages Max Plank to propose a new concept to describe the black body radiation. He proposes that light is emitted as discrete quanta called photons. The energy of each quanta is directly proportional to the light frequency. This new quantum concept opens a new horizon in physics. It encourages De- Brogglie to prose also that particles like electrons behave as discrete quanta. This new concept of quanta encourages Schrodinger and Heisenberg in dependently, to formulate the so-called quantum laws [28, 29]. These quantum laws open a new era in physic s and succeed in explaining a large number of atomic phenomena.

Later on Schrodinger equation, based on classical Newton energy for slow particles, has promoted to describe fast particles. Klein –Gordon and Dirac made this development where they formulated relativistic quantum mechanics [30]. Klein nonlinear equation describes spin less bosons, while Dirac linear one describes fermions [31, 32].

Although both relativistic equation describe fast particle, but they suffer from the lack of a simple expression which recognized all potentials. Another problem is relate to the fact that, ion no single equation can describe the behavior of bosons at the same time.

Different attempts have made to modify quantum relativistic equation to widen their scope in describing physical phenomena [33].

The relativistic modified version of Nagua [34]. Utilized the quantum relativistic equation beside periodicity condition to find the harmonic oscillator solution. A paper published by Fatima [35].

Showed that relativistic potential dependent equation derived from Generalized Special Relativity (GSR) can described the behavior of bio photons as well as photons propagated in free space.

1.2 Research Problem:

The concept of energy in general relativity does not satisfy Newton limt.it does not also conform to observations. The particle spin plays an important role in quantum mechanics. According to relativistic quantum mechanics [36], two different quantum equations was been used to describe integral and half-integral spin quantum numbers. The former one is Klein-Gordon equation, while the later one is Dirac equation. This make the spin mathematical for one work complex [37].

1.3 Aim of the work:

The aim of this work is to use generalized special relativity to formulate new expression for the linear energy. One also need to construct a new relativistic Klein Gordon equation, which can describe spin phenomena.

1.4 Thesis layout:

The thesis consists of five chapters. Chapter one is introduction, while chapter two is concerned with theoretical background, Chapter three is devoted for Dirac equation, and Klein Gordon equation. The literature Review is in chapter four. The new models, discussion and conclusion are in chapter five.

Chapter Two
Nuclear Model

2.1 Introduction

These chapter covers the physics need to understand the nuclear structure, application of nuclear physics, the atoms and nuclear. The difference in energy between the nuclear ground state and the first excited state is especially large for these nuclei; we find magic number and models.

2.2 Nuclear Models and Stability

The aim of this is to understand how certain combinations of N neutrons and Z protons form ground states and to understand the masses, spins and parities of those states. The known (N, Z) combinations are shown in Fig. 2.1. The great majority of nuclear species contain excess neutrons or protons and are therefore β-unstable. Many heavy nuclei decay by α-particle emission or by other forms of spontaneous fission into lighter elements. Another aim of this to understand why certain nuclei are stable against these decays and what determines the dominant decay modes of unstable nuclei. Finally, forbidden combinations of (N, Z) are those outside the lines in Fig. 2.1 marked "last proton/neutron unbound." Such nuclei rapidly (within $\sim 10^{-20}$s) shed neutrons or protons until they reach a bound configuration.

The problem of calculating the energies, spins and parities of nuclei is one of the most difficult problems of theoretical physics. To the extent that nuclei can be considered as bound states of nucleons (rather than of quarks and gluons), one can start with empirically established two-nucleon potentials, and then, in principle, calculate the eigenstates and energies of many nucleon systems. In practice, the problem is intractable because the number of nucleons in a nucleus with $A > 3$ is much too large to perform a direct calculation but is too small to use the techniques of statistical mechanics. We also note that it is sometimes suggested that intrinsic three-body forces are necessary to explain the details of nuclear binding.

However, if we put together all the empirical information we have learned, it is possible to construct efficient phenomenological models for nuclear structure. In addition, this provides an introduction to the characteristics and physical content to the simplest models. This will lead us to a good explanation of nuclear binding energies and to a general view of the stability of nuclear structures [38].

Much can be understood about nuclei by supposing that, inside the nucleus, individual nucleons move in a potential well defined by the mean interaction with the other nucleons. Mean potential model and derive some

important conclusions about the relative binding energies of different isobars. To complement the mean potential model, we will introduce the liquid-drop model that treats the nucleus as a semi-classical liquid object. When combined with certain conclusions based on the mean potential model, this will allow us to derive Bethe and Weizs¨acker's semi-empirical mass formula that gives the binding energy as a function of the neutron number N and proton number Z. also we will come back to the mean potential model in the form of the Fermi-gas model. This model will allow us to calculate some of the parameters in the Bethe–Weizs¨acker formula.
In the shell model, we will further modify the mean-field theory to explain the observed nuclear shell structure that lead to certain nuclei with "magic numbers" of neutrons or protons to have especially large binding energies. Armed with our understanding of nuclear binding, in β- instability we will identify those nuclei that are observed to be radioactive either via β- decay or α-decay [38].

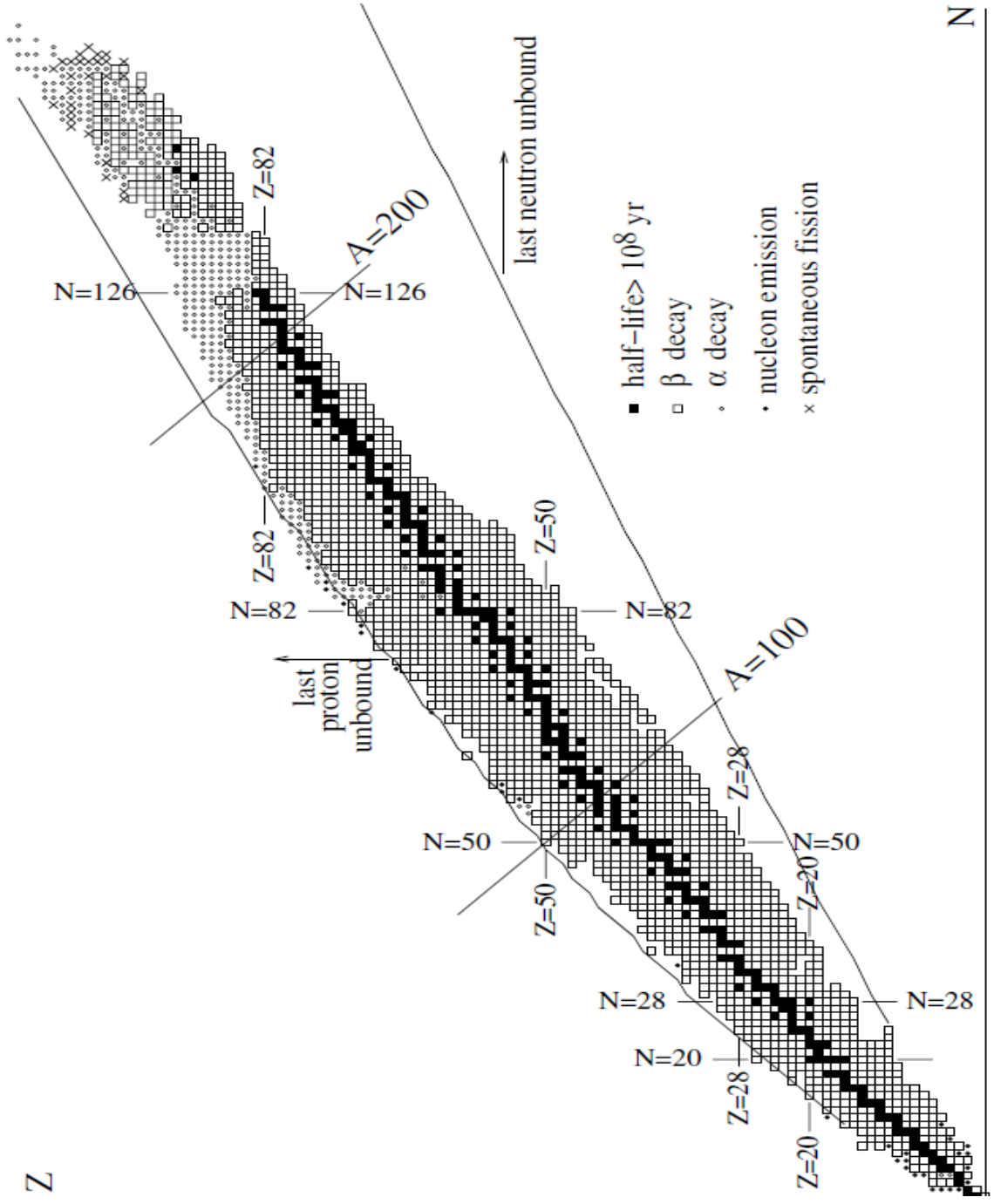

Fig. 2.1. The nuclei. The black squares are long-lived nuclei present on Earth. Combinations of (N, Z) that lie outside the lines marked "last proton/neutron unbound" are predicted to be unbound by the semi-empirical mass formula [38].

2.3 Mean Potential Model

The mean potential model relies on the observation that, to good approximation, individual nucleons behave inside the nucleus as independent particles placed in a mean potential (or mean field) due to the other nucleons.

In order to obtain a qualitative description of this mean potential V (**r**), we write it as the sum of potentials v(**r** – **r**$^{-}$_) between a nucleon at **r** and a nucleon at **r**$^{-}$:

V (**r**) $= \int v(r - r^{-})p(r^{-})dr^{-}$. (2.3.1)

In this equation, the nuclear density ρ ((r^{-})), is proportional to the probability per unit volume to find a nucleus in the vicinity of **r**$^{-}$. It is precisely that function.

One now recall what one know about v and ρ. The strong nuclear interaction $v(r - r^{-})$ is attractive and short range. It falls to zero rapidly at distances larger than ∼ 2 fm, while the typical diameter on a nucleus is "much" bigger, of the order of 6 fm for a light nucleus such as oxygen and of 14 fm for lead. In order to simplify the expression, let us approximate the potential v by a delta function (i.e. a point-like interaction).

$v(r - r^{-}) \sim - v_{\circ}\partial(r - r^{-})$ (2.3.2)

The constant $v_{\circ}$ can be taken as a free parameter but we would expect that the integral of this potential be the same as that of the original two-nucleon potential:

$v_{\circ} = \int \pi d^{3}$rv(r)∼200MeV$fm^{3}$ (2.3.3)

Where we have used the values. The mean potential is then [1].

Simply

V (r) = $-v_{\circ}$ρ(r). (2.3.4)

Using ρ ∼ 0.15 fm$^{-3,}$ we expect to find a potential depth of roughly

V (r < R) ∼ −30MeV, (2.3.5)

Where R is the radius of the nucleus.

Suggest that in first approximation the mean potential has the used analytic expression is the Saxon–Woods potential

$$V(r) = -\frac{V0}{1 + \exp(r - R)/R} \quad (2.3.6)$$

Where V_0 is a potential depth of the order of 30 to 60 MeV and R is the Radius of the nucleus R ∼ 1.2A$^{1/3}$ fm. An even simpler potential which leads to qualitatively similar results is the harmonic oscillator potential drawn on:

$$V(r) = V_{\circ}\left[1 - \left(\frac{r}{R}\right)\right] = -V_{\circ} + \frac{1}{2}M\omega^{2}r^{2} \;\; r < R \quad (2.3.7)$$

With$V_\circ = \frac{1}{2}M\omega^2 r^2$, and V (r > R) = 0. Contrary to what one could believe from Fig. 2.2, the low-lying wave functions of the two potential wells (a) and (b) are very similar. Quantitatively, their scalar products are of the order of 0.9999 for the ground state and 0.9995 for the first few excited states for an appropriate choice of the parameter ω in b. The first few energy levels of the potentials a and b hardly differ.

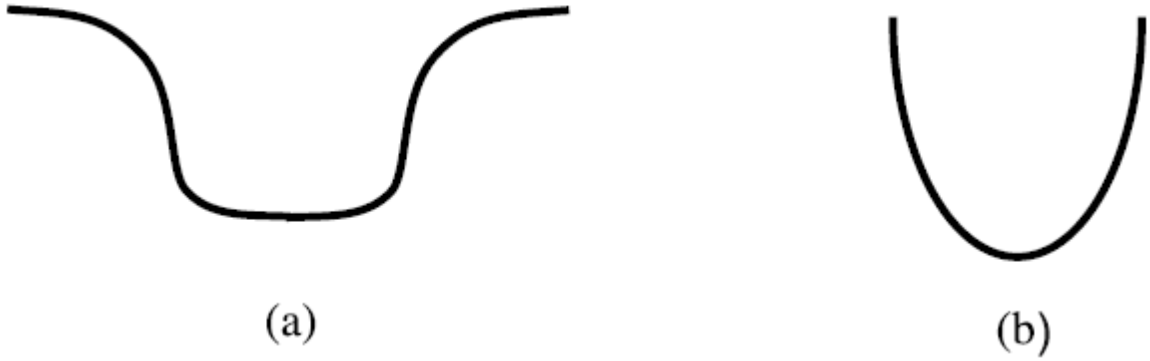

Fig 2.2 the mean potential and its approximation by a harmonic potential.

In this model, where the nucleons can move independently from one another, and where the protons and the neutrons separately obey the Pauli principle, the energy levels and configurations are obtained in an analogous way to that for complex atoms in the Hartree approximation. As for the electrons in such atoms, the proton and neutron orbitals are independent fermion levels.

It is instructive, for instance, to consider, within the mean potential notion, the stability of various A = 7 nuclei, schematically drawn on Fig. 2.3. The figure reminds us that, because of the Pauli principle, nuclei with a large excess of neutrons over protons or vice versa require placing the nucleons in high-energy levels. This suggests that the lowest energy configuration will be the ones with nearly equal numbers of protons and neutrons, 7Li or 7Be. We expect that the other configurations can β-decay to one of these two nuclei by transforming neutrons to protons or vice versa. The observed masses of the A = 7 nuclei, shown in Fig. 2.4, confirm this basic picture:

• The nucleus ^{7}Li is the most bound of all. It is stable, and more strongly Bound than its mirror nucleus be which suffers from the larger Coulomb repulsion between the 4 protons. In this nucleus, the actual energy levels of the protons are increased by the Coulomb interaction. The physical

properties of these two nuclei, which form an isospin doublet, are very similar.

• The mirror nuclei ^{7}B and ^{7}He can β-decay, respectively, to ^{7}Be and ^{7}Li. In fact, the excess protons or neutrons are placed in levels that are so high that neutron emission is possible for ^{7}He and 3-proton emission for ^{7}B and these are the dominant decay modes. When nucleon emission is possible [38].

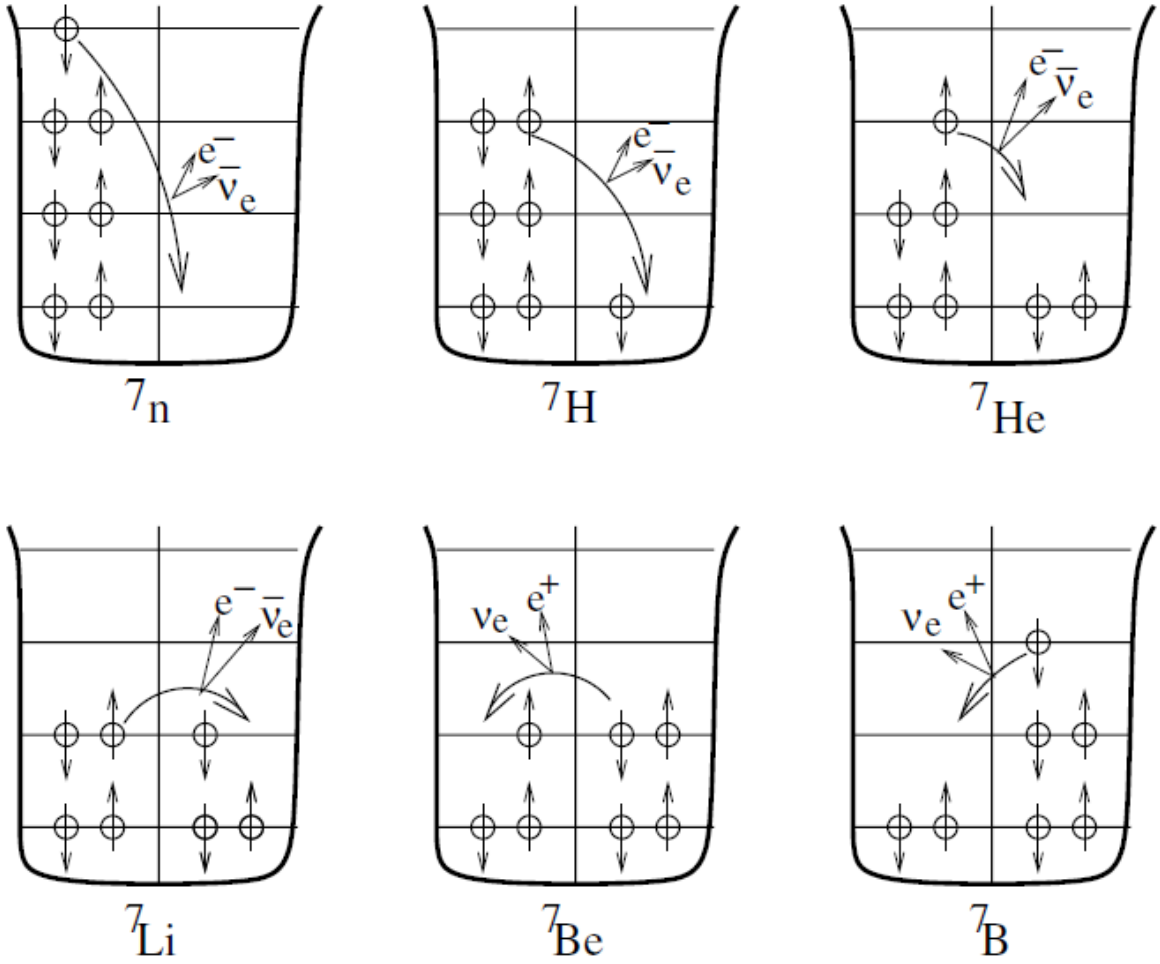

Fig. 2.3. Occupation of the lowest lying levels in the mean potential for various isobars A = 7.

The level spacing's are schematic and do not have realistic positions. The proton orbitals are shown at the same level as the neutron orbitals whereas in reality the electrostatic repulsion raises the protons with respect to the neutrons. The curved arrows show possible neutron–proton and proton–neutron transitions. If energetically possible, a neutron can transform to a proton by emitting a e−¯ve Pair. If energetically possible, a proton can transform to a neutron by emitting a e+ve pair or by absorbing an atomic e−

and emitting a ve. As explained in the text, which of these decays is actually energetically possible depends on the relative alignment of the neutron and proton orbitals [38].

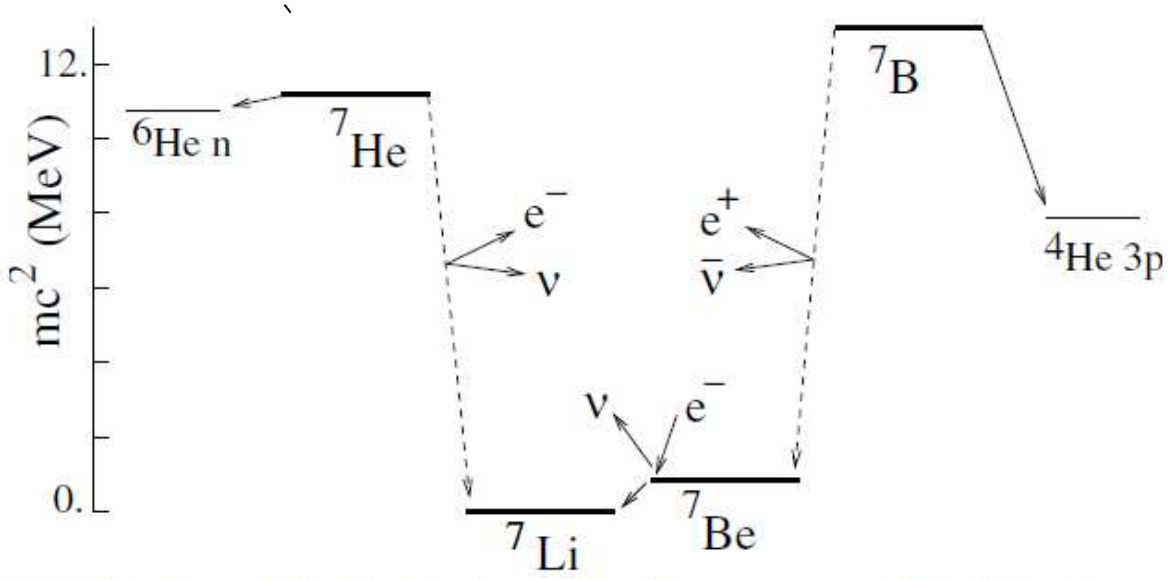

Fig. 2.4. Energies of the $A = 7$ isobars. Also shown are two unbound $A = 7$ states, ^{6}He n and ^{4}He 3p.

This picture of a nucleus formed with independent nuclei in a mean potential allows us to understand several aspects of nuclear phenomenology.

• For a given A, the minimum energy will be attained for optimum numbers of protons and neutrons. If protons were not charged, their levels would be the same as those of neutrons and the optimum would correspond to N = Z (or Z ± 1 for odd A). This is the case for light nuclei, but as A increases, the proton levels are increased compared to the neutron levels owing to Coulomb repulsion, and the optimum combination has N > Z. For mirror nuclei, those related by exchanging N and Z, the Coulomb repulsion makes the nucleus N >Z more strongly bound than the nucleus Z >N.

• The binding energies are stronger when nucleons can be grouped into pairs of neutrons and pairs of protons with opposite spin. Since the nucleon–nucleon force is attractive, the energy is lowered if nucleons are placed near each other but, according to the Pauli principle, this is possible only if they have opposite spins. There are several manifestations of this pairing effect. Among the 160 even-A, β-stable[1] nuclei, only the four light nuclei, ^{2}H, ^{6}Li, ^{10}B, ^{14}N, are "odd-odd", the others being all "even-even." 1

• The Pauli principle explains why neutrons can be stable in nuclei while free neutrons are unstable. Possible β-decays of neutrons in 7n, 7H, 7He and

^{7}Li are indicated by the arrows in Fig. 2.3. In order for a neutron to transform into a proton by β-decay, the final proton must find an energy level such that the process n → pe$^-$ $\bar{}$ve is energetically possible. If all lower levels are occupied, that may be impossible. This is the case for ^{7}Li because the Coulomb interaction raises the proton levels by slightly more than ($m_n - m_p - m_e$) c^2 = 0.78MeV. Neutrons can therefore be "stabilized " by the Pauli principle.

• Conversely, in a nucleus a proton can be "destabilized" if the reaction p → n+e+ν_e can occur. This is possible if the proton orbitals are raised, via the Coulomb interaction, by more than ($m_n+m_e-m_p$) c^2 = 1.80MeV with respect to the neutron orbitals. In the case of ^{7}Li and ^{7}Be shown in Fig. 2.4, the proton levels are raised by an amount between ($m_n + m_e - m_p$) c2 and ($m_n-m_e-m_p$) c^2 so that neither nucleus can β-decay. (The atom ^{7}Be is unstable because of the electron-capture reaction of an internal electron of the atomic cloud ^{7}Be e$^-$ →^{7} Li ve.)

One now come back to equation (2.3.7) to determine what value should be assigned to the parameter ω to reproduce the observed characteristics of nuclei. The two forms in this equation, one find

$$\omega\,(A) = \left(\frac{2V_\circ}{M}\right)^{1/2} R^{-1} \qquad (2.3.8)$$

Equation (2.3.5) suggests that V_0 is independent of A while empirically we know that R is proportional to $A^{1/3}$. Equation (2.3.8) then tells us that ω is proportional to $A^{-1/3}$. To get the phenomenologically correct value, we take V_0 = 20MeV and R = $1.12A^{1/3}$ which yields

$$\hbar\omega = \left(\frac{2V_\circ}{m_p c^2}\right)^{1/2} \frac{\hbar c}{R} \sim 35MeV \times A^{-1/3} \qquad (2.3.9)$$

One can now calculate the binding energy B (A = 2N = 2Z) in this model. The levels of the three-dimensional harmonic oscillator are En = (n+3/2)$\bar{}$hω with a degeneracy g_n = (n+1)(n+2)/2. The levels are filled up to n = n_{max} such that:

$$A = \sum_{n=0}^{nmax} g_n \sim 2n_{max}^3/3 \qquad (2.3.10)$$

i.e. $n_{max} \sim (3A/2)^{1/3.}$ (This holds for A large; one can work out a simple but clumsy interpolating expression valid for all A's.) The corresponding energy is

$$E = -AV0 + 4\sum_{n=0}^{nmax} g_n \left(n + 3/2\right)\hbar\omega \sim -AV_\circ + \frac{\hbar\omega n^4}{2} \qquad (2.3.11)$$

Using the expressions for $\bar{}$hω and n_{max} we find

$$\sim -8MeV \times A \qquad (2.3.12)$$

i.e. the canonical binding energy of 8MeV per nucleon[38].

2.4 The Nuclear Force

The force that binds protons and neutrons together in the nucleus, despite the electrical repulsion of the protons, is an example of the strong interaction that we mentioned in the context of nuclear structure, this interaction is called the nuclear force. Here are some of its characteristics. First, it does not depend on charge; neutrons as well as protons are bound, and the binding is the same for both. Second, it has short range, of the order of nuclear dimensions— that is, (Otherwise, the nucleus would grow by pulling in additional protons and neutrons). However, within its range, the nuclear force is much stronger than electrical forces; otherwise, the nucleus could never be stable. It would be nice if we could write a simple equation like Newton's law of gravitation or Coulomb's law for this force. The nearly constant density of nuclear matter and the nearly constant binding energy per nucleon of larger nuclides show that a particular nucleon cannot interact simultaneously with all the other nucleons in a nucleus, but only with those few in its immediate vicinity. This is different from electrical forces; every proton in the nucleus repels every other one. This limited number of interactions is called saturation; it is analogous to covalent, bonding in molecules and solids. Finally, the nuclear force favors binding of pairs of protons or neutrons with opposite spins and [39]. Of pairs of pairs—that is, a pair of protons and a pair of neutrons, each pair having opposite spins. Hence, the alpha particle (two protons and two neutrons) is an exceptionally stable nucleus for its mass number. We will see other evidence for pairing effects in nuclei in the next subsection. We described an analogous pairing that binds opposite-spin electrons in Cooper pairs in the BCS theory of superconductivity.)

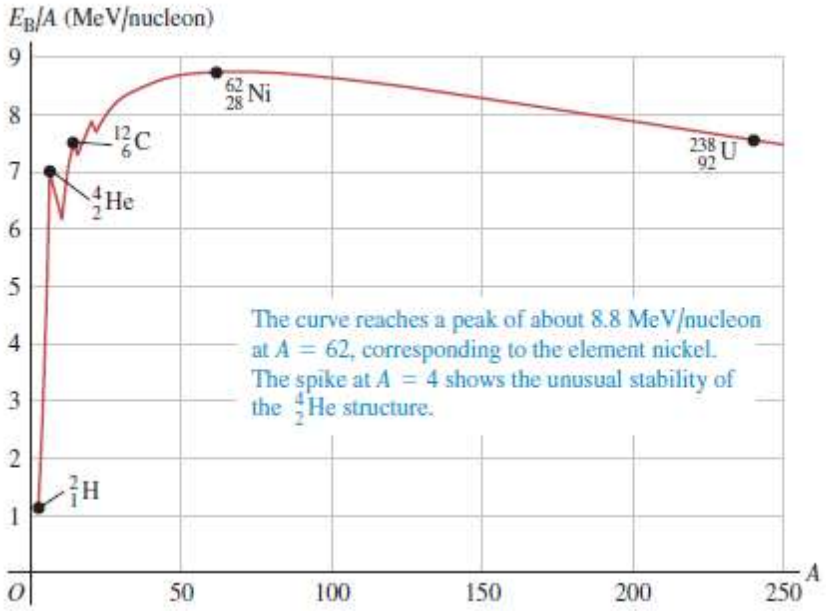

Fig 2.5 Approximate binding energy per nucleon as a function of mass number A [39].

The analysis of nuclear structure is more complex than the analysis of many electron atoms. Two different kinds of interactions are involved (electrical and nuclear), and the nuclear force is not yet completely understood. Even so, we can gain some insight into nuclear structure by the use of simple models. We will discuss briefly two rather different but successful models, the liquid-drop model and the shell model [39].

2.5 Models and Theories of Nuclear Physics

Nuclei are held together by the strong nuclear force between nucleons, so we start this topic by looking at the form of this, which is more complicated than that generated by simple one-particle exchange. Much of the phenomenological evidence comes from low-energy nucleon–nucleon scattering experiments which we will simply quote, but we will interpret the results in terms of the fundamental strong interaction between quarks. The rest of the chapter is devoted to various models and theories that are constructed to explain nuclear data in particular domains [40].

2.6 The Nucleon -- Nucleon Potential

The existence of stable nuclei implies that over all the net nucleon -nucleon force must be attractive and much stronger than the Coulomb force, although it cannot be attractive for all separations, or otherwise nuclei would collapse in on themselves. Therefore, at very short ranges there must be a repulsive core. However, the repulsive core can be ignored in low-energy nuclear structure problems because low-energy particles cannot probe the short-

distance behavior of the potential. In lowest order, the potential may be represented dominantly by a central term (i.e. one that is a function only of the radial separation of the particles), although there is also a smaller non-central part. One know from proton–proton scattering experiments1 that the nucleon–nucleon force is short-range, of the same order as the size of the nucleus, and thus does not correspond to the exchange of gluons, as in the fundamental strong interaction. A schematic diagram of the resulting potential is shown in Figure 2.6. In practice, of course this strong interaction potential must be combined with the Coulomb potential in the case in the case of protons [40].

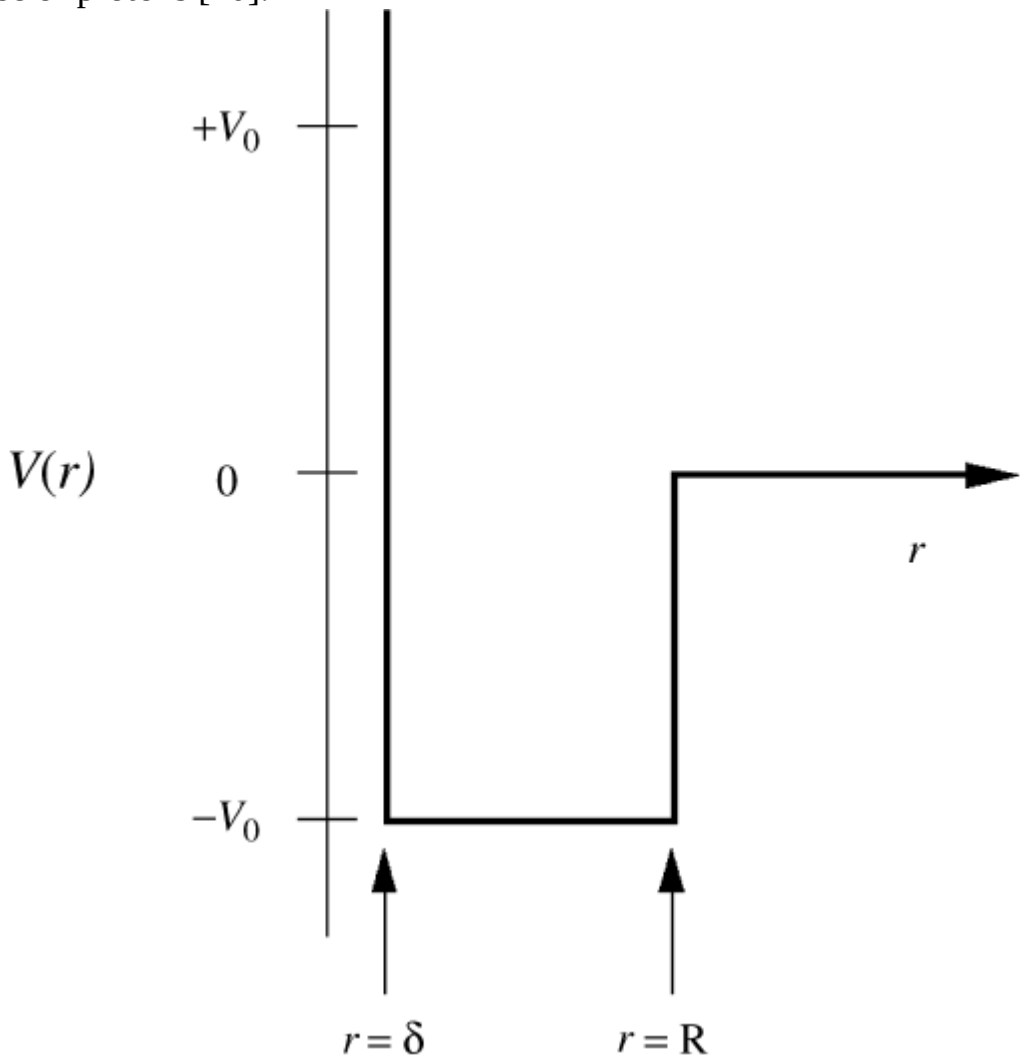

Figure 2.6 Idealized square well representation of the strong interaction nucleon-nucleon potential.

The distance R is the range of the nuclear force and $\partial \leq$ R is the distance at which the short-range repulsion becomes important. The depth V_0 is approximately 40 MeV.

A comparison of nn and pp scattering data (after allowing for the Coulomb interaction) shows that the nuclear force is charge symmetric (pp = nn) and almost charge-independent (pp = nn = pn)^2 , that there is also evidence for this from nuclear physics. Charge-symmetry is seen in comparisons of the energy levels of mirror nuclei and evidence for charge-independence comes from the energy levels of triplets of related nuclei with the same A values. Nucleon–nucleon forces are, however, spin [3] dependent. The force between a proton and neutron in an overall spin-1 state (i.e. with spins parallel) is strong enough to support a weakly bound state (the deuteron), whereas the potential corresponding to the spin-0 state (i.e. spins antiparallel) has no bound states. Finally, nuclear forces saturate. This describes that fact that a nucleon in typical nucleus experiences attractive interactions only with a limited number of the many other nucleons and is a consequence of the short-range nature of the force. The evidence for this is the form of the nuclear binding energy curve.

Ideally, one would like to be able to interpret the nucleon–nucleon potential in terms of the fundamental strong quark–quark interactions. It is not yet possible to give a complete explanation along these lines, but it is possible to go some way in this direction. If we draw an analogy with atomic and molecular structure, with quarks playing the role of electrons. Then possibilities are: an ionic-type bond, a van der Waals type of force, or a covalent bond.3 The first can be ruled out because the confining forces are too strong to permit a quark to be ‘lent’ from one nucleon to another and the second can also be ruled out because the resulting two-gluonex change is too weak. This leaves a covalent bond due to the sharing of single quarks between the nucleons analogous to the covalent bond that binds the hydrogen molecule. However, nucleons have to remain ‘colour less’ during this process and so the shared quark from one nucleon has to have the same colour as the shared quark from the other nucleon. The effect of this is to reduce the effective force (because there are three possible colour states) and by itself, it is unable to explain the depth of the observed potential. In addition to the three (valence) quarks within the nucleon there are also present quark–antiquark pairs due to vacuum fluctuations.4 Such pairs can be colour less and so can also be shared between the nucleons. These quarks actually play a greater role in generating the nuclear strong interaction than single quarks. The lightest such diquarks will be pions and this exchange gives the largest contribution to the attractive part of the nucleon–nucleon force [40].

In principle, the short-range repulsion could be due to the exchange of heavier diquarks (i.e. mesons), possibly also in different overall spin states.

Experiment provides many suitable meson candidates, in agreement with the predictions of the quark model, and each exchange would give rise to a specific contribution to the overall nucleon–nucleon potential, by analogy with the Yukawa potential resulting from the exchange of a spin-0 meson,. It is indeed possible to obtain excellent fits to nucleon–nucleon scattering data in a model with several such exchanges. Thus, this approach can yield a satisfactory potential model, but is semi-phenomenological only, as it requires the couplings of each of the exchanged particles to be found by fitting nucleon–nucleon scattering data. (The couplings that result broadly agree with values found from other sources.) Boson-exchange models therefore cannot give a fundamental explanation of the repulsion. The reason for the repulsion at small separations in the quark model lies in the spin dependence of the quark–quark strong interaction, which like the phenomenological nucleon– nucleon interaction, is strongly spin-dependent. We have discussed this in the context of calculating hadron masses. When the two nucleons are very close, the wave function is effectively that for a 6-quark system with zero angular momentum between the quarks, i.e. a symmetric spatial wave function. Since the colour wave function is antisymmetric, it follows that the spin wave function is symmetric. However, the potential energy increases if all the quarks remain in the L = 0 state with spins aligned.6 The two-nucleon system will try to minimize its 'chromomagnetic' energy, but this will compete with the need to have a symmetric spin wave function. The optimum configuration at small separations is when one pair of quarks is in an L = 1 state, although the excitation energy is comparable to the decrease in chromomagnetic energy, so there will still be a net increase in energy at small separations.

Some tantalizing clues exist about the role of the quark–gluon interaction in nuclear interactions, such as the small nuclear effects in deep inelastic lepton scattering mentioned. There is also a considerable experimental programme in existence [40], to learn more about the nature of the strong nucleon–nucleon force in terms of the fundamental quark–gluon strong interaction and further progress in this area may well result in the next few years. Meanwhile, in the absence of a fundamental theory to describe the nuclear force, specific models and theories are used to interpret the phenomena in different areas of nuclear physics. In and, we will discuss a number of such approaches [40].

2.7 The Liquid-Drop Model

One of the first nuclear models, proposed in 1935 by Bohr, is based on the short range of nuclear forces, together with the additivity of volumes and of binding energies. It is called the liquid-drop model. Nucleons interact

strongly with their nearest neighbors, just as molecules do in a drop of water. Therefore, one can attempt to describe their properties by the corresponding quantities, i.e. the radius, the density, the surface tension and the volume energy [37, 38].

The individual nucleons are analogous to molecules of a liquid, held together by short-range interactions and surface-tension effects. We can use this simple picture to derive a formula for the estimated total binding energy of a nucleus. We will include five contributions:

1. We have remarked that nuclear forces show saturation; an individual nucleon interacts only with a few of its nearest neighbors. This effect gives a binding energy term that is proportional to the number of nucleons. We write this term as C_1A where C_1 is an experimentally determined constant.
2. The nucleons on the surface of the nucleus are less tightly bound than those in the interior because they have no neighbors outside the surface. This decrease in the binding energy gives a negative energy term proportional to the surface area $4\pi R^2$ Because R is proportional to$A^{1/3,}$ this term is proportional to $A^{2/3}$ we write it as$C_2A^{2/3}$ where is $–C_2$,another constant.
3. Every one of the Z protons repels every one of the (z-1) other protons. The total repulsive electric potential energy is proportional to z (z-1) and inversely proportional to the radius R and thus to this energy term [39], is negative because the nucleons are less tightly bound than they would be without the electrical repulsion. We write this correction as $-C_3Z$ (Z-1) $A1^{/3.}$
4. To be in a stable, low-energy state, the nucleus must have a balance Between the energies associated with the neutrons and with the protons. This means that N is close to Z for small A and N is greater than Z (but not too much greater) for larger A. We need a negative energy term corresponding to the difference [N-Z]. The best agreement with observed binding energies is obtained if this term is proportional to $(N-Z)^2$ If we use N=A-Z to express this energy in terms of A and Z, this correction is $–C_4$ $(A-2Z)^2/A$.
5. Finally, the nuclear force favors pairing of protons and of neutrons. This energy term is positive (more binding) if both Z and N are even, negative (less binding) if both Z and N are odd, and zero otherwise. The best fit to the data occurs with the form+-$C_5A^{-4/3}$ for this term. The total estimated binding energy E_B is the sum of these five terms:

(Nuclear binding energy)[2].

$$E_B = C_1 - C_2A^{2/3} - C_3\frac{Z(Z-1)}{A^{1/3}} - C_4\frac{(A-2Z)^2}{A} \pm C_5A^{-4/3} \qquad (2.7.1)$$

The constantsC_1, C_2, C3, C_4 and C_5, chosen to make this formula best fit the observed binding energies of nuclides, are

C5 = 39 MeV

C4 = 23.69 MeV
C3 = 0.7100 MeV
C2 = 17.80 MeV
C1 = 15.75 MeV
C1, C2, C3, C4, C5,

The liquid-drop model and the mass formula derived from it are quite successful in correlating nuclear masses, and we will see later that they are a great help in understanding decay processes of unstable nuclides. Some other aspects of nuclei, such as angular momentum and excited states, are better approached with different models [39].

2.7.1 The Bethe–Weizs¨acker Mass Formula

An excellent parametrization of the binding energies of nuclei in their ground state was proposed in 1935 by Bethe and Weizs¨acker. This formula relies on the liquid-drop analogy but also incorporates two quantum ingredients we mentioned in the previous section. One is an asymmetry energy, which tends to favor equal numbers of protons and neutrons. The other is a pairing energy, which favors configurations where two identical fermions are paired. The mass formula of Bethe and Weizs¨acker is

$$B(A, Z) = a_v A - a_s A^{2/3} - a_c Z^2 / A^{1/3} - a_a (N - Z) \quad A + \delta(A) . \quad (2.7.2)$$

The coefficients a_i are chosen so as to give a good approximation to the Observed binding energies. A good combination is the following:

a_v = 15.753 MeV
a_s = 17.804 MeV
a_c = 0.7103 MeV
a_a = 23.69 MeV

And

$$\delta A = \begin{cases} 33.6A - 3/4 \text{ if N and Z are even} \\ -33.6A - \frac{3}{4} \text{ if Nand Z are odd} \\ 0 \qquad \text{si A} = \text{N} + \text{Z is odd} \end{cases}$$

.

The numerical values of the parameters must be determined empirically (other than a_c), but the A and Z, dependence of each term reflects simple physical properties.

• The first term is a volume term which reflects the nearest-neighbor interactions, and which by itself would lead to a constant binding energy per nucleon B/A ∼ 16 MeV.

• The term a_s, which lowers the binding energy, is a surface term. Internal nucleons feel isotropic interactions whereas nucleons near the surface of the nucleus feel forces coming only from the inside. Therefore, this is a surface

Tension term a_s, proportional to the area $4\pi R^2 \sim A^{2/3}$.

• The term a_c is the Coulomb repulsion term of protons, proportional to Q2/R, i.e. $\sim Z^2/A^{1/3}$. This term is calculable. It is smaller than the nuclear terms for small values of Z. It favors a neutron excess over protons.

• Conversely, the asymmetry term a_a favors symmetry between protons and neutrons (isospin). In the absence of electric forces, Z = N is energetically favorable [38].

• Finally, the term δ (A) is a quantum pairing term.

The existence of the Coulomb term and the asymmetry term means that for each A there is a nucleus of maximum binding energy found by setting $\partial B/\partial Z = 0$. As we will see below, the maximally bound nucleus has Z = N = A/2 for low A where the asymmetry term dominates but the Coulomb term favors N >Z for large A.

The predicted binding energy for the maximally bound nucleus is shown in Fig. 2.5 as a function of A along with the observed binding energies. The figure only shows even–odd nuclei where the pairing term vanishes. The figure also shows the contributions of various terms in the mass formula. We can see that, as A increases, the surface term loses its importance in (favor of the Coulomb term. The binding energy has a broad maximum in the neighborhood of A ~ 56 which corresponds to the even-Z isotopes of iron and nickel [38].

Light nuclei can undergo exothermic fusion reactions until they reach the most strongly bound nuclei in the vicinity of A ~ 56. These reactions correspond to the various stages of nuclear burning in stars. For large A's, the increasing comparative contribution of the Coulomb term lowers the binding energy. This explains why heavy nuclei can release energy in fission reactions or in α-decay. In practice, this is observed mainly for very heavy nuclei A > 212 because lifetimes are in general too large for smaller nuclei.

For the even–odd nuclei, the binding energy follows a parabola in Z for a given A. The minimum of the parabola, i.e. the number of neutrons and protons which corresponds to the maximum binding energy of the nucleus gives the value Z (A) for the most bound isotope [38]. :

$$\frac{\partial B}{\partial Z} = 0 \Rightarrow Z(A) = \frac{A}{2 + a_c A^{\frac{2}{3}}/2a_a} \sim \frac{A/2}{1 + 0.0075\, A^{2/3}} \qquad (2.7.3)$$

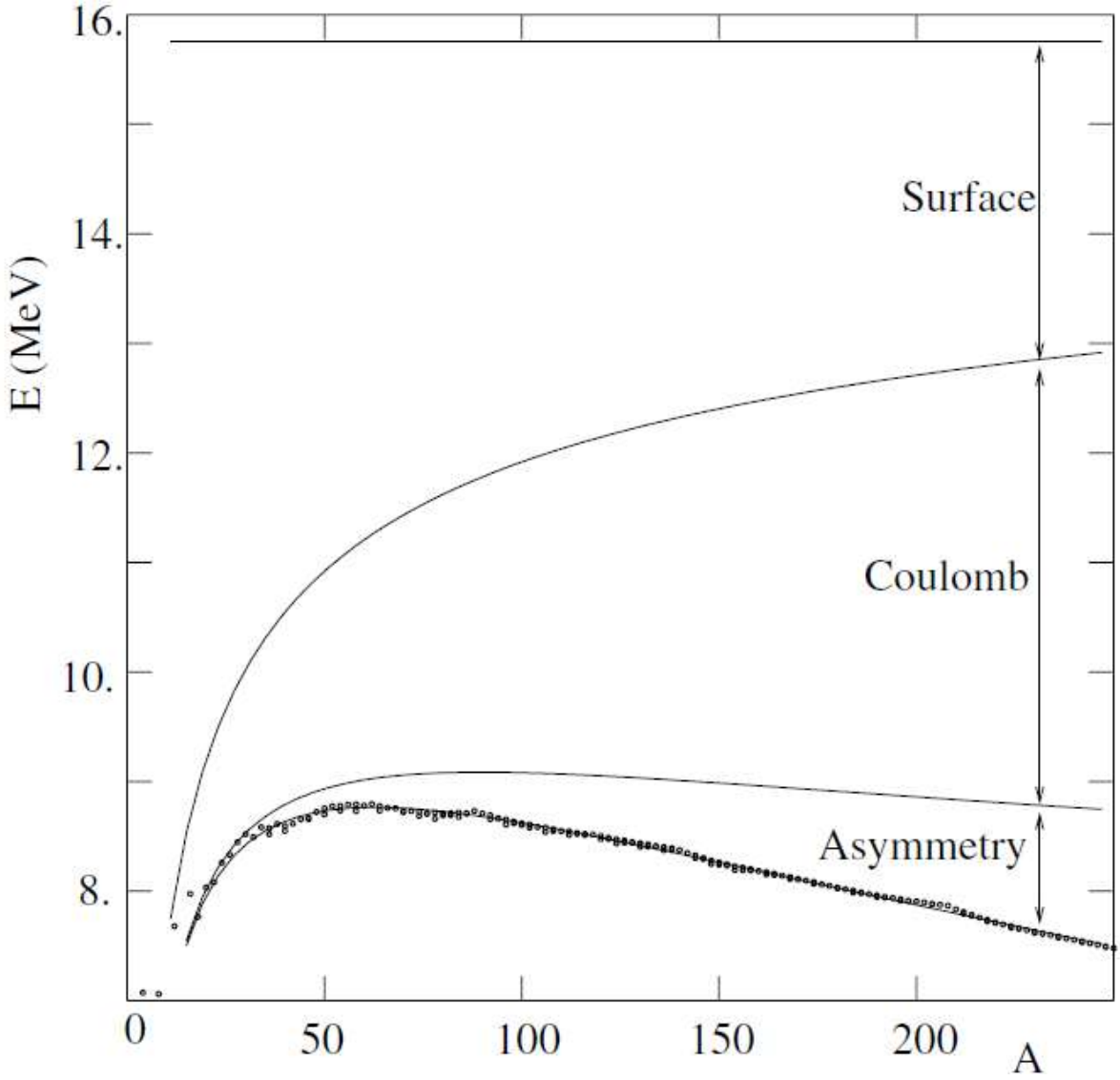

Fig. 2.7. The observed binding energies as a function of A and the predictions of the mass formula (2.13).

For each value of A, the most bound value of Z is used corresponding to Z = A/2 for light nuclei but Z < A/2 for heavy nuclei. Only even–odd combinations of A and Z are considered where the pairing term of the mass formula vanishes. Contributions to the binding energy per nucleon of the various terms in the mass formula [38].

Into account the neutron–proton mass difference in order to make sure of the stability against β-decay. The only stable nuclei for odd A are obtained by minimizing the atomic mass m (A, Z)+Z_{me} [38],(we neglect the binding energies of the atomic electrons). This leads to a slightly different value for the Z (A) of the stable atom:

$$Z(A) = \frac{\left(1 + \frac{\delta_{npe}}{4a_a}\right)}{1 + \frac{a_c A^{2/3}}{4a_a}} \sim \frac{A/2}{1 + 0.0075A^{2/3}}) \qquad (2.7.4)$$

Where $\delta_{npe} = m_n - m_p - m_e = 0.75$MeV. This formula shows that light nuclei have a slight preference for protons over neutrons because of their smaller mass while heavy nuclei have an excess of neutrons over protons because an extra amount of nuclear binding must compensate for the Coulomb repulsion. For even A, the binding energies follow two parabolas, one for even–even nuclei, the other for odd–odd ones. An example is shown for A = 112 on Fig. 2.6. In the case of even–even nuclei, it can happen that an unstable odd-odd nucleus lies between two β-stable even-even isotopes. The more massive of the two β-stable nuclei can decay via 2β-decay to the less massive. The lifetime for this process is generally of order or greater than 1020 y_r so for practical purposes there are often two stable isobars for even A.

The Bethe–Weizs¨acker formula predicts the maximum number of protons for a given N and the maximum number of neutrons for a given Z. The limits are determined by requiring that the last added proton or last added neutron be bound, i.e.

$B(Z + 1, N) - B(Z, N) > 0, B(Z, N + 1) - B(Z, N) > 0 \qquad (2.7.5)$

Or equivalently

$$\frac{\partial B/(Z,N)}{\partial Z} > 0, \frac{\partial B/(Z,N)}{\partial N} > 0 \qquad (2.7.6)$$

The locus of points (Z, N) where these inequalities become equalities establishes determines the region where bound states exist. The limits predicted by the mass formula are shown in Fig. 2.1. These lines are called the proton and neutron drip-lines. As expected, some nuclei just outside the drip-lines are observed to decay rapidly by nucleon emission. Combinations of (Z, N) far outside the drip-lines are not observed. That nucleon emission is observed as a decay mode of many excited nuclear states [38].

2.8 The Fermi Gas Model

The Fermi gas model is a quantitative quantum-mechanical application of the mean potential model discussed qualitatively. It allows one to account semi-quantitatively for various terms in the Bethe–Weizs¨acker formula. In this model, nuclei are considered to be composed of two fermion gases, a neutron gas and a proton gas. The particles do not interact, but they are confined in a sphere, which has the dimension of the nucleus. The interactions appear implicitly through the assumption that the nucleons are confined in the sphere.

The liquid-drop model is based on the saturation of nuclear forces and one relates the energy of the system to its geometric properties. The Fermi model is based on the quantum statistics effects on the energy of confined fermions. The Fermi model provides a means to calculate the constants av, as and aa in the Bethe–Weizs¨acker formula, directly from the density ρ of the nuclear matter. Its semi-quantitative success further justifies for this formula [38].

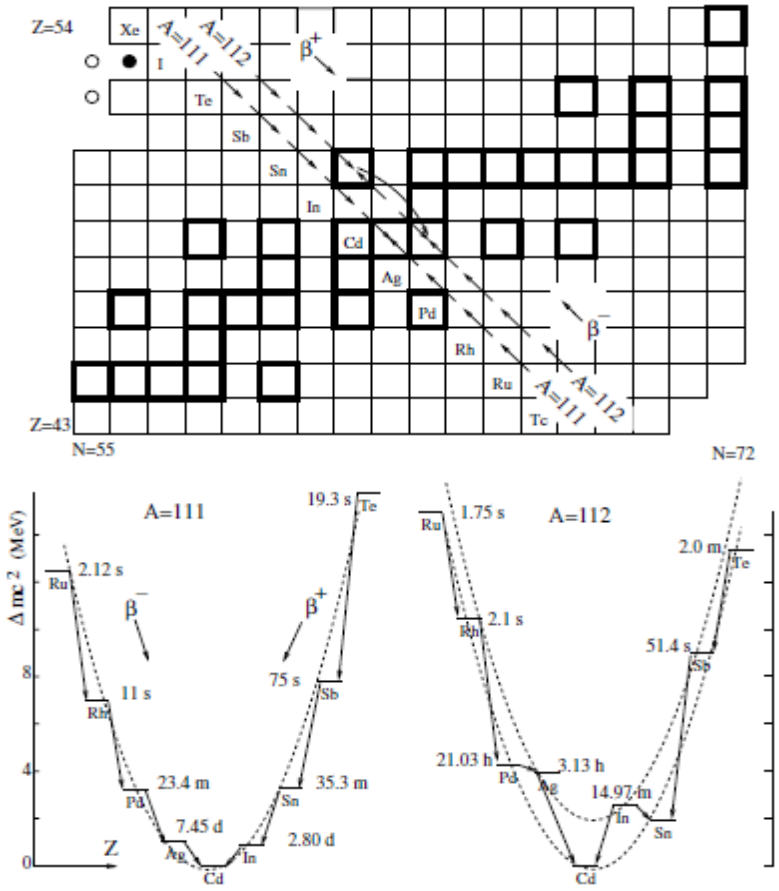

Fig. 2.8 The systematics of β-instability.

The top panel shows a zoom of Fig. 2.1 with the β-stable nuclei shown with the heavy outlines. Nuclei with an excess of neutrons (below the β-stable nuclei) decay by β− emission. Nuclei with an excess of protons (above the β-stable nuclei) decay by β+ emission or electron capture. The bottom panel shows the atomic masses as a function of Z for A = 111 and A = 112. The quantity plotted is the difference between m (Z) and the mass of the lightest isobar. The dashed lines show the predictions of the mass formula (2.13) after being offset to pass through the lowest mass isobars. Note that for even-A, there can be two β-stable isobars, e.g. 112Sn and 112Cd. The former

decays by 2β-decay to the latter. The intermediate nucleus 112In can decay to both.

In this model, the protons and neutrons that make up the nucleus are assumed to comprise two independent systems of nucleons, each freely moving inside the nuclear volume subject to the constraints of the Pauli principle. The potential felt by every nucleon is the superposition of the potentials due to all the other nucleons. In the case of neutrons, this is assumed to be a finite-depth square well; for protons, the Coulomb potential modifies this.

For a given ground state nucleus, the energy levels will fill up from the bottom of the well. The energy of the highest level that is completely filled is called the Fermi level of energy E_F and has a momentum $p_F = (2ME_F)^{1/2}$, where M is the mass of the nucleon. Within [40]. The volume V, the number of states with a momentum between p and p + dp is given by the density of states factor [40].

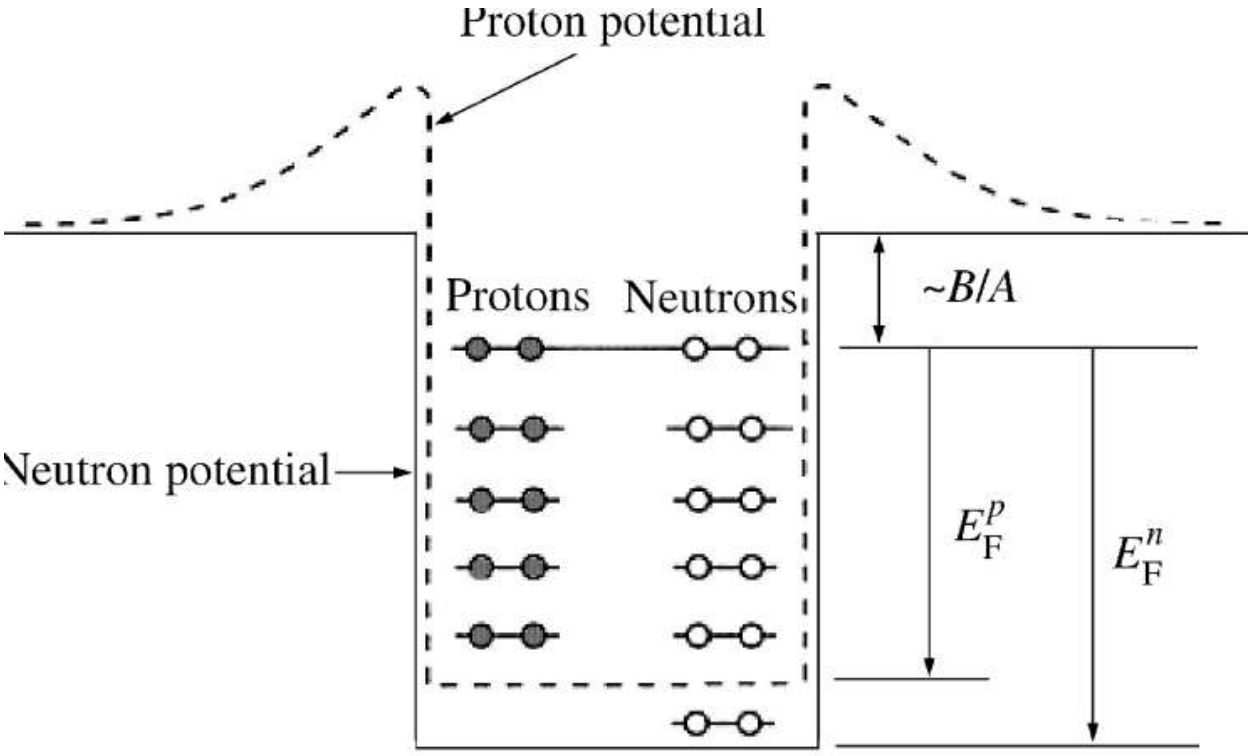

Figure 2.9 Proton and neutron potentials and states in the Fermi gas model [40].

$$n(p)dp = \frac{4\pi V}{(2\pi\hbar)^3} p^2 dp \qquad (2.8.1)$$

which is derived in Appendix A. Since every state can contain two fermions of the same species, we can have (using $n = 2\int_0^{Pf} dn$)

$N = \frac{V(P_F^n)^3}{3\pi^2\hbar^3} and\ Z = \frac{V\left(P_F^P\right)^3}{3\pi^2\hbar^3}$ (2.8.2)

Neutrons and protons, respectively, with a nuclear volume

$V = \frac{4}{3}\pi \mathrm{R}^3 = \frac{4}{3}\pi R_\circ^3 A$ (2.8.3)

Where experimentally R_0 = 1:21 fm, as we have seen from electron and hadron scattering experiments Assuming for the moment that the depths of the neutron and proton wells are the same, we find for a nucleus with Z = N = A/2, the Fermi momentum

$P_F = P_F^n = \frac{\hbar}{R_\circ}\left(\frac{9\pi}{8}\right)^{1/3} \approx 250 MeV/C.$ (2.8.4)

Thus, the nucleons move freely within the nucleus with quite large momenta. The Fermi energy is

EF =$p2_F$/2M ≈ 33 MeV (2.8.5)

The difference between the top of the well and the Fermi level is constant for most heavy nuclei and is just the average binding energy per nucleon.

˜B = B/A = 7–8 MeV. The depth of the potential and the Fermi energy=

$V_o = E_F + \tilde{B} \approx 40 MeV$ (2.8.6)

Heavy nuclei generally have a surplus of neutrons. Since the Fermi levels of the protons and neutrons in a stable nucleus have to be equal (otherwise the nucleus can become more stable by β decay) this implies that the depth of the potential well for the neutron gas has to be deeper than for the proton gas, as shown in Figure 2.9. Protons are therefore on average less tightly bound in nuclei than are neutrons.

We can use the Fermi gas model to give a theoretical expression for some of the dependence of the binding energy on the surplus of neutrons, as follows. First, we define the average kinetic energy per nucleon as [40].

$(E_{kin}) \equiv \left[\int_\circ^{p_f} E_{kin}\, p^2 dp\right]\left[\int_\circ^{p_f} p^2\, dp\right]^{-1}$ (2.8.7)

Evaluating the integrals gives:

$(E_{kin}) = \frac{3P_f^2}{52M} \approx 20\ mEv$ (2.8.8)

The total kinetic energy of the nucleus is then

$E_{kin}(N,Z) = N\langle E_n\rangle + Z\langle E_P\rangle = \frac{3}{10M}\left[N\left(P_f^n\right)^2\right] + \mathrm{Z}\left(P_f^n\right)^2$ (2.8.9)

Which may be re-expressed as

$E_{kin}(N,Z) = \frac{3}{10M}\frac{\hbar^2}{R_\circ^2}\left(\frac{9\pi}{4}\right)^{2/3}\left[\frac{N^{5/3}+z^{5/3}}{A^{2/3}}\right]$ (2.8.10)

Where again we have taken the radii of the proton and neutron wells to be equal. This expression is for fixed abut varying N and has a minimum at N = Z. Hence, the binding energy gets smaller for N ≠ Z. If we set N = (A +Δ)/2, where Δ= N - Z, and expand Equation (2.8.8) as a power series in Δ/A we obtain:

$$E_{kin}(N,Z) = \frac{3}{10M}\frac{\hbar^2}{R_o^2}\left(\frac{9\pi}{4}\right)^{2/3}\left[A + \frac{5}{9}\frac{(N-Z)^2}{A} + \cdots \ldots .\right] \qquad (2.8.11)$$

Which gives the dependence on the neutron excess. The first term contributes to the volume term in the semi-empirical mass formula (SEMF), while the second describes the correction that results from having N ≠Z. This is a contribution to the asymmetry term we have met before in the SEMF and grows as the square of the neutron excess. Evaluating this term from Equation (2.8.11)

2.9 Collective Model

The Rainwater model is equivalent to assuming an aspherical liquid drop and A age Bohr (the son of Neils Bohr) and Mottelson showed that many properties of heavy nuclei could be ascribed to the surface motion of such a drop. However, the single particle shell model cannot be abandoned because it explains many general features of nuclear structure. The problem was therefore to reconcile the shell model with the liquid-drop model. The outcome is the collective model.

This model views the nucleus as having a hard core of nucleons in filled shells, as in the shell model, with outer valence nucleons that behave like the surface molecules of a liquid drop. The motions of the latter introduce non-sphericity in the core that in turn causes the quantum states of the valence nucleons to change from the unperturbed states of the shell model. Such a nucleus can both rotate and vibrate and these new degrees of freedom give rise to rotational and vibrational energy levels. For example, the rotational levels are given by E_J = (J+1) _h^2/2I, where I is the moment of inertia and J is the spin of the nucleus. The predictions of this simple model are quite good for small J, but overestimate the energies for larger J. Vibrational modes are due predominantly to shape oscillations, where the nucleus oscillates between prolate and oblate ellipsoids. Radial oscillations are much rarer because nuclear matter is relatively incompressible. The energy levels are well approximated by a simple harmonic oscillator potential with spacing $\nabla E = \hbar\omega$, where! Is the oscillator frequency. In practice, the energy levels of deformed nuclei are very complicated, because there is often

coupling between the various modes of excitation, but nevertheless many predictions of the collective model are confirmed experimentally[41].

2.10 Shell Model

Atomic theory based on the shell model has provided remarkable clarification of the complicated details of atomic structure. In this model, we fill the shells with electrons in order of increasing energy [42].

In spite of the shell model is successes to expression for nuclear spins for ground state, but we find many type cannot be for the theoretical value for the shell model with experimental measured [43].

The nuclear shell model is based on the analogous model for the orbital structure of atomic electrons in atoms. In some areas, it gives more detailed predictions than the Fermi gas model and it can address Questions that the latter model cannot. Firstly, we recap the main features of the atomic case [40].

The shell model of nuclear structure is analogous to the central-field approximation in atomic physics, we picture each nucleon as moving in a potential that represent the averaged-out effect of all the other nucleons. This may not seem to be a very promising approach; the nuclear force is very strong, very short range, and therefore strongly distance dependent. However, in some respects, this model turns out to work fairly well [39].

The potential-energy function for the nuclear force is the same for protons as for neutrons. The corners are somewhat rounded because the nucleus does not have a sharply defined surface. For protons, there is an additional potential energy associated with electrical repulsion. We consider each proton to interact with a sphere of uniform charge density, with radius R and total charge we shows the nuclear, electric, and total potential energies for a proton as functions of the distance r from the center of the nucleus questions that the latter model cannot. Firstly, we recap the main features of the atomic case [39].

2. 10.1 Shell Structure of Atoms

The binding energy of electrons in atoms is due primarily to the central Coulomb potential. This is a complicated problem to solve in general because in a multi electron atom we have to take account of not only the Coulomb field of the nucleus, but also the fields of all the other electrons. Analytic solutions are not usually possible. However, many of the general features of the simplest case of hydrogen carry over to more complicated cases, so it is worth recalling the former [39,44].

Atomic energy levels are characterized by a quantum number n = 1, 2, 3, 4, . .
Called the principal quantum number. This is defined so that it determines the energy of the system.. For any n there are energy-degenerate levels with orbital angular momentum quantum numbers given by:

$$L=0, 1, 2, 3 \ldots (n-1) \qquad (2.10.1)$$

(This restriction follows from the form of the Coulomb potential) and for any value of L there are (2L+ 1) sub-states with different values of the projection of orbital angular momentum along any chosen axis (the magnetic quantum number):

$$m_L=-L,-L+1,\ldots..,0,1,2\ldots.,L-1,L \qquad (2.10.2)$$

Due to the rotational symmetry of the Coulomb potential, all such sub-states are degenerate in energy. Furthermore, since electrons have spin-1/2, each of the above [40].

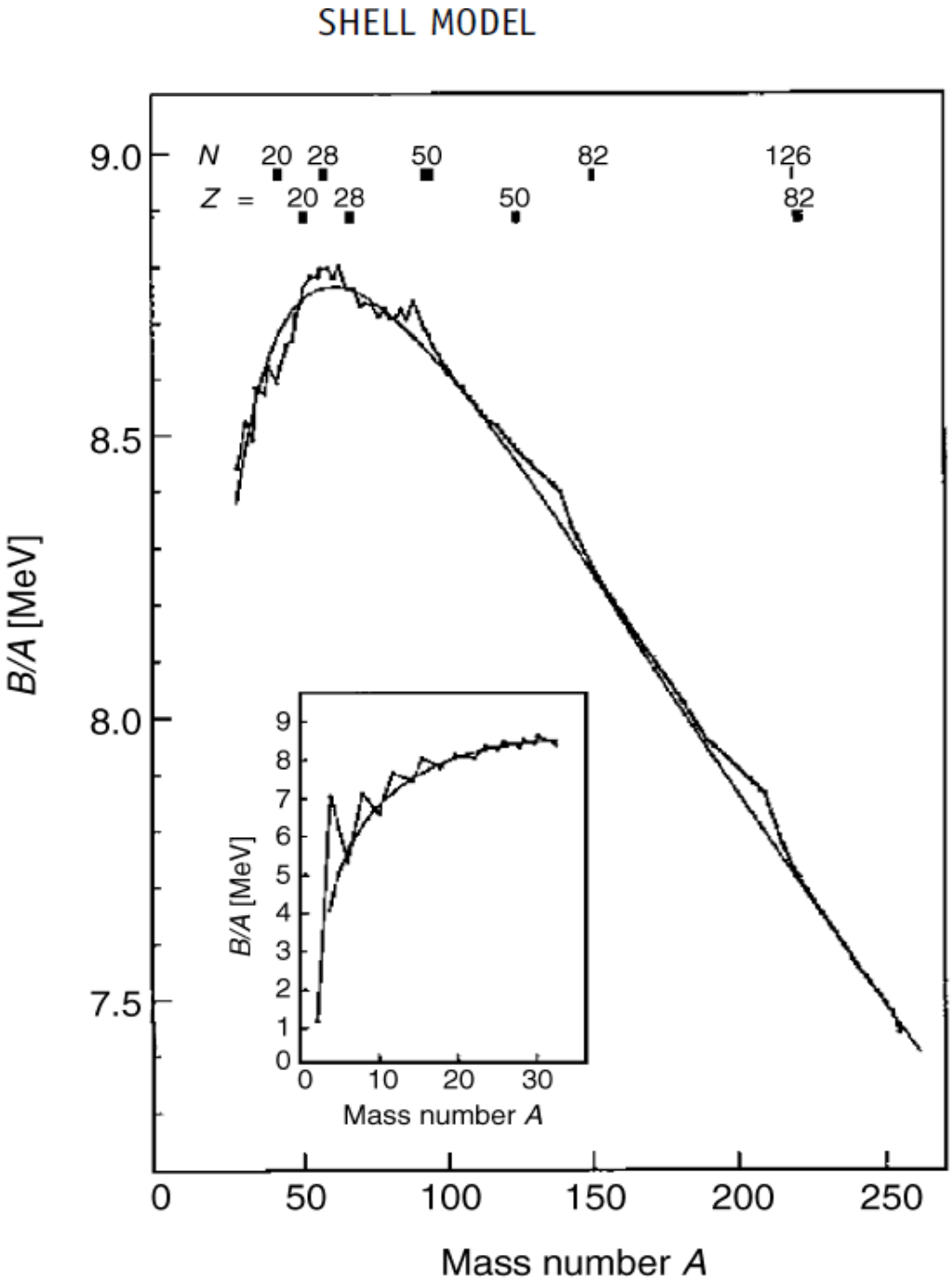

Figuer2.10.binding energy per nucleon for even value of A: the solid curve is the SEMF (fromBo69) [40].

2.10.2 The Shell Model and Magic Numbers

In atomic physics, the ionization energy E_I , i.e. the energy needed to extract an electron from a neutral atom with Z electrons, displays discontinuities around Z = 2, 10, 18, 36, 54 and 86, i.e. for noble gases. These discontinuities are associated with closed electron shells [38].

An analogous phenomenon occurs in nuclear physics. There exist many experimental indications showing that atomic nuclei possess a shell-structure and that they can be constructed, like atoms, by filling successive shells of an effective potential well. For example, the nuclear analogs of atomic ionization energies are the "separation energies" Sn and Sp which are necessary in order to extract a neutron or a proton from a nucleus

$$Sn = B(Z,N) - B(Z,N-1) \quad Sp = B(Z,N) - B(Z-1,N) \quad . (2.10.3)$$

These two quantities present discontinuities at special values of N or Z, which are called magic numbers. The most commonly mentioned are:

$$2\ 8\ 20\ 28\ 50\ 82\ 126 \quad . (2.10.4)$$

As an example, Fig. 2.11. Gives the neutron separation energy of lead isotopes (Z = 82) as a function of N. The discontinuity at the magic number N = 126 is clearly seen.

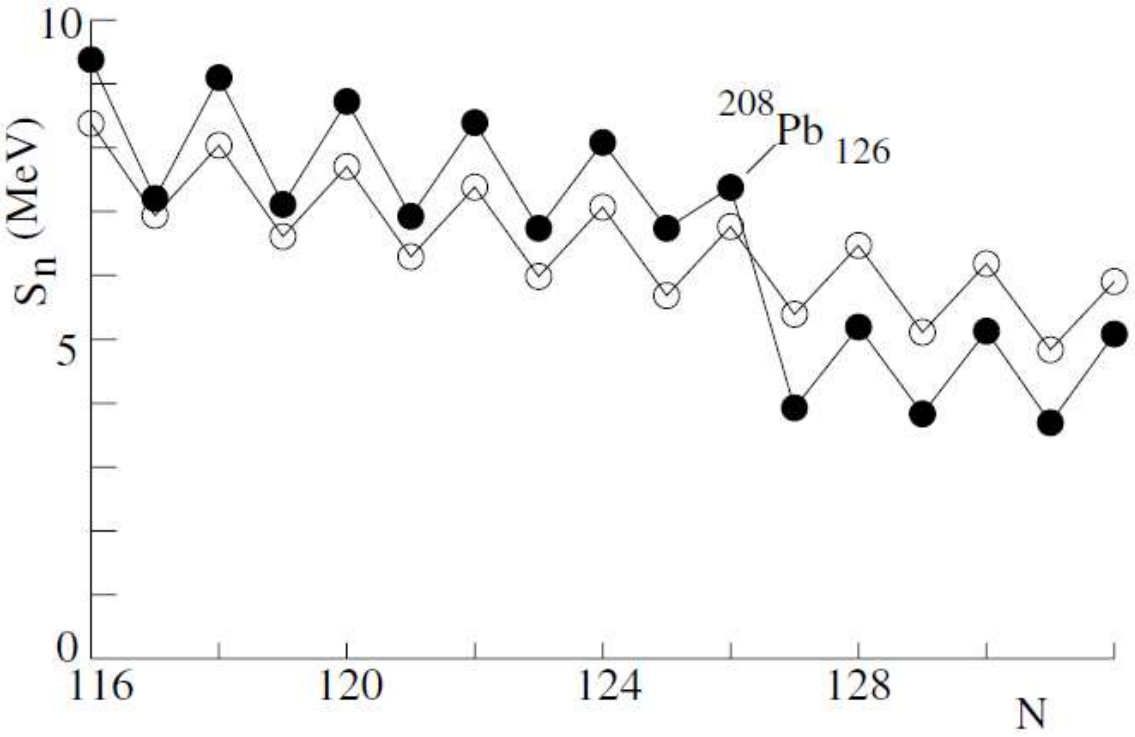

Fig 2.11 The neutron separation energy in lead isotopes as a function of N. The filled dots show the measured values and the open dots show the predictions of the Bethe–Weizs¨acker formula.

The discontinuity in the separation energies is due to the excess binding energy for magic nuclei as compared to that predicted by the semi-empirical Bethe–Weizs¨acker mass formula. One can see this in Fig. 2.12 which plots the excess binding energy as a function of N and Z. Large positive values of B/A(experimental)-B/A(theory) are observed in the vicinity of the magic numbers for neutrons N as well as for protons Z , Figure 2.13 shows the

difference as a function of N and Z in the vicinity of the magic numbers 28, 50, 82 and 126.

Just as the energy, necessary to liberate a neutron is especially large at magic numbers, the difference in energy between the nuclear ground state and the first excited state is especially large for these nuclei. Table 2.1 gives this energy as a function of N (even) for Hg (Z = 80), Pb (Z = 82) and Po (Z = 84). Only even–even nuclei are considered since these all have similar nucleon structures with the ground state having $J^P = 0^+$ and a first excited state generally having $J^P = 2^+$. The table shows a strong peak at the doubly magic ^{208}Pb. As discussed in Sect. 1.3, the large energy difference between rotations [38].

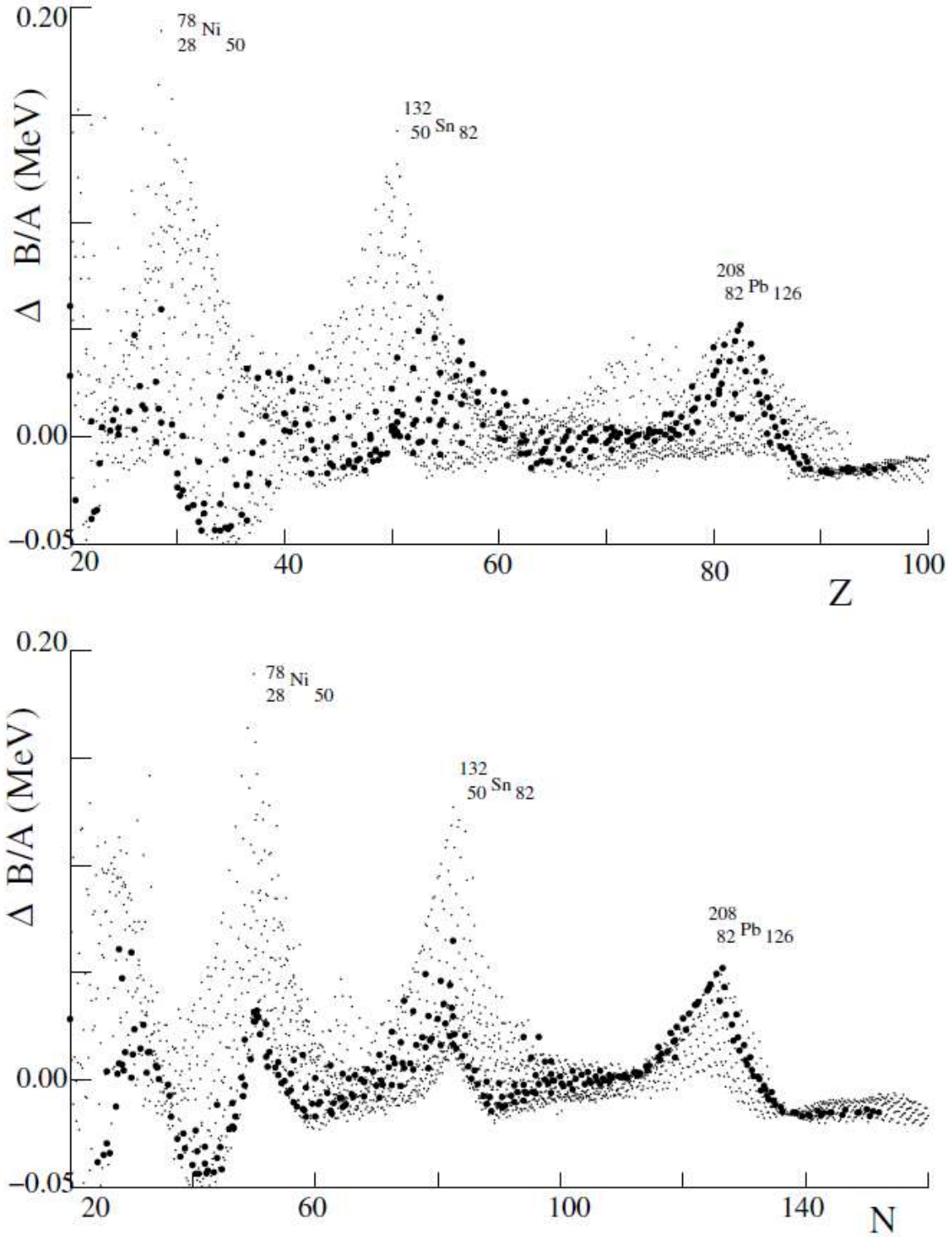

Fig. 2.12. Difference in MeV between the measured value of *B/A* and the value calculated with the empirical mass formula as a function of the number of protons *Z* (top) and of the number of neutrons *N* (bottom).
The large dots are for β-stable nuclei. One can see maxima for the magic numbers *Z*, *N* = 20, 28, 50, 82, and 126.

The largest excesses are for the doubly magic nuclides as indicated. **Fig.**

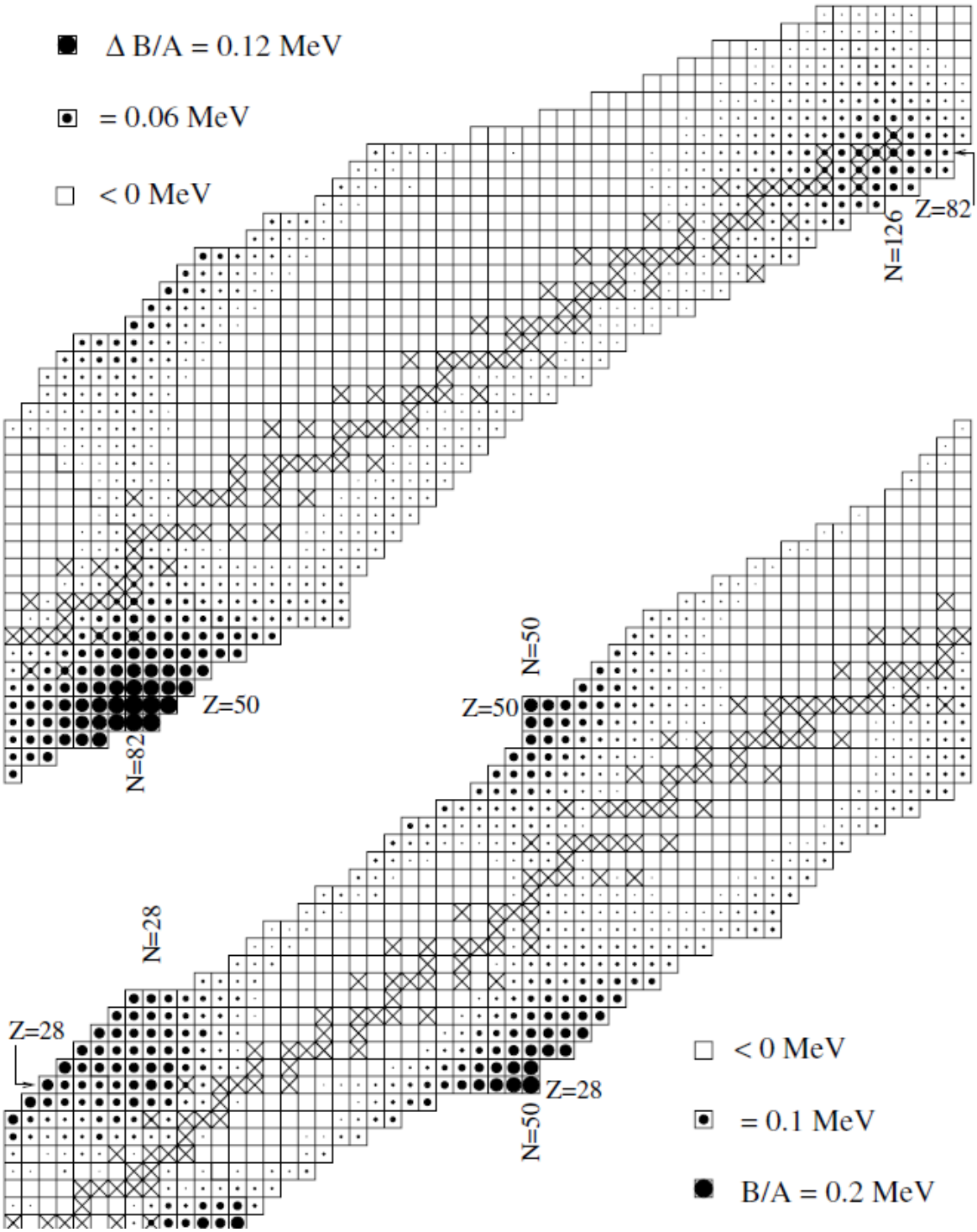

Fig. 2.13. Difference between the measured value of *B/A* and the value calculated with the mass formula as a function of *N* and *Z*. The size of the black dot increases with the difference.

One can see the hills corresponding to the values of the magic numbers 28, 50, 82 and 126. Crosses mark β-stable nuclei [38].

2.10.3 The Shell Model and the Spin-Orbit Interaction

It is possible to understand the nuclear shell structure within the framework of a modified mean field model. If we assume that the mean potential energy is harmonic, the energy levels are:

$En = (n + 3/2)\bar{}\,h\omega \quad n = n_x + n_y + n_z = 0, 1, 2, 3 \ldots ,$ (2.10.5)

where n_x,y,z are the quantum numbers for the three orthogonal directions and can take on positive semi-definite integers. If we fill up a harmonic well with nucleons, 2 can be placed in the one $n = 0$ orbital, i.e. the (n_x, n_y, n_z) = (0, 0, 0). We can place 6 in the $n = 1$ level because there are 3 orbitals, (1, 0, 0), (0, 1, 0) and (0, 0, 1). The number N (n) are listed in the third row of Table 2.2.

We note that the harmonic potential, like the Coulomb potential, has the peculiarity that the energies depend only on the principal quantum number n and not on the angular momentum quantum number l. The angular momentum states, $|n, l,m\_$ can be constructed by taking linear combinations of the $|n_x, n_y, n_z\_$ states . The allowed values of l for each n are shown in the second line of Table 2.2.

Table 2.10.1 The number N of nucleons per shell for a harmonic potential.

n	0	1	2	3	4	5	6
1	0	1	0,2	1,3	0,2,4	1,3,5	0,2,4,6
N(n)	2	6	12	20	30	42	56
∑N	2	8	20	40	70	112	168

(2.10.6)

The magic numbers corresponding to all shells filled below the maximum n would then be 2, 8, 20, 40, 70, 112 and 168. It might be expected that one could find another simple potential that would give the correct numbers. In general, one would find that energies would depend on two quantum numbers: the angular momentum quantum number [45]. l and a second giving the number of nodes of the radial wave function. An example of such a l-splitting is shown in Fig. 2.10. Unfortunately, it turns out that there is no simple potential that gives the correct magic numbers. The solution to this problem, found in 1949 by M. G¨oppert Mayer, and by D. Haxel J. Jensen and H. Suess, is to add a spin orbit interaction for each nucleon [1].

$\hat{H} = \mathrm{Vs} - \mathrm{o(r)}\hat{l}.\hat{s}/\hbar^2$ (2.10.7)

Without the spin-orbit term, the energy does not depend on whether the nucleon spin is aligned or anti-aligned with the orbital angular momentum. The spin orbit term breaks the degeneracy so that the energy now depends on three quantum numbers, the principal number n, the orbital angular momentum quantum number l and the total angular momentum quantum number j = l±1/2. We note that the expectation value of $\hat{l}.\hat{s}$ is given by:

$$\frac{\hat{l}.\hat{s}}{\hbar^2} = \frac{j(j+1)-l(l+1)-s(s+1)}{2} \qquad s = \frac{1}{2}$$
$$= \frac{l}{2} for j = l + \frac{1}{2}$$
$$= -\frac{l+1}{2} for\ j = l - \frac{1}{2} \qquad (2.10.8)$$

For a given value of n, the energy levels are then changed by an amount proportional to this function of j and l. For Vs−o < 0 the states with the spin aligned with the orbital angular momentum (j = l+1/2) have their energies lowered while the states with the spin anti-aligned (j = l − 1/2) have their energies raised.

The orbitals with this interaction included (with an appropriately chosen Vs−o) are shown in Fig. 2.10. The predicted magic numbers correspond to orbitals with a large gap separating them from the next highest orbital. For the lowest levels, the spin-orbit splitting (2.40) is sufficiently small that the original magic numbers, 2, 8, and 20, are retained. For the higher levels, the splitting becomes important and the gaps now appear at the numbers 28, 50, 82 and 126.. We note that this model predicts that the number 184 should be magic.

Besides predicting the correct magic numbers, the shell model also correctly predicts the spins and parities of many nuclear states. The ground states of even–even nuclei are expected to be 0+ because all nucleons are paired with a partner of opposite angular momentum. The ground states of odd–even nuclei should then take the quantum numbers of the one unpaired nucleon. For example, $^{17}{}_{9}F_8$ and $^{17}{}_{8}O_9$ have one unpaired nucleon outside a doubly magic $^{16}{}_{8}O_8$ core [1]. Figure 2.10 tells us that the unpaired nucleon is in a l = 2, j = 5/2. The spin parity of the nucleus is predicted to by 5/2+ since the parity of the orbital is −1l. This agrees with observation. The first excited states of $^{17}{}_{9}F_8$ and $^{17}{}_{8}O_9$, corresponding to raising the unpaired nucleon to the next higher orbital, are predicted to be 1/2+, once again in agreement with observation [39].

On the other hand, $^{15}{}_{8}N_7$ and $^{15}{}_{8}O_7$ have one "hole" in their ^{16}O core. The ground state quantum numbers should then be the quantum numbers of

the hole which are l = 1 and j = 1/2 according to Fig. 2.14. The quantum numbers of the ground state are then predicted to be 1/2−, in agreement with observation [38].

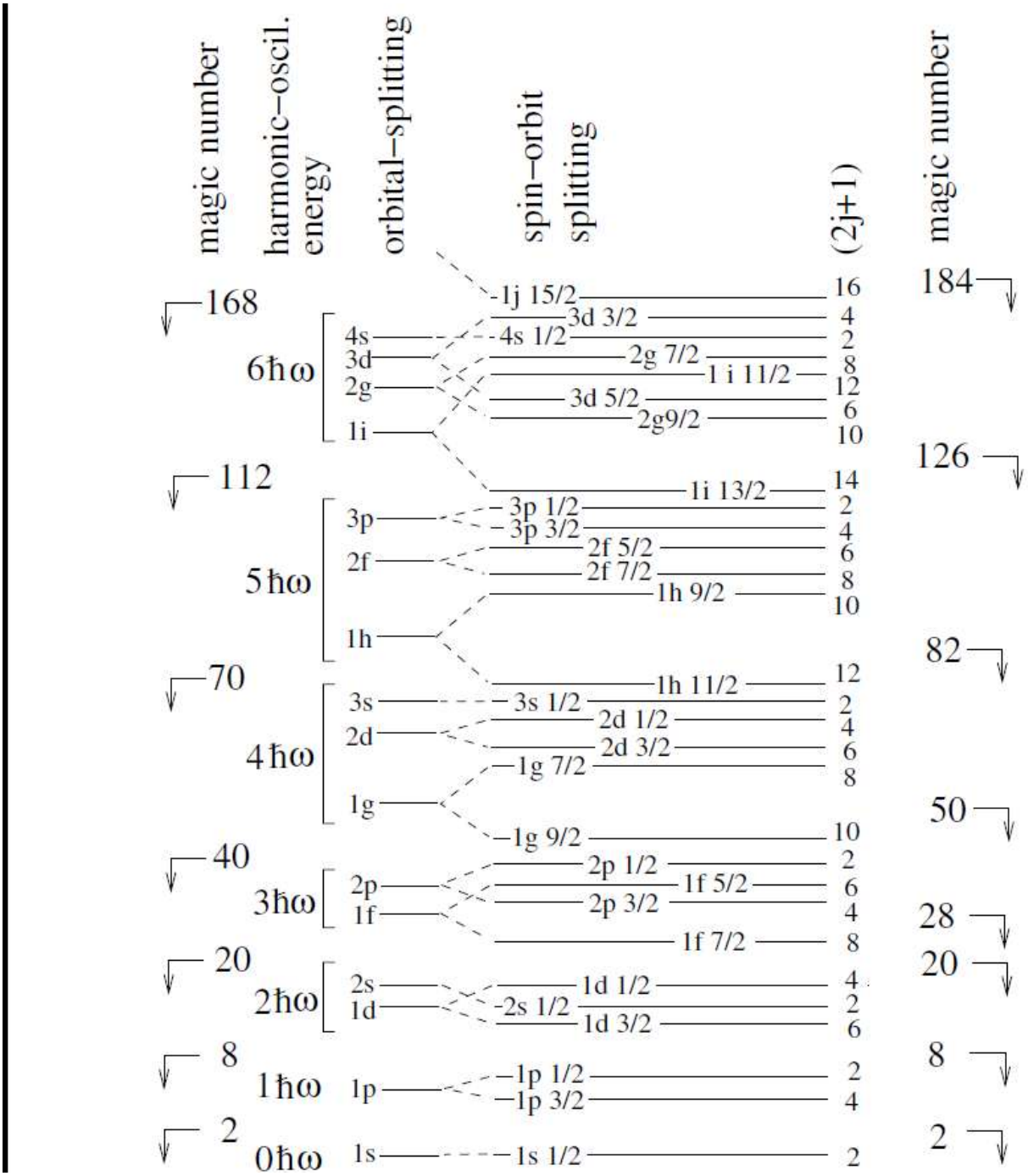

Fig. 2.14. Nucleon orbitals in a model with a spin-orbit interaction. The two leftmost columns show the magic numbers and energies for a pure harmonic potential. The splitting of different values of the orbital angular

momentum *l* can be arranged by modifying the central potential. Finally, the spin-orbit coupling splits the levels so that they depend on the relative orientation of the spin and orbital angular momentum. The number of nucleons per level $(2j + 1)$ and the resulting magic numbers are shown on the right.

The shell model also makes predictions for nuclear magnetic moments. As for the total angular momentum, the magnetic moments results from a combination of the spin and orbital angular momentum. However, in this case, the weighting is different because the gyromagnetic ratio of the spin differs from that of the orbital angular momentum.

Shell model calculations are important in many other aspects of nuclear physics, for example in the calculation of β-decay rates. The calculations are quite complicated and are beyond the scope of this book. Interested readers are referred to the advanced textbooks [38].

2.10.4 Some Consequences of Nuclear Shell Structure

Nuclear shell structure is reflected in many nuclear properties and in the Relative natural abundances of nuclei. This is especially true for doubly magic nuclei like 4He2, $^{16}O_8$ and $^{40}Ca_{20}$ all of which have especially large binding energies. The natural abundances of ^{40}Ca is 97% while that of $^{44}Ca_{24}$ is only 2% in spite of the fact that the semi-empirical mass formula predicts a greater binding energy for ^{44}Ca. The doubly magic ^{100}Sn50 is far from the stability line (^{100}Ru56) but has an exceptionally long half-life of 0.94 s. The same can be said for, $^{48}Ni_{20}$, the mirror of $^{48}Ca_{28}$ which is also doubly magic. $^{56}Ni_{28}$ is the final nucleus produced in stars before decaying to ^{56}Co and then ^{56}Fe. Finally, $^{208}{}_{82}Pb_{12}6$ is the only heavy double magic. It, along with its neighbors ^{206}Pb and ^{207}Pb,.

Nuclei with only one closed shell are called “semi-magic”:

- Isotopes of nickel, Z = 28;
- Isotopes of tin, Z = 50;
- Isotopes of lead, Z = 82;
- Isotones N = 28 (^{50}Ti, ^{51}V, ^{52}Cr,^{54}Fe , etc.)
- Isotones N = 50 (^{86}Kr, ^{87}Rb, ^{88}Sr, ^{89}Y, ^{9}0Zr, etc.)
- Isotones N = 82 (^{136}Xe, ^{13}8Ba, ^{139}La, ^{140}Ce, ^{141}Pr, etc.)

These nuclei have [1].

- a binding energy greater than that predicted by the semi-empirical mass formula,
- a large number of stable isotopes or isotones,
- a large natural abundances,
- a large energy separation from the first excited state,
- a small neutron capture cross-section (magic-N only).

The exceptionally large binding energy of doubly magic ^{4}He makes α decay the preferred mode of A non-conserving decays. Nuclei with 209 < A < 240 all cascade via a series of β and α decays to stable isotopes of lead and thallium. Even the light nuclei ^{5}He, ^{5}Li and ^{8}Be decay by α emission with lifetimes of order 10−16 s.

While ^{5}He rapidly α decays, ^{6}He has a relatively long lifetime of 806 ms. This nucleus α particle. This system has the peculiarity that while being stable, none of the two-body subsystems (n-n or n-α) are stable. Such systems are called "Borromean" after three brothers from the Borromeo family of Milan. The three brothers were very close and their coat-of-arms showed three rings configured so that breaking any one ring would separate the other two.

Shell structure is a necessary ingredient in the explanation of nuclear deformation. We note that the Bethe–Weizs¨acker mass formula predicts that nuclei should be spherical, since any deformation at constant volume increases the surface term. This can be quantified by a "deformation potential energy" as illustrated in Fig. 2.15. In the liquid-drop model, a local minimum is found at vanishing deformation corresponding to spherical nuclei. If the nucleus is unstable to spontaneous fission, the absolute minimum is at large deformation corresponding to two separated fission fragments.

Since the liquid-drop model predicts spherical nuclei, observed deformation must be due to nuclear shell structure. Deformations are then linked to how nucleons fill available orbitals. For instance, even–even nuclei have paired nucleons. If the nucleons tend to populate the high-m orbitals of the outer shell of angular momentum l, then the nucleus will be oblate. If they tend to populate low-m orbitals, the nucleus will be prolate. Which of [1].these cases occurs depends on the details of the complicated nuclear Hamiltonian. The most deformed nuclei are prolate. Because of these quantum effects, the deformation energy in Fig. 2.15 will have a local minimum at non-vanishing deformation for non-magic nuclei. It is also possible that a local minimum occurs for super-deformed configurations. These metastable configurations are seen in rotation band spectra.

We note that the shell model predicts and "island of stability" of super heavy nuclei near the magic number (A, N, Z) = (298, 184, 114) and (310, 90 2.184, 126). The lifetime are estimated to be as high as 106 yr making them of more than purely scientific interest.

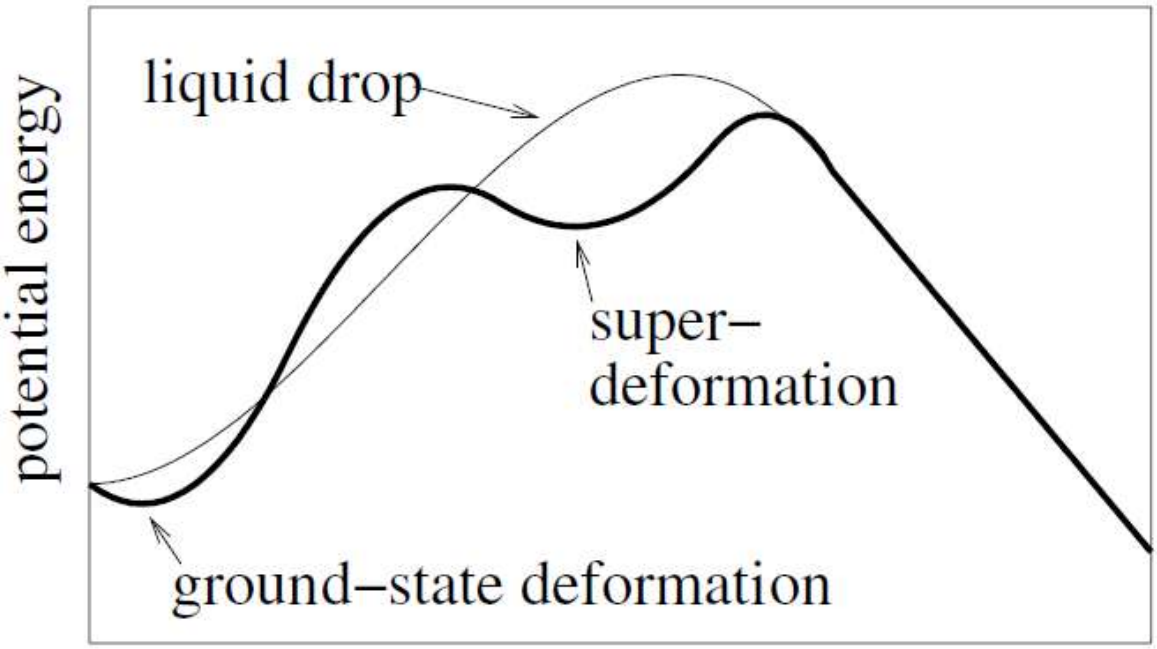

Fig. 2.15. Nuclear energies as a function of deformation. The liquid drop model predicts that the energy has a local minimum for vanishing deformation because this minimizes the surface energy term, in high-*Z* nuclei the energy eventually decreases for large deformations because of Coulomb repulsion, leading to spontaneous fission of the nucleus.) As explained in the text, the shell structure leads to a deformation of the ground state for nuclei with unfilled shells. Super-deformed local minima may also exist [38].

Finally, we mention that an active area or research concerns the study of magic number for neutron – rich nuclei far from the bottom of the stability valley. It is suspected that for such nuclides the shell structure modified .this effect is important for the calculation of the nucleosynthesis in the r-process [38].

2.11 Nuclear Magic Numbers

In nuclear physics, there is also evidence for magic numbers, i.e. Values of Z and N at which the nuclear binding is particularly strong. This can been seen from the B/A curves of Figure 2.14. Where at certain values of N and Z the data lie above the SEMF curve. This is also shown in Figure 2.10, where the inset shows the low-A region magnified. (The figure only shows results for even values of the mass number A.) The nuclear magic numbers was found from experiment to be [40].

N = 2; 8; 20; 28; 50; 82; 126

Z = 2; 8; 20; 28; 50; 82 (2.11.1)

and correspond to one or more closed shells, plus eight nucleons filling the s and p sub-shells of a nucleus with a particular value of n. Nuclei with both N and Z having one of these values are called doubly magic, and have even greater stability. An example is the helium nucleus, the α particle [40].

Shell structure is also suggested by a number of other phenomena. For example: 'magic' nuclei have many more stable isotopes than other nuclei; they have very small electric dipole moments, which means they are almost spherical, the most tightly bound shape; and neutron capture cross-sections show sharp drops compared with neighbouring nuclei. However, to proceed further we need to know something about the effective potential [38, 40].

A simple Coulomb potential is clearly not appropriate and we need some form that describes the effective potential of all the other nucleons. Since the strong nuclear force is short- ranged, we would expect the potential to follow the form of the density distribution of nucleons in the nucleus. For medium and heavy nuclei, we have seen that the Fermi distribution fits the data and the corresponding potential is called the Woods–Saxon form [40].

$$v_{central}(r) = \frac{-V_\circ}{1+e^{(r-R)/a}} \qquad (2.11.2)$$

However, although these potentials can be shown to offer an explanation for the lowest magic numbers, they do not work for the higher ones. This is true of all purely central potentials. The crucial step in understanding the origin of the magic numbers was taken in 1949 by Mayer and Jensen who suggested that by analogy with atomic physics there should also be a spin–orbit part, so that the total potential is

$$V_{total} = V_{central}(r) + Vls(r)L \,.\, S \qquad (2.11.3)$$

where L and S are the orbital and spin angular momentum operators for a single nucleon and $V_{ls}(r)$ is an arbitrary function of the radial coordinate.8 This form for the total potential is the same as that used in atomic physics except for the presence of the function $V_{ls}(r)$. Once we have coupling between L and S then m_L and m_s are no longer 'good' quantum numbers and we have to work with eigenstates of [40].The Total angular momentum vector J, defined by J = L + S. Squaring this, we have

$$J^2 = L^2 + S^2 + 2L.S \qquad (2.11.4)$$

$$L.S = \frac{1}{2}(J^2 - L^2 - S^2) \qquad (2.11.5)$$

Hence the expectation value of L. S, which we write as L_S, is

$$L_S = \frac{\hbar^2}{2}[j(j+1) - l(l+1) - s(s+1)] = \begin{Bmatrix} \frac{l}{2} for\ j = l + \frac{l}{2} \\ -\frac{(l+1)}{2} for j = -\frac{l}{2} \end{Bmatrix} \qquad (2.11.6)$$

(We are always dealing with a single nucleon, so that s ½) The splitting between the two levels is thus;

$$\Delta E_{LS} = \frac{2L+1}{2}\hbar^2(V_{LS}) \qquad (2.11.7)$$

Experimentally, it is found that V‘sr is negative, which means that the state wit j= $l + \frac{l}{2}$ has a lower energy than the state with j = $l - \frac{l}{2}$. This is the opposite of the situation in atoms. In addition, the splitting are substantial and increase linearly with ‘. Hence for higher L crossings between levels can occur. Namely, for large L the splitting of any two neighbouring degenerate levels can shift the j = l - $-\frac{l}{2}$ state of the initial lower level to lie above the j = $l + \frac{l}{2}$ level of the previously higher level.

An example of the resulting splittings up to the 1G state is shown in Figure 2.16, where the usual atomic spectroscopic notation has been used, i.e. levels are written n‘j with S, P, D, F, G, . . . : used for L= 0, 1, 2, 3, 4, ... Magic numbers occur when there are particularly large gaps between groups of levels. Note that there is no restriction on the values of ‘for a given n because, unlike in the atomic case, the strong nuclear potential is not Coulomb-like.

The configuration of a real nuclide (which of course has both neutrons and protons) describes the filling of its energy levels (sub-shells), for protons and for neutrons, where k is the occupancy of the given sub-shell. Sometimes, for brevity, the completely filled [40].

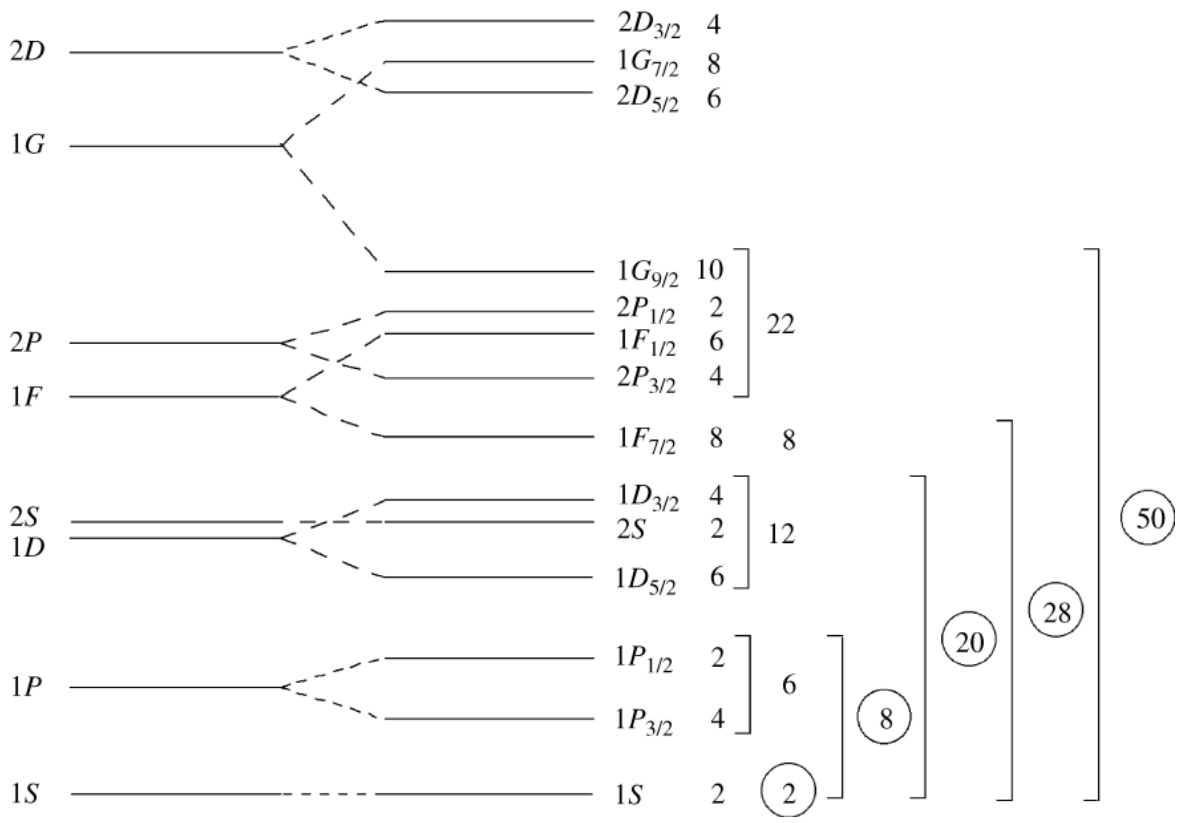

Figure 2.16 Low-lying energy levels in a single-particle shell model using a Woods—Saxon potential plus spin--orbit term.

circled integers correspond to nuclear magic numbers sub-shells are not listed, and if the highest sub-shell is nearly filled, k can be given as a negative number, indicating how far from being filled that sub-shell is. Using the ordering diagram above, and remembering that the maximum occupancy of each sub-shell is 2j + 1, we predict, for example, the configuration for $^{17}8_{O}$ to be:

$$\left(ls_{\frac{1}{2}}\right)^2\left(lp_{\frac{3}{2}}\right)^4\left(lp_{\frac{1}{2}}\right)^2 \; for\ the\ protons \qquad (2.11.8)$$

$$\left(ls_{\frac{1}{2}}\right)^2\left(lp_{\frac{3}{2}}\right)^4\left(lp_{\frac{1}{2}}\right)^2\left(ld_{\frac{5}{2}}\right)^1 \quad for\ the\ neutrons \qquad (2.11.9)$$

Notice that all the proton sub-shells are filled, and that all the neutrons are in filled sub-shells except for the last one, which is in a sub-shell on its own. Most of the ground state properties of $^{17}{}_{8}O$ can therefore be found from just stating the neutron configuration as $\left(ld_{\frac{5}{2}}\right)^1$ [3].

2.12 Spins, Parities and Magnetic Dipole Moments

The nuclear shell model can be used to make predictions about the spins of ground states.A filled sub-shell must have zero total angular momentum, because j is always an integer-plus-a-half, so the occupancy of the sub-shell, 2j+1, is always an even number. This means that in a filled sub-shell, for each nucleon of a given m_j=(j_z) there is another having the opposite m_j. Thus the pair have a combined m_j of zero and so the complete sub-shell will also have zero m_j. Since this is true whatever axis we choose for z, the total angular momentum must also be zero. Since magic number nuclides have closed sub-shells, such nuclides are predicted to have zero contribution to the nuclear spin from the neutrons or protons or both, whichever are magic numbers. Hence magic-Z/magic-N nuclei are predicted to have zero nuclear spin. This is indeed found to be the case experimentally[40].

In fact, it is found that all even-Z/even-N nuclei have zero nuclear spin. We can therefore make the hypothesis that for ground state nuclei, pairs of neutrons and pairs of protons in a given sub-shell always couple to give a combined angular momentum of zero, even when the sub-shell is not filled. This is called the pairing hypothesis. We can now see why it is the last proton and/or last neutron that determines the net nuclear spin, because these are the only ones that may not be paired up. In odd-A nuclides there is only one unpaired nucleon, so we can predict precisely what the nuclear spin will be by referring to the filling diagram. For even- A/odd-Z/odd-N nuclides, however, we will have both an unpaired proton and an unpaired neutron. We cannot then make a precise prediction about the net spin because of the vectorial way that angular momenta combine; all we can say is that the nuclear spin will lie in the range[$j_p - _{jn}$] to (j_p j_n).

Predictions can also be made about nuclear parities. First, recall the following properties of parity: (1) parity is the transformation r--r; (2) the wave function of a single-particle quantum state will contain an angular part proportional to the spherical harmonic Y^l_m (θ,ϕ)and under the parity transformation[3]: $pY_m^1(\theta,\phi) = (-)Y_m^l(\theta,\phi)$

a single-particle state will also have an intrinsic parity, which for nucleons is defined to be positive. Thus the parity of a single-particle nucleon state depends exclusively on the orbital angular momentum quantum number with $P = (-1)^L$ The total parity of a multi particle state is the product of the parities of the individual particles. A pair of nucleons with the same ‘will therefore always have a combined parity of 1. The pairing hypothesis then tells us that the total parity of a nucleus is found from the product of the parities of the last proton and the last neutron. Therefore, we can predict the parity of any nuclide, including the odd/odd ones, and these predictions are in agreement

with experiment. Unless the nuclear spin is zero, we expect nuclei to have magnetic (dipole) moments, since both the proton and the neutron have intrinsic magnetic moments, and the proton is electrically charged, so it can produce a magnetic moment when it has orbital motion. The shell [40] model can make predictions about these moments. Using a notation similar to that used in atomic physics, we can write the nuclear magnetic moment as:

$$\mu = g_j j \mu N$$

where μN is the nuclear magneton that was used in the discussion of hadron magnetic moments in Section 3.3.3, gj is the Lande´ g-factor and j is the nuclear spin quantum number. For brevity we can write simply _ μN nuclear magnetons. We will find that the shell model does not give very accurate predictions for magnetic moments, even for the even–odd nuclei where there is only a single unpaired nucleon in the ground state.We will therefore not consider at all the much more problematic case of the odd–odd nuclei having an unpaired proton and an unpaired neutron. For the even–odd nuclei, we would expect all the paired nucleons to contribute zero net magnetic moment, for the same reason that they do not contribute to the nuclear spin. Predicting the nuclear magnetic moment is then a matter of finding the correct way to combine the orbital and intrinsic components of magnetic moment of the single unpaired nucleon. We need to combine the spin component of the moment, $g_s s$, with the orbital component, $g_l l$ (where g_s and g_l are the g factors for spin and orbital angular momentum.) to give the total moment gj j. The general formula for doing this is:

$$g_j = \frac{j(j+1)+l(l+1)-s(s+1)}{2j(j+1)} g_l + \frac{j(j+1)-l(l+1)+s(s+1)}{2j(j+1)} g_s \qquad (2.12.1)$$

Which simplifies considerably because we always have $j = l \pm \frac{1}{2}$ Thus

$$Jg_j = g_l l + \frac{g_s}{2} for\ j = l + \frac{1}{2}$$

$$Jg_j = g_l J\left(1 + \frac{1}{2l+1}\right) - g_s J\left(\frac{1}{2l+1}\right) for\ j = l - \frac{1}{2} \qquad (2.12.2)$$

Since g_l = 1 for a proton and 0 for a neutron, and g_s is approximely +5.6 for the proton and -3.8 for the neutron, Equations (2.11.3) yield the results (where g proton(neutron) is the g-factor for nuclei with an odd proton(neutron))[40].

$$jg\ proton = l + \frac{1}{2} \times 5.6 = j + 2.3 for l - \frac{1}{2}$$

$$jg\ proton = j\left(1 + \frac{1}{2l+1}\right) - 5.6 \times j\left(\frac{1}{2l+1}\right) = j - \frac{2.3j}{j+1}\ for j = l - \frac{1}{2} \quad (2.12.3)$$

$$jg\ neutron = -\frac{1}{2} \times 3.8 = -1.9 for\ j = j = l + \frac{1}{2}$$

$$jg\ neutron = 3.8 \times j\left(\frac{1}{2l+1}\right) = \frac{1.9j}{j+1}\ for\ j = l - \frac{1}{2} \quad (2.12.4)$$

Accurate values of magnetic dipole moments are available for a wide range of nuclei and plots of a sample of measured values for a range of odd-Z and odd-N nuclei across [40].

Chapter Three

Equations of Quantum Mechanics

3.1 Introduction

This chapter is explain the equation of quantum mechanics, firstly with derivation Schrodinger equation, Klein-Gordon equation, and Dirac equation.

3.2 Schrodinger Equation

The Schrodinger equation is a linear particle differential, that describes the wave function or state function of quantum mechanical system, its useful key result in quantum in quantum mechanics, its fundamental equation , also Schrodinger equation describe the dynamics of a system of N particle . This description can be obtained from generalization of dynamics of single particle [46].

The Schrodinger Equation Has Two Form

One in which time explicitly appears, and so describes how wave function of particle will evolve in time. In general, the wave function behaves like a wave, and so the equation is often referred to as the time dependence [46].

3.2.1 Derivation Schrodinger Wave Equation

The other is the equation in which he time dependent has been removed and hence is known as the time independent Schrodinger equation and is found to describe. These are not separate, independent equation, the time independent equation can be derived readily from the time dependent equation [46, 47].

The time dependent Schrodinger equation wave equation of the discussion of the particle in an infinite potential well, it was observed the wave functions of a particle fixed energy E, the form of the wave function

$$\psi(r,t) = Ae^{i(kx-\omega t)} \qquad (3.2.1)$$

$$E = K_E + P_E$$

$$E = \frac{1}{2}mv^2 + V$$

The particle of momentum

$p = \hbar k$, $E = \hbar\omega$, $p = \frac{h}{2\pi}\left(\frac{2\pi}{\lambda}\right) = \hbar k$

$p = mv$, $E = \frac{1}{2}mv^2 = \frac{m^2v^2}{2m} = \frac{p^2}{2m}$

$E = \frac{1}{2}mv^2 + u = \frac{p^2}{2m} + u$

$E = \frac{p^2}{2m} + u$ (3.2.2)

$\psi = e^{i(kx-\omega t)}$ (3.2.3)

Differential equation

$\frac{\partial\psi}{\partial x} = -ike^{i(kx-\omega t)} = ik\psi$ (3.2.4)

$\frac{\partial^2\psi}{\partial x^2} = -k^2\psi$ (3.2.5)

Which can be written, using:

$E = \frac{p^2}{2m} = \frac{\hbar^2k^2}{2m}$

$\frac{-\hbar^2}{2m}\frac{\partial^2\psi}{\partial x^2} = \frac{p^2}{2m}\psi$ (3.2.6)

Similarly: $\frac{\partial\psi}{\partial t} = -i\omega\psi$ (3.2.7)

Which can be written using E= $\hbar\omega$

$i\hbar\frac{\partial\psi}{\partial t} = \hbar\omega\psi = E\psi$ (3.2.8)

We now generalize this to the situation in which there is both a kinetic energy and potential energy present, then

$E = \frac{p^2}{2m} + v(x)$, $so\ that$

$E\psi = \frac{p^2}{2m}\psi + v(x)\psi$ (3.2.9)

Where ψ is now the wave function particle moving in the presence of a potential v(x). If we assume that the result equation (3.2.6) and (3.2. 8) still apply in this case, then we have [47, 48].

$$-\frac{\hbar^2}{2m}\frac{\partial^2\psi}{\partial x^2}+v(x)\psi=i\hbar\frac{\partial\psi}{\partial t} \qquad (3.2.10)$$

Which is the famous time dependent Schrodinger wave equation, it is setting up and solving this equation. Even though this equation does not look like the familiar wave equation that describes, for instance, the harmonic wave function for a free particle of energy E and momentum[37,47].

$$\psi(x,t)=Ae^{-i(px-Et)/\hbar} \qquad (3.\ 2.11)$$

Is a solution of this equation with for particle, v(x) =0, when the wave express for the body in three domination, the equation of free body:

$$\psi=Ae^{(pr-Et)} \qquad (3.2.12)$$

$$pr=p_x x+p_y y+p_z z$$

The Schrodinger equation for general formula:

$$i\hbar\frac{\partial^{-2}\psi}{\partial t^2}=-\frac{\hbar^2}{2m}\nabla^2\psi+\mathrm{v}\psi \qquad (3.2.13)$$

$$H=i\hbar\frac{\partial\psi}{\partial t} \qquad (3.2.14)$$

H: Called Hamiltonian

The Time in Dependent Schrodinger Equation:

We have seen that the wave function looks like for a free particle of energy E, one or the other of the harmonic wave function. In both cases, the time dependent entered into the wave function via a complex exponential factor eEp[-iEt/ $\hbar$] a solution into the Schrodinger wave equation of the form[47]

$$\psi(x,t)=\psi(x)e^{-it/\hbar} \qquad (3.2.15)$$

1f we substitute this trail solution into Schrodinger wave equation, and make use of the meaning of particle derivation, one get

$$\frac{-\hbar^2}{2m}\frac{d^2\psi(x)}{dx^2}+v(x)\psi(x)=E\psi(x) \qquad (3.2.16)$$

If we rearrange the terms, we end up with

$$\frac{\hbar^2}{2m}\frac{d^2\psi(x)}{dx^2} + \big(E - V(x)\big)\psi(x) = 0 \qquad (3.2.17)$$

Which is the time independent Schrodinger equation, we note hear the quantity E. Which have identified as the energy of the particle is a free parameter in this equation [47].

3.3 The Klein –Gordon Equation

One can obtained in exactly the same way, being with relativistic energy momentum relation, the energy of particle [21, 48]:

$$E = \frac{p^2}{2m} + V \qquad (3.3.1)$$

Applying the quantum prescription:

$$p = \frac{\hbar}{i}\nabla \ , \ E = i\hbar\frac{\partial}{\partial t} \qquad (3.3.2)$$

And letting the resulting operator act on the wave function ψ

$$E = i\hbar\frac{\partial\psi}{\partial t} \ , \ \nabla^2\psi = \frac{\partial\psi^2}{\partial x^2} = \frac{p^2}{\hbar^2}\psi \qquad (3.3.3)$$

$$\psi = Ae^{\frac{i}{\hbar}(pr-Et)} \qquad (3.3.4)$$

$$\frac{-\hbar^2}{2m}\nabla^2\psi = \frac{p^2}{2m}\psi$$

Substitute (3.3.1) at ψ on (3.3.3) we obtained:

$$E\psi = \frac{P^2}{2m}\psi = V\psi$$

$$i\hbar\frac{\partial\psi}{\partial t} = \frac{\hbar^2\nabla^2}{2m}\psi + V\psi \qquad (3.3.5)$$

$$\frac{-\hbar^2\nabla^2}{2m}\psi + V\psi = i\hbar\frac{\partial\psi}{\partial t} \qquad (3.3.6)$$

The equation is Schrodinger equation, the Klein-Gordon had given by

$$E^2 - P^2C^2 = m_\circ^2c^4\theta_r$$

$$E = \sqrt{C^2P^2 + m_\circ^2c^4} \qquad (3.3.7)$$

E=Energy of particle p=momentum, m_0=electron mass constant

$$p^\mu p_\mu - m^2c^2 = 0 \qquad (3.3.8)$$

One leave out the potential energy, we will stick to free particle surprisingly, and the quantum prescription requires no relativistic modification in four – vector notion .it reads [49].

$$p_\mu = i\hbar\partial_\mu \qquad (3.3.9)$$

$$\partial_\mu = \frac{\partial}{\partial x}\mu \qquad (3.3.10)$$

$$\partial_\circ = \frac{1}{c}\frac{\partial}{\partial t}, \quad \partial_1 = \frac{\partial}{\partial x}, \ \partial_2 = \frac{\partial}{\partial y}, \partial_3 = \frac{\partial}{\partial z} \qquad (3.3.11)$$

Putting equation (3.3.7) into equation (3.3.8) and letting the derivation Acton a wave functionψ, we obtain:

$$-\hbar^2\partial^\mu\partial_\mu\psi - m^2c^2\psi = 0 \qquad (3.3.12)$$

$$\text{Or } -\frac{1}{c^2}\frac{\partial^2\psi}{\partial t^2} + \nabla^2\psi = \left(\frac{mc}{\hbar}\right)^2\psi \qquad (3.3.13)$$

The equation (3.3.13) is Klein –Gordon equation free particle, and find electromagnetic field, the equation become:

$$(E - e\phi^2) = (CP - eA)^2 + m_o^2c^4 \qquad (3.3.14)$$

This equation equivalence the classical equation:

$$H = \frac{1}{2m}\left(p - \frac{e}{c}A\right)^2 + e\phi \qquad (3.3.15)$$

A=magnetic field, ϕ ≡normal electric field

$$E = i\frac{d}{c}\frac{A}{dt} - \overline{\nabla}\emptyset \ , \ H = \overline{\nabla} \times A$$

Multiply equation (3.3.14) at ψ we obtained:

$$(E - e\phi^2)\psi = (CP - eA)^2\psi + m_o^2c^4\psi \qquad (3.3.15)$$

Let:

$$E = \frac{-\hbar\partial}{i\partial t} \ and \ p = \frac{\hbar\overline{\nabla}}{i} \qquad (3.3.16)$$

Let equation (3.3.16) in equation (3.3.15) we 0btained the general Klein-Gordon equation [49].

$$\left[\left(i\hbar\frac{\partial}{\partial t} - e\phi\right)^2 - c^2\left(\frac{\hbar}{i}\nabla - \frac{e}{c}A\right)^2 - m_o^2c^4\right]\psi = 0$$

$$-\hbar^2\frac{\partial^2}{\partial t^2} - 2ie\phi\frac{\partial}{\partial t} - ie\hbar\frac{\partial\phi}{\partial t} + e^2\phi^2)\psi$$

$$(-\hbar^2c^2\nabla^2 + 2ie\hbar cA.\nabla + ie\hbar c\overline{\nabla}.A + e^2A^2 + m_o^2c^4)\psi \quad (3.3.17)$$

3.4 The Dirac Equation

Perpetration itself flawed in relativistic quantum theory, and restored the Klein –Gordon equation to its rightful place, while keeping the Dirac equation for particle of spine ½.

Dirac's basic strategy was to factor the energy, momentum relation, this would be easy if we had only p^0 (that is powered zero), the relativistic energy equation [50].

$$E = \sqrt{c^2p^2 + m_o^2c^4} \quad (3.4.1)$$

$$(p^o)^2 - m^2c^2 = (p^o + mc)(p^o - mc) = 0 \quad (3.4.2)$$

When then obtain two first order equation:

$$(p^o + mc) = 0\,, or \quad (p^o - mc) = 0 \quad (3.4.3)$$

Either one of which guarantees that;

$p^\mu p_\mu - m^2c^2 = 0$, but it is a different matter when the other three components of p^μ are included, in that case we are looking for something of the form [48, 51].

$$(p^\mu p_\mu - m^2c^2) = (B^kP_k + mc)(\gamma^\lambda p_\lambda - mc) \quad (3.4.4)$$

Where $B^k and \gamma^\lambda$ eight coefficients to be determined, multiplying out the right –hand side, we have:

$$B^k\gamma^\lambda P_k p_\lambda - mc(B^k - \gamma^k)P_k - m^2c^2$$

We don't want any terms linear in P_k, so we must choose $(B^k = \gamma^k)$ to finish the job, we need to find coefficient γ^k such that;

$$(p^\mu p_\mu = \gamma^k\gamma^\lambda P_k p_\lambda$$

Which is to say:

$$(p^o)^2 - (p^1)^2 - (p^2)^2 - (p^3)^2 = (\gamma^o)^2(p^o)^2 + (\gamma^1)^2(p^1)^2 +$$
$$(\gamma^2)^2(p^2)^2 + (\gamma^3)^2(p^3)^2 + (\gamma^o\gamma^1 + \gamma^1\gamma^o)p_op_1 + (\gamma^o\gamma^2 + \gamma^2\gamma^o)p_op_2 +$$

$(\gamma^o\gamma^3 + \gamma^3\gamma^o)p_o p_3 + (\gamma^1\gamma^2 + \gamma^2\gamma^1)p_1 p_2 + (\gamma^1\gamma^3 + \gamma^3\gamma^1)p_1 p_3 + (\gamma^2\gamma^3 + \gamma^3\gamma^2)p_2 p_3$

(3.4.5)

We could pick $\gamma^o = 1\ and\ \gamma^1 = \gamma^2 = \gamma^3 = i$ we just might be able to find a set such that [48]:

$$(\gamma^o)^2 = 1, (\gamma^1)^2 = (\gamma^2)^2 = (\gamma^3)^2 = -1$$

$\gamma^\mu\gamma^\nu + \gamma^\nu\gamma^\mu = 0\ , for\ \mu \neq \nu$ (3.4.6)

Or more succinctly:

$\{\ \gamma^\mu\gamma^\nu\} = 2g^{\mu\nu}$ (3.4.7)

Write equation (3.4.4) out (long hand).

$$(p^o)^2 - (p^1)^2 - (p^2)^2 - (p^3)^2 - m^2c^2 = (B^oP^o - B^1P^1 - B^2P^2 - B^3P^3 + mc)(\gamma^o p^o - \gamma^1 p^1 - \gamma^2 p^2 - \gamma^3 p^3 - mc)$$

Where $g^{\mu\nu}$ is the Minkowski metric?

{A, B}= AB+BA (3.4.8)

We will used the standard "Bjor-Ken and Drell" convention:

$\gamma^o \begin{pmatrix} 1 & 0 \\ 0 & -1 \end{pmatrix}, \begin{pmatrix} 0 & \sigma i \\ -\sigma i & 0 \end{pmatrix}$ (3.4.9)

Where $\sigma i (i = 1,2,3)$.

The relativistic energy momentum relation does factor:

$(p^\mu p_\mu - m^2c^2) = (\gamma^k p_k + mc)(\gamma^\lambda p_\lambda - mc) = 0$ (3.4.10)

We obtain the Dirac equation, now by peeling of one term (it does not really matter which one but this is conventional choice.

$\gamma^\mu p_\mu - mc = 0$ (3.4.11)

$p_\mu \rightarrow i\hbar\partial_{\mu,}$ And let the result act on the wave function ψ

$i\hbar\gamma^\mu\partial_\mu\psi - mc\psi = 0$ (3.4.12)

Dirac Equation

$$\sigma_x = \begin{pmatrix} 0 & 1 \\ 1 & 0 \end{pmatrix} \sigma_y = \begin{pmatrix} 0 & -i \\ i & 0 \end{pmatrix} \sigma_2 = \begin{pmatrix} 1 & 0 \\ 0 & 1 \end{pmatrix}$$

$$\alpha_2 \begin{pmatrix} 0 & \sigma_x \\ \alpha_x & 0 \end{pmatrix} \alpha_y = \begin{pmatrix} 1 & \sigma_y \\ \sigma_y & -1 \end{pmatrix}$$

$$\alpha_{3\begin{pmatrix} 0 & \sigma_x \\ \alpha_z & 0 \end{pmatrix}\beta_y} = \begin{pmatrix} 1 & 0 \\ 0 & -1 \end{pmatrix} \quad (3.4.13)$$

$$i = \begin{pmatrix} 1 & 0 \\ 0 & 1 \end{pmatrix}$$

$$a_x = \begin{pmatrix} 0001 \\ 0010 \\ 0100 \\ 1000 \end{pmatrix} a_z = \begin{pmatrix} 000-i \\ 00i0 \\ 0-i00 \\ i000 \end{pmatrix}$$

$$a_z = \begin{pmatrix} 0010 \\ 000-1 \\ 1000 \\ 0-i00 \end{pmatrix}, B = \begin{pmatrix} 1000 \\ 0100 \\ 00-10 \\ 000-1 \end{pmatrix} \quad (3.4.14)$$

Note: Dirac function that is now a four-element column Matrix:

$$\psi = \begin{pmatrix} \psi 1 \\ \psi 2 \\ \psi 3 \\ \psi 4 \end{pmatrix} \quad (3.4.15)$$

$$E\psi = C\alpha + P\psi + Bm_o c^2 \psi$$

Substitute: $i\hbar \frac{\partial \psi}{\partial t} = E\psi, \frac{\hbar}{i} \nabla \psi = p\psi$

Equation:

$$\psi = Ae^{\frac{i}{\hbar}(px - Bu)}$$

$$\nabla^2 \psi = \frac{\partial^2 \psi}{\partial x^2} = \frac{p^2}{\hbar^2} \psi$$

We find the Dirac equation time:

$$i\hbar \frac{\partial \psi}{\partial t} = c_\alpha \frac{h}{i} \nabla \psi + m_o c^2 \psi = \frac{ch}{i} \alpha . \nabla + m_o c^2 \psi \quad (3.4.16)$$

$\psi i \equiv spinors$

We find the Dirac equation UN dependent time of form [43]

$$[a.p = \frac{q}{c}A] + \mathrm{q}\emptyset + \mathrm{Bm}c^2]\psi(r) = g_i\psi_i(r) \qquad (3.4.17)$$

$$\psi = e^{-i-\frac{6ji}{\hbar}}\psi_i(r)$$

3.5 Equation of Spherically Symmetric Potential

For Spherically Symmetric Potential Schrodinger equation gives [17]

$$\ddot{u} - \frac{2m}{\hbar^2}ru + k^2u = \frac{2mc}{\hbar^2}\frac{u}{r} \qquad (3.5.1)$$

$$\ddot{u} - \frac{2m}{\hbar^2}kr^2u + k^2u = \frac{c_1}{r^2}u \qquad (3.5.2)$$

Where u stand for the radial part of wave function, while

$$k^2 = \frac{2mE}{\hbar^2}$$

$$c_2 = \frac{m}{\hbar^2}k, \qquad c_1 = \frac{2m\hbar^2 l(l+1)}{\hbar^2(2m)} \qquad (3.5.3)$$

Re arranging (3.5.2) yields

$$\ddot{u} - c_2r^2u + k^2u - \frac{c_1}{r^2}u = 0 \qquad (3.5.4)$$

One can redefine the variables such that to get

$$y = \propto r \quad , \qquad dr = \frac{1}{\propto}dy$$

$$u^{"} = \frac{d^2u}{dy^2} = \frac{1}{\propto^2}\frac{d^2u}{dr^2} = \frac{1}{\propto^2}\ddot{u}$$

There fore

$$\ddot{u} = \propto^2 u^{"} \qquad (3.5.5)$$

In view of equation (3.5.4) one gets

$$\propto^2 u^{"} - c_2r^2u + k^2u - \frac{c_1}{r^2}u = 0$$

$$\propto^2 u^{"} - \frac{c_2y^2}{\alpha^2}u + k^2u - \frac{c_1\alpha^2}{y^2}u = 0$$

Hence

$$u^{"} - \frac{c_2}{\alpha^4} y^2 u + \frac{k^2}{\alpha^2} u - \frac{c_1}{y^2} u = 0 \qquad (3.5.6)$$

With

$$\propto^4 = c_2 \ , \quad \lambda = \frac{k^2}{\alpha^2} \qquad \lambda = \frac{2mE}{\hbar^2 \alpha} \qquad (3.5.7)$$

Therefore, equation (3.5.6) reduces to

$$u^{"} + (\lambda - y^2)u - \frac{c_1}{y^2} u = 0 \qquad (3.5.8)$$

To solve this equation assume

$$u = He^{-\frac{1}{2}y^2}$$

$$u^{"} = \left(H^{"} - 2yH^{/} + y^2 H - H\right)e^{-\frac{1}{2}y^2} \qquad (3.5.9)$$

Sub (3.5.9) in (3.5.8) to get

$$H^{"} - 2yH^{/} + y^2 H - H + \lambda H - y^2 H - \frac{c_1}{y^2} H = 0$$

$$H^{"} - 2yH^{/} + (\lambda - 1)H - \frac{c_1}{y^2} H = 0$$

The function H can be defined to be

$$H = \sum a_s \, y^s \ , \ H^{/} = \sum S a_s y^{s-1}$$

$$H^{"} = \sum s(s-1) a_s \, y^{s-2}$$

$$\sum_s s(s-1) a_s \, y^{s-1} - 2 \sum s a_s \, y^s + (\lambda - 1) \sum a_s \, y^s - c_1 \sum_s a_s y^{s-2} = 0 \qquad (3.5.10)$$

In first and last term let

$$s \to s + 2$$

$$\sum (s+2)(s+1) a_{s+2} y^s \sum_s [\lambda - 1 - 2s] a_s y^s - c_1 \sum a_{s+2} y^s = 0 \qquad (3.5.11)$$

Equating ea e ff of y^s

$$[(s+2)(s+1) - c_1] a_{s+2} = [2s + 1 - \lambda] a_s$$

$$a_{s+2} = \frac{[2s+1-\lambda] a_s}{(s+1)(s+2) - c_1}$$

Since the last term is a_n , thus

$a_n \neq 0 \quad , \; a_n + 1 = 0 \quad , \; a_{n+2} = 0$

Therefore

$0 = a_{n+2} = \frac{[2n+1-\lambda]a_n}{(n+1)(n+2)-c_1}$

$2n + 1 - \lambda = 0 \qquad , \qquad \lambda = 2n + 1$

In view of equation (3.5.7) and (3.5.3)

$\lambda = \frac{k^2}{\propto^2} =$

$\propto^2 = \sqrt{c_2} = \sqrt{\frac{m^2\omega^2}{\hbar^2}} = \frac{m\omega}{\hbar}$

$k^2 = \frac{2mE}{\hbar^2}$

$\lambda = \frac{2mE\hbar}{\hbar^2(m\omega)} = \frac{2E}{\hbar\omega} = 2n + 1 = \lambda$ (3.5.12)

Thus, the energy have given by

$E = \frac{1}{2}\hbar\omega(2n + 1) = \hbar\omega\left(n + \frac{1}{2}\right)$ (3.5.13)

The total angular momentum have given by

$j = l + s \, , \; j^2 = l^2 + s^2 + 2l.s$

$\frac{\hbar\omega}{2}(2n + 1) = \frac{\hbar\omega}{2}(2n - 1) + \hbar\omega$

$= \frac{\hbar\omega}{2}[N + 2\hbar\omega]$ (3.5.14)

Also

$cos\theta = \frac{l.s}{l_s}$

$\hbar l[(l + 1)]^{\frac{1}{2}} = \hbar l(1 + \frac{1}{l})^{\frac{1}{2}} = \hbar l\left(1 + \frac{1}{2}l\right) \; = \hbar l$ (3.5.15)

The orbital angular momentum Eigen equation satisfies

$L^2Y = ay \qquad a = \hbar^2 l(l + 1)$ (3.5.16)

The spins and angular momentum L multiplication gives

S.L = $\frac{1}{2}\hbar\sqrt{l(l+1)} = \frac{1}{2}\hbar l$

$$S.Lcos\theta = \frac{1}{2}\hbar l(l+1)cos\theta \qquad (3.5.17)$$

3. 6 Generalized Special Relativistic Quantum Equation

The GSR energy is given by

$$E = \frac{m_\circ c^2}{\sqrt{g_{\circ\circ} - \frac{v^2}{c^2}}} = \frac{m_\circ c^2}{\sqrt{\frac{g_{\circ\circ}m^2c^4 - m^2v^2c^2}{m^2c^4}}} \qquad (3.6.1)$$

Thus

$$E = \frac{m_\circ c^2 E}{\sqrt{g_{\circ\circ}E^2 - c^2p^2}} \qquad (3.6.2)$$

Since the time component of the matric is given by

$$g_{\circ\circ} = \left(1 - \frac{2\emptyset}{c^2}\right) \qquad (3.6.3)$$

Where $\emptyset$ is potential per unit mass, it follows that

$$g_{\circ\circ}E^2 - c^2p^2 = m_\circ^2c^4$$

$$\left(1 - \frac{2\emptyset}{c^2}\right)E^2 = c^2p^2 + m_\circ^2c^4$$

$$\left(1 - \frac{2m\emptyset}{mc^2}\right)E^2 = c^2p^2 + m_\circ^2c^4$$

$$\left(1 - \frac{2V}{E}\right)E^2 = c^2p^2 + m_\circ^2c^4$$

Hence

$$E^2 - 2VE = c^2p^2 + m_\circ^2c^4$$

$$E^2\psi - 2VE = c^2p^2\psi + m_\circ^2c^4\psi \qquad (3.6.4)$$

The quantum equation can be obtained by suggesting the wave function to be

$$\psi = Ae^{\frac{i}{\hbar}(px - Et)}$$

Differentiating w.r.t time gives

$$i\hbar\frac{\partial\psi}{\partial t} = E\psi - \hbar^2\frac{\partial^2\varphi}{\partial t^2} = E^{2\psi}$$

In addition, w.r.t coordinate gives

$$\frac{\hbar}{i}\nabla\psi = p\psi,\ -\hbar^2\nabla^2\psi = p^2\psi$$

Inserting in (4.5.20) gives

$$-\hbar^2\frac{\partial^2\psi}{\partial t^2} - 2iV\hbar\frac{\partial\psi}{\partial t} = -c^2\hbar^2\nabla^2\psi + m_\circ^2c^4\psi \qquad (3.6.5)$$

Splitting the time and coordinate parts gives

$$\psi = e^{\frac{-i}{\hbar}Et}u(r), \qquad \frac{\partial\psi}{\partial t} = -\frac{i}{\hbar}Eue\ , \qquad \frac{\partial^2\psi}{\partial t^2} = -\frac{1}{\hbar^2}E^2ue^{\frac{-i}{\hbar}Et}$$

Inserting again in (3.6.4) gives

$$(E^2u + 2EVu)e^{\frac{-i}{\hbar}Et} = (-c^2\hbar^2\nabla^2u + m_\circ^2c^4u)e^{-\frac{i}{\hbar}Et}$$

$$c^2\hbar^2\nabla^2u + E^2u + 2EVu - m_\circ^2c^4u = 0$$

Rearranging yields

$$\frac{c^2\hbar^2}{E}\nabla^2u + Eu - 2Vu - \frac{m_\circ^2c^4}{E}u = 0$$

For large rest mass

$$E = mc^2 \approx m_\circ c^2$$

Thus, one gets

$$\frac{\hbar^2}{m_\circ}\nabla^2u + Eu - 2Vu - m_\circ c^2u = 0$$

$$\nabla^2u + \frac{E^2}{c^2\hbar^2}u - \frac{2EV}{c^2\hbar^2}u - \frac{m_\circ^2c^4}{c^2\hbar^2}u = 0 \qquad (3.6.6)$$

In spherical coordinate. This equation can be written using (3.5.4) to be

$$\ddot{u} + K^2u - c_2r^2u - \frac{c_1}{r^2}u = 0$$

Where

$$K^2 = \frac{\left(E^2 - m_\circ^2c^4\right)}{c^2\hbar^2}\ , \quad c_2 = \frac{2EK}{2c^2\hbar^2}\ , \quad c_1 = \frac{l(l+1)E}{c^2\hbar^2}$$

And

$y = \alpha r\ ,\ \alpha^4 = c_2\ ,\ \lambda = \frac{K^2}{\alpha^2}$

$\alpha^4 = c_2 = \frac{Em\omega^2}{c^2\hbar^2} = \frac{m^2c^2\omega^2}{c^2\hbar^2} = \frac{m^2\omega^2}{\hbar^2}$

$\alpha^2 = \frac{m\omega}{\hbar}$,

Also

$\lambda = \frac{K^2}{\alpha^2} = \frac{E^2}{c^2\hbar^2}\left(\frac{h}{m\omega}\right) = \frac{E^2}{mc^2(\hbar\omega)} = \frac{E^2}{E(\hbar\omega)}$ (3.6.7)

If one neglect $m_\circ$, it follows that

$m_\circ$: $m_\circ \approx 0$, $\lambda = \frac{E}{\hbar\omega}$, $\lambda = 2n + 1$

$E = (2n + 1)\hbar\omega$

However $m_{\circ \neq 0}$, one gets

$\lambda = \frac{E^2}{c^2\hbar^2}\left(\frac{h}{m\omega}\right) - \frac{m_\circ^2c^4(h)}{c^2\hbar^2m\omega} = \frac{E}{\hbar\omega} - \frac{m_\circ^2c^4}{\hbar\omega(mc^2)} = \frac{E}{\hbar\omega} - \frac{m_\circ^2c^4}{\hbar\omega E}$

$E^2 - m_\circ^2c^4 = (2n + 1)\hbar\omega E$

$E^2 = (2n + 1)\hbar\omega E + m_\circ^2c^4 = (2n + 1)$ (3.6.8)

The magnetic moment of atom μ can be used to find the nuclear magnetic flux density B, which interacts with proton and neutron magnetic moment, in terms of well-known parameters to be

$\mu = iA = i(\pi r^2) = \frac{-e}{2m}l$

A is the orbital area, r is the radius. The current i is given by

$i = \frac{\mu}{\pi r^2}$

$B = \frac{\mu_\circ i}{2r} = \frac{\mu_\circ \mu}{2\pi r^3} = \frac{-\mu_\circ e}{4\pi m r^3}l$ (3.6.9)

The interaction potential between nucleon spin and nuclear magnetic field is given by

$V_m = -\mu_s.Bcos\theta = -\frac{e}{m}S.Bcos\theta$

Thus

$$V_m = \frac{\mu_\circ e^2}{4\pi m r^3} s.l\ cos\theta$$

$$V_m = \frac{\mu_\circ e^2 \hbar^2}{4\pi m r^3}(m_s)\sqrt{l(l+1)cos\theta} = c_\circ(m_s)\sqrt{l(l+1)}\ cos\theta \quad (3.6.10)$$

Numerically

$\mu_\circ = 4\pi \times 10^{-7}$ hen. m^{-1} $\hbar = 6 \times 10^{-34}$ $e = 1.6 \times 10^{-19}$

$m = 9.1 \times 10^{-14}$ $r = 3 \times 10^{-34}$ $\mu_\circ \sim 4\pi$ $\times 10^{-7}\hbar$ $e \sim 10^{-19}$

$m \sim 10^{-31}$ $r \sim 10^{-14}$

$$c_\circ = \frac{10^{-7}\times 10^{-38}\times 10^{-19}}{10^{-31}\times 10^{-42}} h = 10^{-26} \times 10^{-38} \times 10^{31} \times 10^{42} h$$

$$= 10^9 h$$

Thus:

$$V_m = 10^9 h(m_s)\sqrt{l(l+1)}cos\theta = \pm\frac{1}{2} \times 10^9 h\sqrt{l(l+1)}cos\theta$$

$$V_m = \pm\frac{1}{2} \times 10^9 h\sqrt{l(l+1)}cos\theta$$

If n_s is integer such that:

$n_s = 0, \pm 1, \pm 3, \pm 4$ ... ...

Thus, θ can adjust itself, such that:

$cos\theta = \frac{2n_s}{10^9\hbar\sqrt{l(l+1)}}$ To get:

$V_m = \pm n_s$

The Hamiltonian of nuclear spin magnetic interaction is given by:

$\widehat{H} = \widehat{H_\circ} + \widehat{V_m}$

Where the time independent equation become

$\widehat{H}\psi = E\psi$ (3.6.11)

The wave function is given by

$\psi = R(r)y(\theta, \theta)$ (3.6.12)

Hence

$$\widehat{H_\circ}Ry = y\widehat{H_\circ}R = E_\circ yR$$

$$\widehat{V_m}Ry = R\widehat{V_m}\, y = V_m yR$$

Thus:

$$\widehat{H}\psi = \left(\widehat{H_\circ} + \widehat{V_m}\right)Ry = \left(\widehat{H_\circ}R\right)y + R(\widehat{V_m}\, y)$$

$$= E_\circ Ry + V_\circ Ry \; = (E_\circ + V_m)Ry$$

$$\widehat{H}\psi = (E_\circ + V_m)\psi \qquad (3.6.13)$$

Chapter Four

Literature Review

4.1 Introduction

Different attempts was made to explain the nuclear models and the magic number.

4.2 Determination of Nuclear Potential Radii and Its Parameter from Finite – Size Nuclear Model

The atomic nucleus is not a point source. Thus, the assumption of a finite size for a nucleus leads to a departure from Coulomb potential between electron and nucleus. In this work, the nuclear potential charge radius by virtue of the modified finite size nuclear potential. Has been found. The volume of the nuclear potential charge exceeded the nuclear radius by factor $\sqrt{3}$. Due to the extension of the nuclear potential charge, a new and simple $Z^{1/3}$ dependent formula for calculating the radii of the extension of nuclear potential charge is proposed. This work offers a simple way to predict the nuclear charge radius from the assumption of nuclear finite sized model [52].

This work also revealed the important advantage of finite – size nuclear model in determining the nuclear charge radius. The "spherical nuclear" radius *R* can be replaced by *R*p for the distribution of proton charge beyond the radius of the atomic nucleons.

Methodology:

The size of a nucleus is characterized by, R_{rms} or by the radius *R* of the uniform sphere [53]. Both the quantities are related. The mean squared radii of neutron, proton, charge and mass distribution can be defined as follows:

$$\langle r\rangle_c^2 = \frac{\int_0^\infty r^2 4\pi r^2(r)dr}{\int_0^\infty 4\pi r^2 p(r)dr}$$

Where $\rho(r)$ is the nuclear charge density [54]. For a uniformly Charged sphere [$\rho(r)$ = constant] of radius *R*. For $r > R$, this Gives:

$$\langle r\rangle^2 = \frac{\int_0^R r^4 dr}{\int_0^R r^2 dr} = \frac{3}{5}R^2$$

So that the radius of a sphere

$$R = \sqrt{\frac{5}{3}}\langle r_c^2\rangle^{\frac{1}{2}} \qquad (4.2.1)$$

The root-mean-square nuclear matter radii (*R*rms) and the density distributions contain an important insight on nuclear potentials and nuclear wave functions [55]. If the nucleus is a point charge with the distance of electron from the nucleus, *r* and $k = (4\pi\varepsilon 0,)^{-1}$ then its potential is given by:

$$U(r) = -K\frac{ze^2}{r} \qquad (4.2.2)$$

The nuclear potential and electron wave function change when the nucleus is described as a finite-size source with a uniform distribution of charges [3] of radius *R*, then the electron wave function can penetrate to $r \leq R$, and thus the electron spends part of its time inside the nuclear charge distribution, there it feels a very different interaction [56]. Therefore, the potential appropriate for the perturbed electron is no longer of the pure Coulomb form. This is because the electrostatic potential , is no longer due just to the point charge nucleus of electric charge $|e|Z$ [57].

The potential inside a spare of radius *r* due to a point charge $q_{\text{inside}} = e(r/R)^3$, located at the origin is from Coulomb's law:

$$U(r \leq R) = -\frac{ke^2}{r}\left(\frac{r}{R}\right)^3 \qquad (4.2.3)$$

The perturbative potential difference between *r* and *R* is defined by

$$U(r \leq R) = \int_r^R \frac{4\pi epr^2}{r} = \frac{3ke^2}{R^3}\frac{r^2}{2}\frac{R}{r}$$

$$= -\frac{3ke^2}{2R^3}(R^2 - r^2) \qquad (4.2.4)$$

Where $\rho = 3q/4\pi R3$ is the nuclear charge distribution and in this case it is constant [58]. And:

$$R = R_o A^{\frac{1}{3}} \qquad (4.2.5)$$

Thus, for $r \leq R$ we have the potential:

$$U(R) = -\frac{ke^2}{r}\left(\frac{r}{R}\right)^3 - \frac{3ke^2}{2R^3}(R^2 - r^2)$$

$$= -\frac{3ke^2}{2R^3}(3R^2 - r^2) \qquad (4.2.6)$$

Equation (3.2.6) represents the potential for a finite-size charge nucleus [59]. Now we have seen that due to the finite nuclear size, the electric potentials *U*(*R*) and *U*(*r*) of the nucleus are different [60]. Therefore, the spherical electrostatic potential function U(*R*), corresponding to a nuclear charge density distribution, will then be used to replace the common Coulomb potential for a point-like nucleus, [61]. Also compared to a point-like nucleus, the extended nuclear charge distribution also leads to a shift in the energy levels of electron [62, 63].

Assuming uniform charge distribution, one have for a nucleus of charge +*Ze*, the volume.

$$V = \int_o^b \sqrt{1-\frac{z^2}{a^2}}\, pdp \int_o^z dz \int_o^{2\pi} d\phi = \frac{4}{3}\pi ab^2 \qquad (4.2.7)$$

Hence the density:

$$\rho = \frac{3ze}{4\pi ab^2} \qquad (4.2.8)$$

The intrinsic quadrupole moment of a symmetry charged distribution is defined by the relation.

$$Q_o = \frac{1}{e}\int \rho(r)[3(z)^2 - (r)^2]\, dv \qquad (4.2.9)$$

The nucleus is assumed to have asymmetry axis along z' and e is the charge on each proton [64]. Using the fact that $r'^2 = x'^2 + y'^2 + z'^2 = \rho'^2 + z'^2$ and $dv = \rho'\, d\rho'\, d\varphi'\, dz'$, we find:

$$Q_o = \frac{3ze}{4\pi ab^2 e}\iiint p(r)[3z^2 - z^2 - p^2]\mathrm{dv}$$

$$= Z\frac{2}{5}\,(a^2 - b^2) \qquad (4.2.10)$$

A non-zero quadrupole moment Q_0 indicates that the proton distribution is not spherically symmetric. By convection, the value of Q_0 is taken to be positive (i.e. when $a > b$) if the ellipsoid is prolate and negative (i.e. when $a < b$) if the ellipsoid is oblate and zero (i.e. when $a = b$) if the ellipsoid is a sphere. Figure 2 depicts the possible charge (shape) distribution of nuclei.

Nuclear deformation has an influence on the nuclear charge radii. The effective deformation parameters (β_{eff}) are deduced from the intrinsic quadrupole moment (Q_0), which is related to the spectroscopic quadrupole moment (Q) via the well-known formula

$$Q = \frac{Q_o\, I(2l-1)}{(1+3)(2I+3)} \qquad (4.2.11)$$

Thus, the effective deformation parameters can be deduced the quadrupole moments and the charge radii are known. βeff has been deduced for light mirror nuclei .

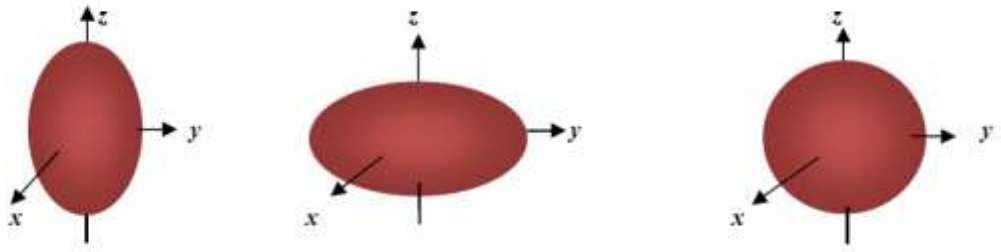

Figure (4. 1) Electric quadrupole moments for different charge distribution.

4.3 Nuclei at or Near Drip-Lines

The magic number and halo and /or skin (neutron) of the nuclei at or near neutron drip-line are studied using axially deformed relativistic mean field model. The density profiles of some of selected nuclei in the light mass region of nuclear landscape are plotted for the purpose. A considerable difference in the densities of neutron and proton can be seen easily in all the cases studied. In addition, single particle energy levels show the visible shell gaps at N = 28 and 40 which corresponds the sudden decrease in the two neutron separation energy. The two results are consistent with each other, while the shell gaps corresponding to the numbers N = 32 and 34 seem not to be supporting the magicity at these numbers in the isotopes considered here [65].

The halo character and the magic number in the nuclei close to or on the neutron drip-line, has been studied also. The density profiles show that the nuclei considered here are having considerable difference in the densities of neutron and proton, which is a clear indication of halo structure. The other part of investigation is magic number in this mass region. The shells at N = 32 or 34 are separated by energy ~1.6 MeV only, as compared to the gaps of ~4.5 MeV at N = 28. The shell gap of ~1.6 is small enough to create the stability required for the number to be a magic number. Therefore, these numbers do not seem show the magic number character.

Formalism:

One use axially deformed relativistic mean field (RMF) model to study the properties of the nuclei. The RMF model has been proved to be a very powerful tool to explain the properties of finite nuclei and infinite nuclear matter [66, 67, 68] for the last two decades. We start with the relativistic Lagrangian density for a nucleon-meson many-body system,

$$\ell = \overline{\psi_\iota}\left(i\gamma^\mu\partial_\mu - M\right)\psi_i + \frac{1}{2}\partial^\mu\sigma\partial_\mu^\sigma - \frac{1}{2}m_\sigma^2\sigma^2 - \frac{1}{2}g_2\sigma^3 - \frac{1}{4}g_3\sigma^4 - g_s\overline{\psi_\iota}\psi_i\sigma - \frac{1}{4}\Omega^{\mu\nu}\Omega_{\mu\nu} + \frac{1}{2}m_\omega^2V^\mu V_\mu + \frac{1}{4}c_3\left(V_\mu V^\mu\right)^2 - g_\omega\overline{\psi_\iota}\ \gamma^\mu\psi_i V_\mu - \frac{1}{4}\vec{B}^{\mu\nu}.\vec{B}_{\mu\nu} + \frac{1}{2}pm^2.\vec{R}^\mu - g_p\overline{\psi_\iota}\ \gamma^\mu\vec{T}\psi_i.\vec{R}^\mu - \frac{1}{4}F^{\mu\nu} - e\vec{\psi}_i\gamma^\mu\frac{(1-T3i)}{2}\psi_i A_\mu \quad (4.3.1)$$

The quadrupole deformation parameter β2 is evaluated from the resulting quadrupole moment [4] using the formula,

$$Q = Q_n + Q_p = \sqrt{\frac{a}{5\pi}}\ AR^2\beta_2 \quad (4.3.2)$$

Where, $R=1.2A^{1/3}$. The total binding energy of the system is,

$$E_{total} = E_{part} + E_{\sigma} + E_{\omega} + E_{p} + E_{c} + E_{pair} + E_{cm} \quad (4.3.3)$$

Where E_{part} is the sum of the single-particle energies of the nucleons and E_{σ}, E_{ω}, E_{ρ}, E_c and E_{pair} are the contributions of the mesons fields, the Coulomb field and the pairing, energy respectively. For the open shell nuclei, effect of pairing interactions is added in the BCS formalism. The pairing gaps for proton (Δp) and neutron (Δn) are calculated from the relations [69]

$$\Delta p = rbsZ^{-\frac{1}{3}}e^{(sI-tI)^2}$$
$$\Delta n = rbsN^{-\frac{1}{3}}e^{-(sI+tI))^2} \quad (4.3.4)$$

Where r=5.72 MeV, s=0.118, t=8.12, b_s=1, and I= (N-Z)/ (N+Z).

4.4 Three-Dimensional Simulations Of pure Deflagration Models for Thermos Nuclear Supernovae

This work is concerned with a systematic study of the pure deflagration model of Type Ia supernovae (SNe Ia) using three-dimensional, high-resolution, full-star hydrodynamical simulations. Nucleosynthetic yields were calculated using Lagrangian tracer particles, and light curves calculated using radiation transport [70].

One tests the effects of the initial conditions on results by varying the number of randomly selected ignition points from 63 to 3500. In addition, the radius of the centered sphere they are confined in from 128 to 384 km. The results show that the rate of nuclear burning depends on the number of ignition points at early times. The density of ignition points at intermediate times. In addition, the radius of the confining sphere later. The results depend primarily on the number of ignition points, but we do not expect this to be the case in general. The simulations with few ignition points release more nuclear energy *E*nuc, have larger kinetic energies *E*K, and produce more 56Ni than those with many ignition points, and differ in the distribution of 56Ni, Si, and C/O in the ejecta. The *M*B and light curves resemble those of under-luminous SNe Iax, while those for simulations with many ignition points are not..

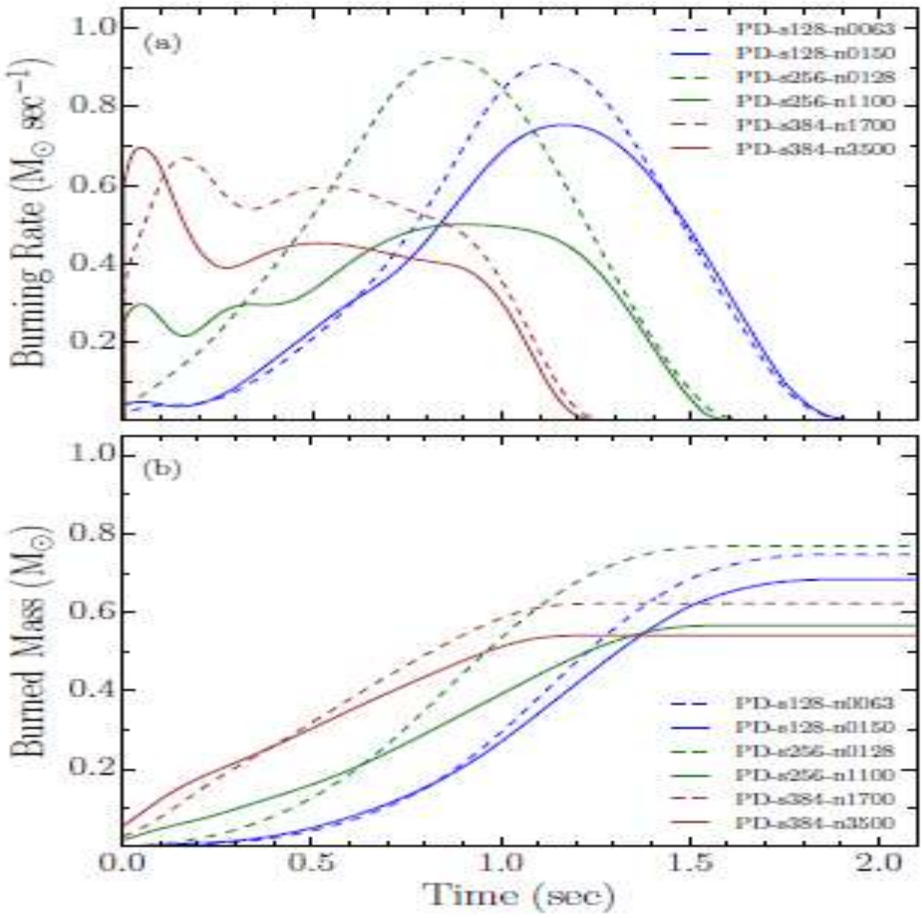

Figure a (4.2): **the nuclear burning rate as a function of time. (b): the burned mass *M*b as a function of time. Blue, green, and brown lines correspond to the pairs of simulations with confining spheres of radii *R*sph = 128, 256 and 384 km.**

The simulations with a small fraction *f* of the volume of the confining sphere filled by ignition point bubbles are shown as dashed lines, while those with nearly the largest possible fraction are shown as solid lines.

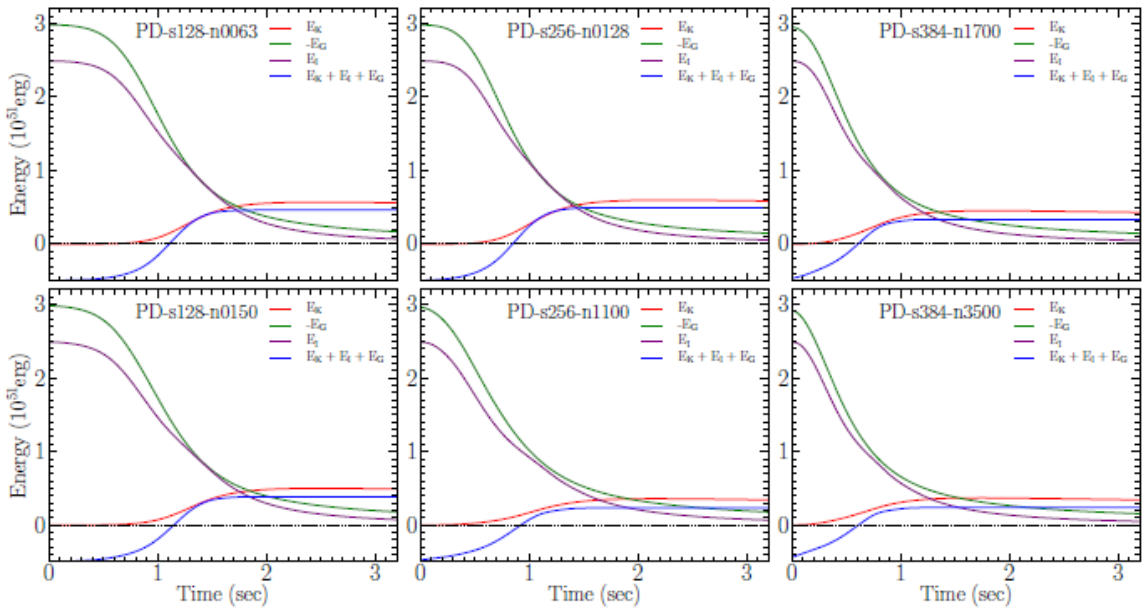

Figure (4.3) Evolution of the internal energy, *E*I, the negative of the gravitational potential energy, −*E*G, and the kinetic energy, *E*K, for all six simulations.

In the simulations with *N*ign ~ 100, *E*I and −*E*G decrease slowly at first, reflecting the initially low burning and the low rate of expansion of the star in these simulations. The opposite is the case in the simulations with *N*ign ~ 103.

4.5 Investigation of the Shell Effect on Neutron Induced Cross Section of Actinides

Investigations has been made concerning the development of the effect of shell structure on neutron induced cross section, evaluations for Actinides elements in the energy range of 0-30 MeV. The EXIFON code, which is based on the analytical model for statistical multistep direct and multistep compound reactions, was used for the calculation of the cross section for (n-2n), (n-p) and (n-α) reaction channels. Results are compared with data from the experimental database, EXFOR from the IAEA nuclear data bank to deduce the shell effect. An empirical relation for the reaction cross section has been established for magic numbers nucleus in the (n-2n) reaction channel in the energy range. Results shows that the odd-even effect has also been observed as the cross section for odd-even nuclei are higher than their neighbouring even-even nuclei and with comparison in term of Shell correction, the cross section is higher when the Shell correction is not considered [71].

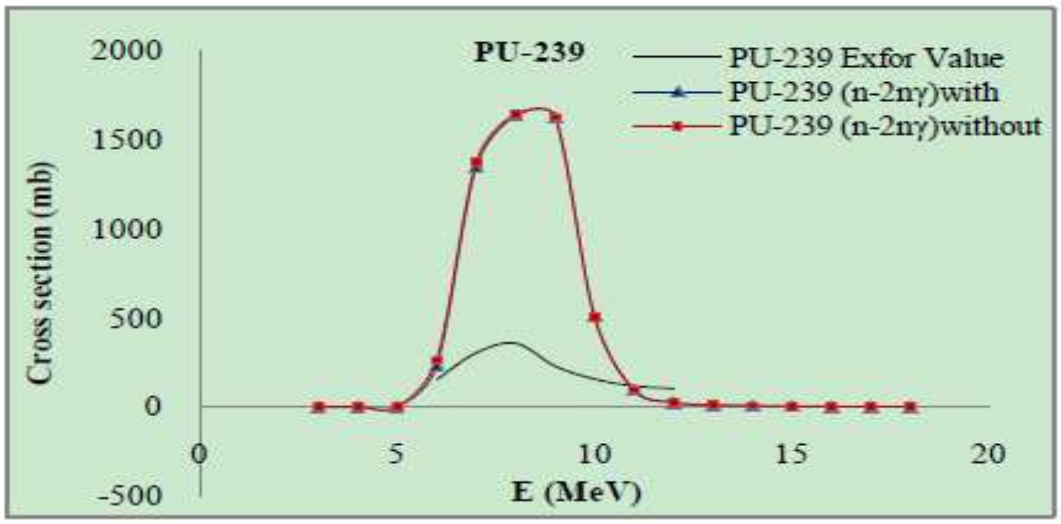

Figure (4.4) Graphical representation of the comparison between the Exofor and the calculated values for (2, 2n) reaction channel for PU-239

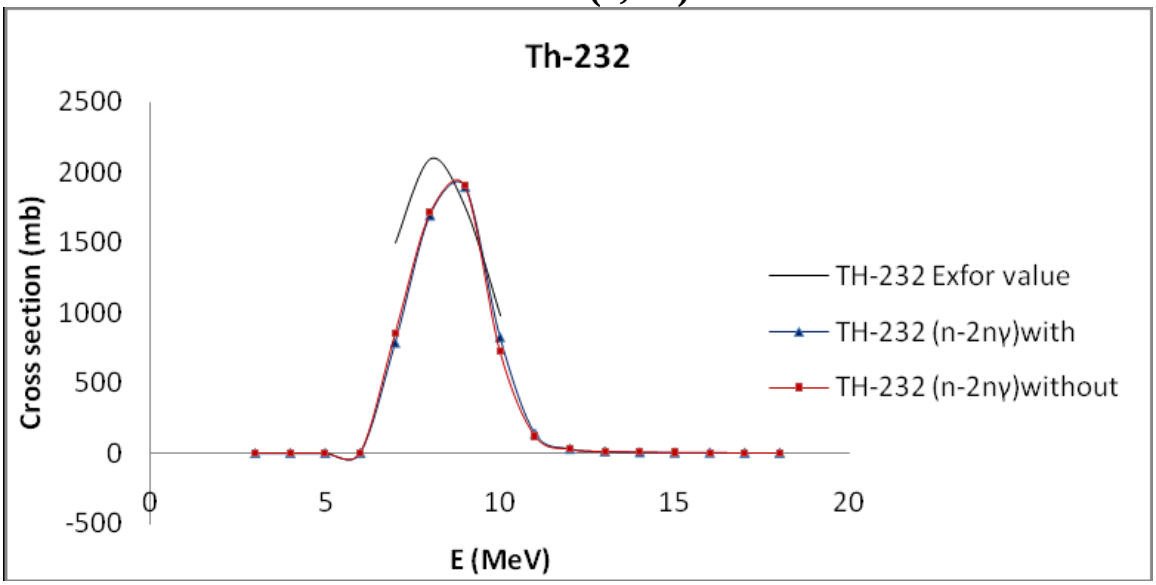

Figure (4.5) Graphical representation of the comparison between the Exofor and the calculated values for (2, 2n) reaction channel for Th-232

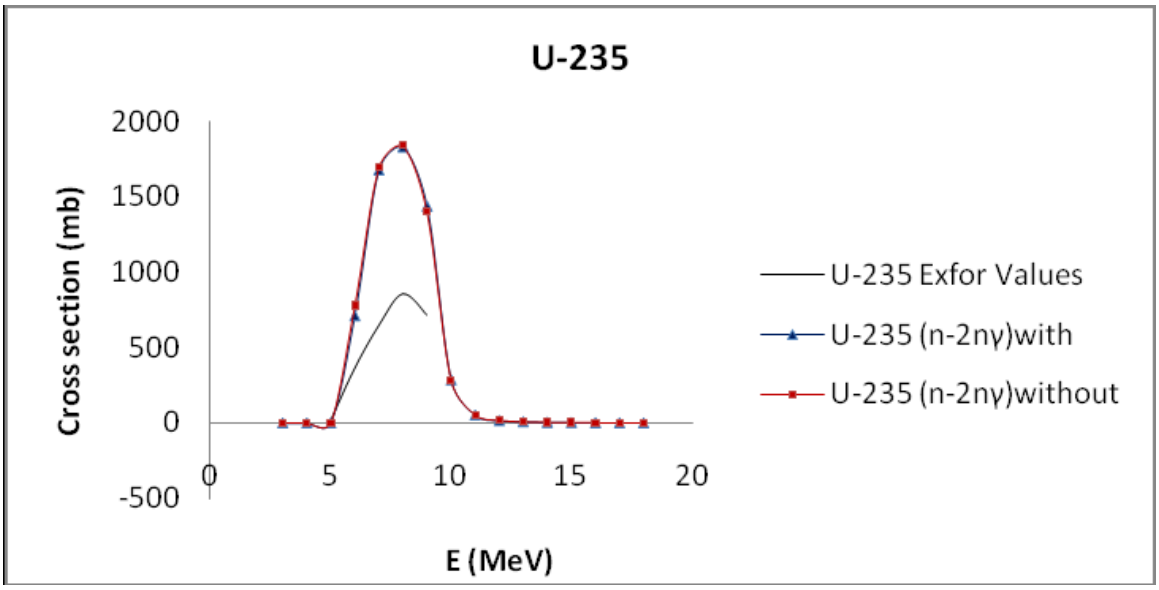

Figure (4.6) Graphical representation of the comparison between the Exofor and the calculated values for (2, 2n) reaction channel for Th 232.

4.6 Nuclear and Neutron Matter Properties Using BHF Approximation

Results of cold and hot symmetric nuclear matter and pure neutron matter calculations are presented. The Brueckner-Hartree-Fock (BHF) approximation + two-body density dependent Skyrme potential which is equivalent to three-body interaction are used. Various modern nucleon-nucleon (NN), CD-Bonn potential, Nijm1 potential, Reid 93 potential and Argonne V18 potential were used. The bulk properties of asym-metric nuclear matter are computed such as the equation of state (EOS) at (T = 0), pressure at (T = 0, 5 and 10 MeV), single particle potential, free energy at (T = 5 and 10 MeV), nuclear matter incompressibility and the symmetry energy. In addition, the bulk properties of pure neutron matter are computed such as the EOS at (T = 0), pressure at (T = 0, 3 and 6 MeV), single particle potential, free energy at (T = 3 and 6MeV). Good agreement is obtained in comparison with previous theoretical models [72].

4.6.1 BHFA and BGE

The G-matrix is defined by:

$$G(\omega) = V + V\frac{Q}{\omega - H_o + i\eta} \qquad (4.6.1)$$

This is known as the Beth-Goldstone equation (BGE);etial for more deaital,[73] ω is the starting energy which is usually the sum of the single particle energies of the states of the interacting nucleons

$$\Omega = e(k) + e(k^{-}) \qquad (4.6.2)$$

V is the bare NN potential, η is an infinitesimal small number, H is the unperturbed energy of the intermediate scattering states. Q is the Pauli projection operator, it pro-jects out states with two nucleons above the Fermi level, and it is given by:

$$Q(k,k^{-}) = (1-\theta_F(k))(1-\theta_F(k^{-})) \qquad (4.6.3)$$

Where Θ_F (k) = 1 for k < k_F and zero otherwise, Θ_F (k) is the occupation probability of a free Fermi gas with a Fermi momentum k_F. In the Brueckner-Goldstone expansion, the average binding energy per nucleon is expanded in a series of terms as follows:

$$\frac{E(k)}{A} = \langle\bar{\Gamma}\rangle + \langle\bar{G}\rangle = \sum_k \frac{\hbar^2k^2}{2m} + \frac{1}{2}\sum_k k\bar{k}\ \left|G(e(k)+e(\bar{k}))\right|k\bar{k} \quad (4.6.4)$$

where |kk' > refers to antisymetrized two-body states. This first order is known as the Brueckner-Hartree-Fock approximation (BHFA). To completely determine the average binding energy one has to define the single particle potential U (k) which contributes to the single particle energies ap-pearing in the G-matrix elements. The structure of the expression (2.4) suggests choosing the following BHF single particle potential

$$U(k) = \sum_{k<k_F} < k\bar{k}\left|G(e(k)+e(\bar{k}))\right|k\bar{k} \qquad (3.6.5)$$

$$\frac{E(k)}{A} = \sum_{k<k_F}\left[\frac{\hbar^2k^2}{2m}+\frac{1}{2}U(k)\right] = \frac{41}{p^2}\int_o^{k_F}\frac{4\pi k^2}{(2\pi)^3}\left(\frac{\hbar^2k^2}{2m}+e(k)\right)dx = \frac{3\hbar^2k_F^2}{10m} + \frac{3}{2k_F^3}\int_o^{k_F}k^2\,dkU(k) \qquad (4.6.6)$$

The G-matrix itself depends on U (k) through the starting energy ω, defined in Eq.(4.6.2) and the lowest order approximation (4.6.4) along with the choice (for the single particle potential. The single particle energy e (k) is defined

$$e(k) = \Gamma + U(k) = \frac{\hbar^2k^2}{2m} + U(k) \qquad (4.6.7)$$

where Γ is the kinetic energy. In the conventional choice for the single particle potential one normally takes the BHF potential for the hole states (k < kF) and zero for particle states (k > kF)

$$U(k) = \sum_{k<k_F} < k\bar{k}\left|G\left(e(k)+e(\bar{k})\right)\right|k\bar{k})k < k_F, k > k_F \qquad (4.6.8)$$

The use of the continuous choice potential implies that the G-matrix elements needed in the self-consistent calcula-tion are complex and the prescription advocated by Mahaux is

$$U(k) = Re\sum_{k<k_F} < k\bar{k}\left|G\left(e(k)+e(\bar{k})\right)\right|k\bar{k}) \qquad (4.6.9)$$

Eqs. (4.6.1) and (4.6.8) represent the main equations that one needs to solve self-consistently. In order to obtain such a self-consistent solution one often assumes a quadratic dependence of the single-particle energy on the momentum of the nucleon in the form

$$e(k) = \begin{cases} \frac{\hbar^2 k^2}{2m^*} + \Delta k \leq k_F \\ \frac{\hbar^2 k^2}{2m^*} \; k > k_F \end{cases} \qquad (4.6.10)$$

Where m* is the effective mass of the nucleon and Δ is a constant. Starting with an appropriate choice for the pa-rameters for the effective m* and the constant Δ, one can solve the Bethe-Goldstone equation and evaluate the sin-gle-particle energy [74].

4.6.2 EOS of the Symmetric Nuclear Matter at (T = 0)

The EOS is the relationship between energy per nucleon and Fermi momentum k_F or density ρ, the minimum point of the curve is called the saturation point. In the present work, one may introduce a Skyrme effective interaction density dependent term in addition to the BHF potential.

$$V(\bar{r_1}, \bar{r_2}) = \sum_{i=1}^{4} r_i (1 + x_i p_\sigma) p^{\propto_i} \partial(\bar{r_1} - \bar{r_2}) \qquad (4.6.11)$$

This is a two-body density dependent potential which is equivalent to three-body interaction. Where ti and xi are interaction parameters, Pσ is the spin exchange operator, ρ is the density, ***r***1and ***r***2 are the position vectors of the particle (1) and particle (2) respectively and αi = (1/3, 2/3, 1/2 and 1).

The results are shown in the figure (3.7), where the energy per particle (E / A) in MeV is plotted against density ρ in fm-3, for symmetric nuclear matter using different potentials in comparison with Freidman and Pandharipande (F and P) [25].

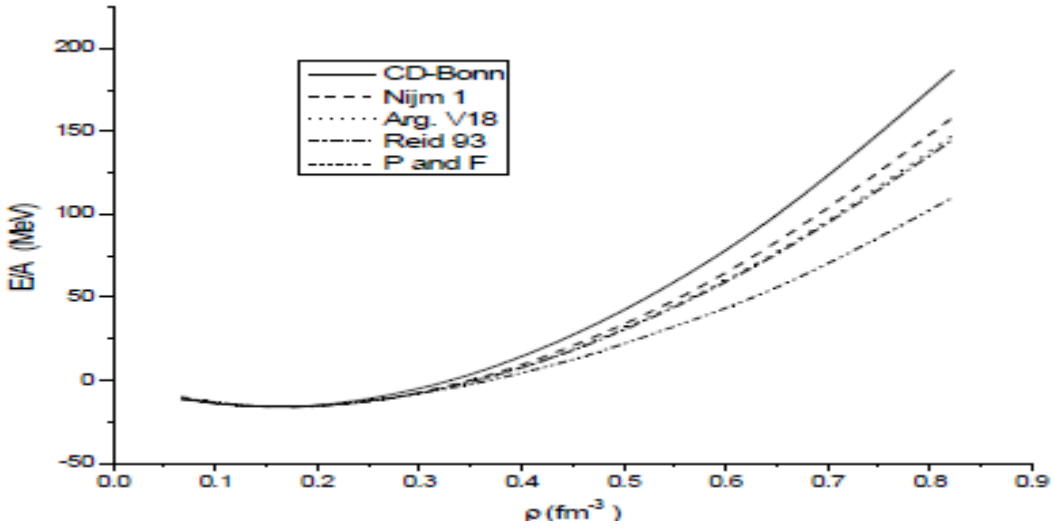

Figure (4.7) E / A in MeV for symmetric nuclear matter at (T=0) as a function of density using different potentials for conventional choice in comparison with F and P [25]

4.6. 3 Pressure of the Symmetric Nuclear Matter at (T = 0)

The pressure for symmetric nuclear matter at T = 0 is de-fined in terms of the energy per particle as

$$p(p) = p^2 \frac{\partial(\frac{E}{A})(p)}{\partial p} \qquad (4.6.12)$$

The results are shown in Fig. (3.8). The values of the pressure are plotted against the density ρ for symmetric nuclear matter for conventional choice using the CD-Bonn potential, the Nijm1 potential, the Argonne v18 potential and the Reid 93 potential in comparison with F and P[25]. From figure (4.8) it is observed that when the density of symmetric nuclear matter increases the pressure of nuclear matter increases.

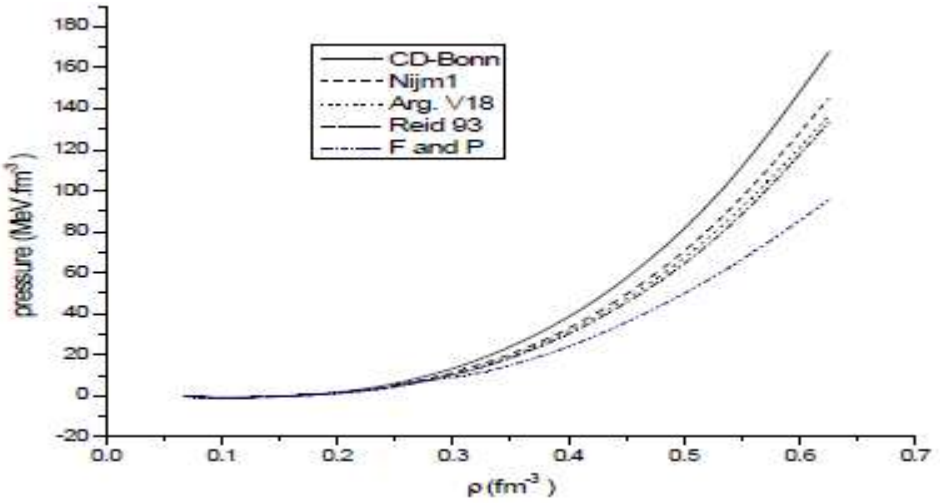

Figure (4.8): The pressure of symmetric nuclear matter at (T = 0) as a function of density using different potentials for conventional choice in comparison with F and P [25].

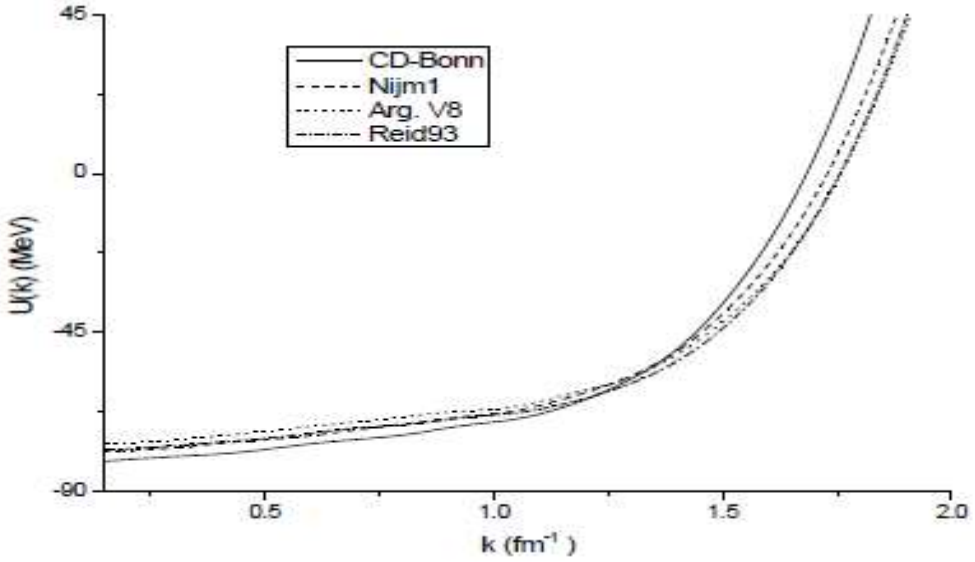

Figure (4.9) the single particle potential for symmetric nuclear as a function of momentum k at (k_F = 1.333 fm-1) for different potentials for conventional choice.

4.7 A Calculation Method of Nuclear Cross-Sections of Proton Beams by the Collective Model and the Extended Nuclear-Shell Theory with Applications to Radiotherapy and Technical Problems.

An analysis of total nuclear cross-sections of various nuclei is presented, which yields detailed knowledge on the different physical processes such as potential/resonance scatter and nuclear reactions. The physical base for poten-tial/resonance scatter and the threshold energy resulting from Coulomb repulsion of nuclei are collective/oscillator models. The part pertaining to the nuclear reactions can only be determined by the microscopic theory (Schrödinger equation and strong interactions). The physical impact is the fluence decrease of proton beams in different media, the stopping power of secondary particles, and a 'translation' of the results of the microscopic theory to the collective model.

The presented results show that a suitable combination of the collective model with extended nuclear shell theory can be adequate to solve problems, which are rather outstanding in many practical problems. Besides the radiotherapy with protons, it should be mentioned that the cross-sections of those nuclei/isotopes are important to reduce the half times of the corresponding isotopes significantly. The storage of long-existing isotopes should be avoided [75].

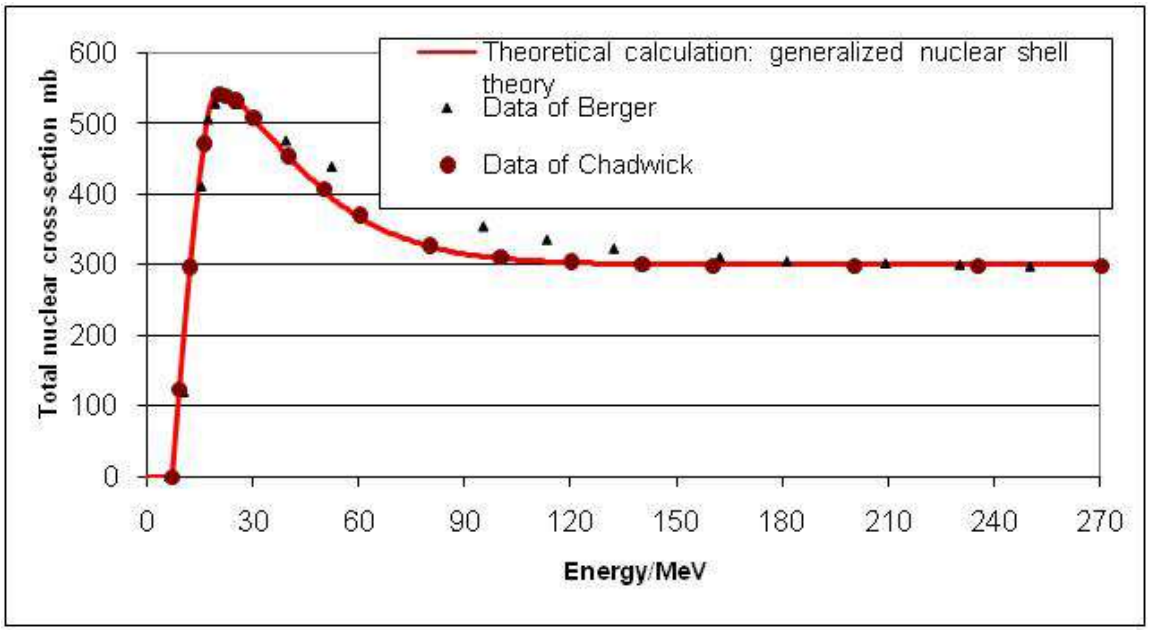

Figure 4.10. Total nuclear cross-section Qtot of oxygen [1 - 5]

4.8 Review on the progress in nuclear fission—experimental methods and theoretical descriptions

New approaches have considerably extended the availability of fissioning systems for the experimental study of nuclear fission, and have provided a full identification of all fission products in *A* and *Z* for the first time. In particular, the transition from symmetric to asymmetric fission around ^{226}Th, some unexpected structures in the mass distributions in the fission of systems around $Z = 80–84$, and an extended systematics of the odd–even effect in the fission fragment *Z* distributions have all been measured[76].

Three classes of model descriptions of fission presently appear to be the most promising or the most successful. Self-consistent quantum-mechanical models fully consider the quantum-mechanical features of the fission process. Intense efforts are presently being made to develop suitable theoretical tools [77].For modeling the non-equilibrium, large-amplitude collective motion leading to fission. Stochastic models provide a fully developed technical framework. The main features of the fission-fragment mass distribution have been well reproduced from mercury to fermium and beyond [78]; however, limited computer resources still impose restrictions,

for example, on the number of collective coordinates and on an elaborate description of the fission dynamics. In an alternative semi-empirical approach [79], considerable progress in describing the fission observables has been achieved by combining several theoretical ideas, which are essentially well known. This approach exploits

(i) The topological properties of a continuous function in multidimensional space.

(ii) The separability of the influence of fragment shells and the macroscopic properties of the compound nucleus.

(iii) The properties of a quantum oscillator coupled to a heat bath of other nuclear degrees of freedom.

(iv) An early freeze-out of collective motion.

(v) The application of statistical mechanics for describing the thermalization of intrinsic excitations in the nascent fragments. This new approach reveals a high degree of regularity and allows the calculation of high-quality data that is relevant to nuclear technology without specifically adjusting the empirical data of individual systems [80].

4.9 Systematic study of the α decay preformation factors of the nuclei around the Z = 82, N = 126 shell closures within the generalized liquid drop model

This study is devoted for the decay preformation factors, and the α decay half-lives of 152 nuclei around $Z = 82$, $N = 126$ closed shells based on the generalized liquid drop model (GLDM) with P_α being extracted from the ratio of the calculated α decay half-life to the experimental one. The results show that there is a remarkable linear relationship between P_α and the product of valance protons (holes) N_p and valance neutrons (holes) N_n. At the same time, it extract the α decay preformation factor values of the even–even nuclei around the $Z = 82$, $N = 126$ closed shells from the study of Sun *et al.* [81]. In which the α decay was calculated by two different microscopic formulas. We find that the α decay preformation factors are also related to $N_p N_n$. Combining with our previous studies. Therefore, seifetal the phenomenon of linear

relationship for the nuclei around the above closed shells is model-independent. This may be caused by the effect of the valence protons (holes) and valence neutrons (holes) around the shell closures. Using the formula obtained by fitting the α decay preformation factor data calculated by the GLDM, to calculate the α decay half-lives of these nuclei. The calculated results agree with the experimental data well [82].

4.10 A search for neutron magicity in the isotopic series of Z = 122, 128 super heavy nuclei

The superheavy nuclei have been examined systematically in the region $158 \leq N \leq 218$, $162 \leq N \leq 212$ for Z = 122 and 128, respectively. The explicit density-dependent meson-exchange (DD-ME) and point-coupling (DD-PC) models within the framework of covariant density functional theory (CDFT) have been used to study the structural and decay properties of the isotopic series which includes the separable form of a finite range of pairing interaction. From the potential energy curves, the ground state properties of nuclei are predicted. Due to the importance of the shell effect in the superheavy region, the Strutinsky shell correction method has been employed for a better understanding of the extra stability of nuclei. The results from neutron pairing energy, two-neutron separation energy (S_2n), single-particle energy levels, and total shell-correction energy strongly support N = 168, 174, and 178 as deformed neutron-magic numbers from both the force parameter, in both the isotopic series. N = 172 and 184 are predicted as spherical magic with DD-ME2 interaction in the Z = 122 isotopic series. Using three different semi-empirical approaches named UNIV2, SemFIS2, and ImSahu, the α-decay properties are studied and compared with available experimental data, FRDM2012 and the WS4 mass model. The stability of synthesized super heavy nuclei can be determined by comparing spontaneous fission half-lives with α-decay half-lives. [83].

4.11 A new View of Nuclear Shells

The nuclear shell structure that has served as a fundamental framework for understanding the arrangement of nucleons exhibits dramatic changes as the neutron to proton ratio in nuclei increases. This paper describes how reaction spectroscopy of the neutron- and proton-rich nuclei has brought about a new revolution towards a more global view of nuclear shells. The relationship between changes in shell structure and the discovery of exotic forms of nuclei such as nuclear halo and skin is discussed. It is

shown that the well-known shell gaps (magic numbers) $N = 8$ and 20 disappear. The discovery of a new magic number at $N = 16$ at the limit of nuclear binding is discussed [84].

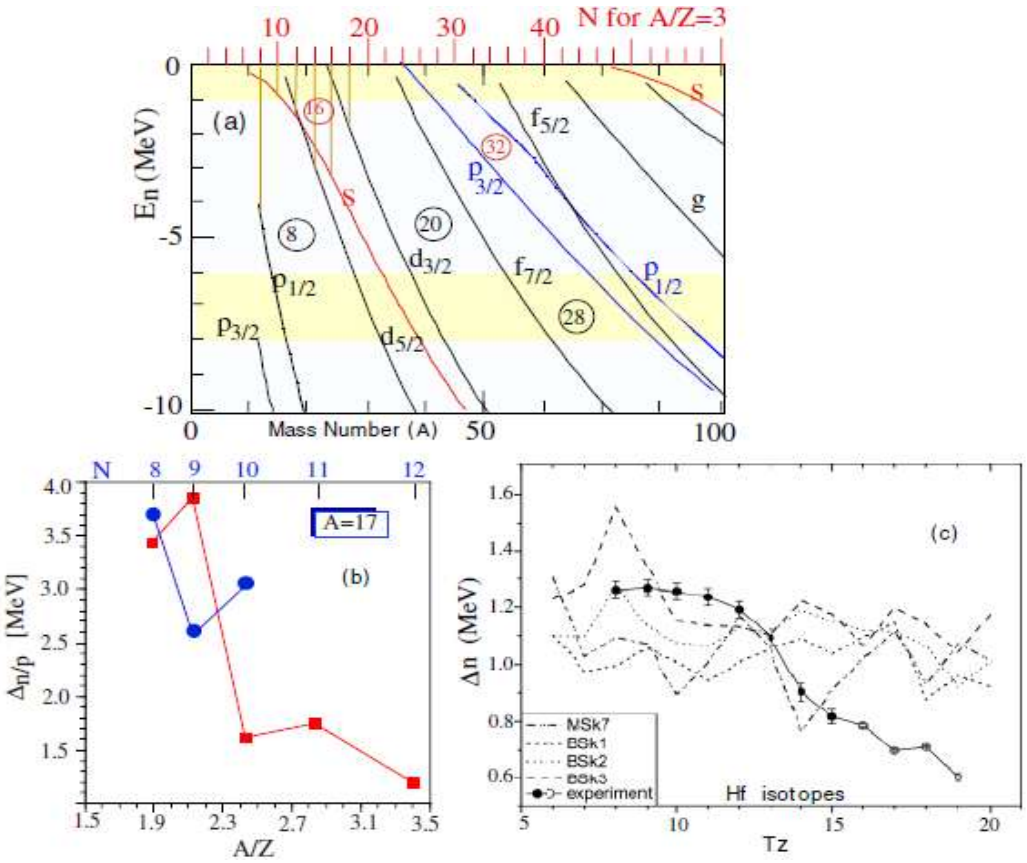

Figure (4.11) (a) Neutron orbitals for nuclei with $A/Z = 3$ calculated in a Woods–Saxon potential [3]. (b) The pairing energy for neutrons (1*n*, squares) and protons (1*p*, circles), according to the definition in [4], plotted against functions of neutron–proton asymmetry *A*/*Z*.
Adapted from [5]. (c) The neutron pairing energy of the Hf isotopes as a function of isospin (*Tz*), adapted from [6]. The neutron pairing energy in (b) and (c) is seen to decrease as the neutron–proton asymmetry increases.

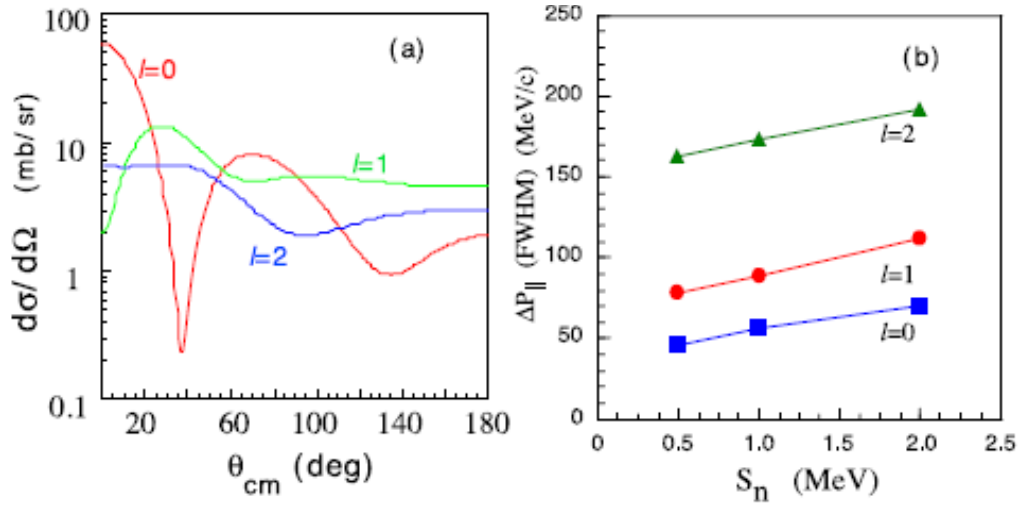

Figure (4.12) (a) Demonstrative distorted wave born approximation (DWBA) calculations of a (d,p) transfer reaction.

The different curves as indexed in the figure show angular distributions for different angular momentum transfers (l = 0, 1 and 2). (b) Demonstrative calculations showing the width of the longitudinal momentum distribution for one-neutron removal from a nucleus plotted as a function of the one-neutron separation energy.

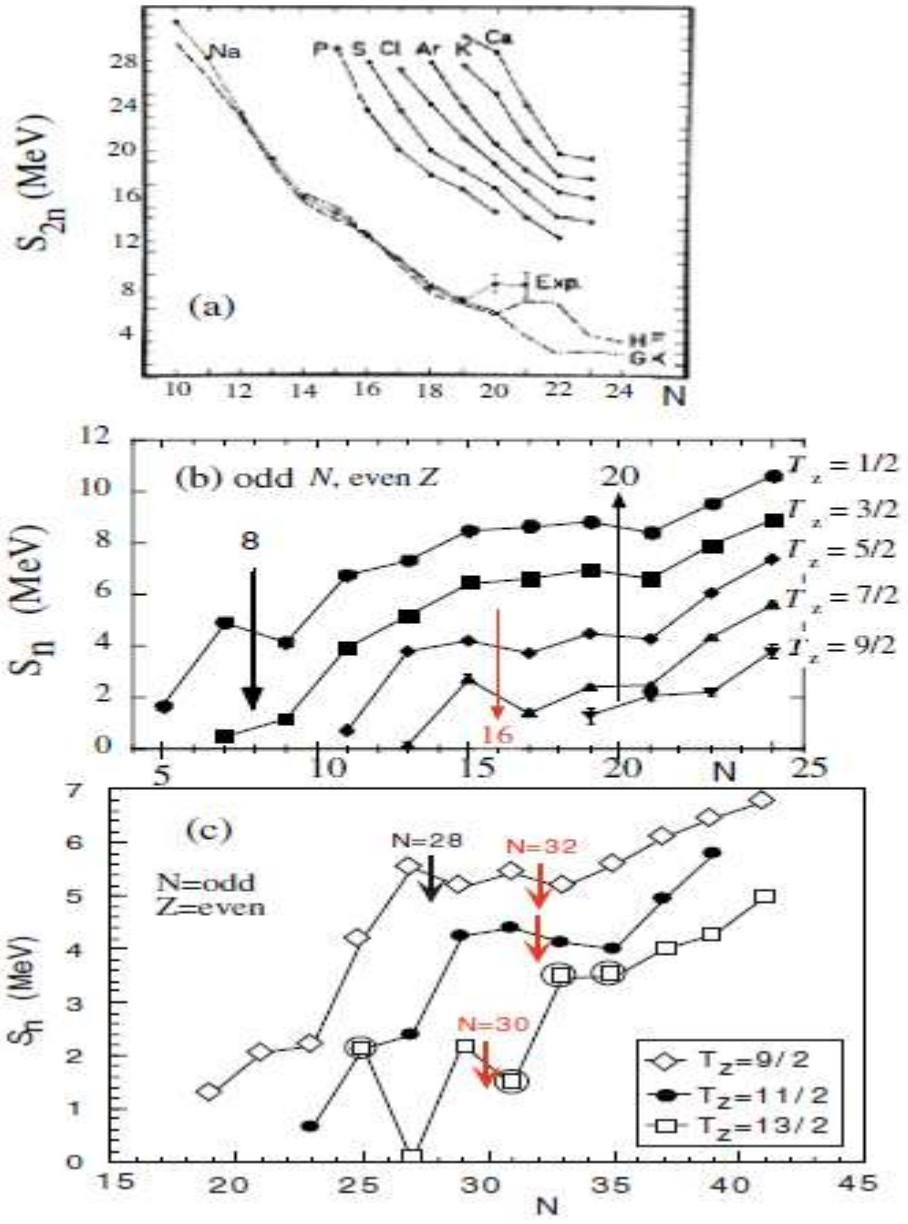

Figure (4.13) (a) Two-neutron separation energies for different isotopes plotted against the neutron number. (b), (c) One-neutron separation energy for different isospin chains plotted against the neutron number.

To avoid fluctuations due to pairing, only the isotopes with N = odd and Z = even are plotted for identifying possible magic numbers. The circled points are masses not measured but taken from evaluation systematics.

4.12 Exotic nuclei and nuclear forces

The shell structure of nuclei has been proposed by Mayer and Jensen, and has been considered to be kept valid basically for all nuclei, with

well-known magic numbers, 2, 8, 20, 28, 50,.. Nuclear forces were shown, very recently, to change this paradigm. One descrier the shell evolution in terms of the monopole interaction of nuclear forces. One will discuss three types of nuclear forces. The first one is the tensor force. The tensor force is one of the most fundamental nuclear forces, but its first-order effect on the shell structure has been clarified only recently in studies on exotic nuclei. The tensor force can change the spin–orbit splitting depending on the occupation of specific orbits. These results in changes of the shell structure in many nuclei, and consequently some of Mayer–Jensen's magic numbers are lost and new ones emerge, in certain nuclei. This mechanism can be understood in an intuitive way, meaning that the effect is general and robust. The second type of nuclear forces is central force. One shows a general but unknown property of the central force in the shell-model Hamiltonian that can describe nuclear properties in a good agreement with experiment.. Actually, by combining the central force with the tensor force, one can understand and foresee how the same proton–neutron interaction drives the shell evolution, for examples such as Sn/Sb isotopes, $N = 20$ nuclei and Ni/Cu isotopes. The distribution of single-particle strength is discussed also in comparison to (e,e'p) experiment on ^{48}Ca. The shell evolution affects shapes of nuclei through Jahn–Teller-type mechanism, and a very interesting example with exotic Si isotopes is discussed. The third type of nuclear force is a three-body force, which originates in the Δ particle excitation as proposed by Fujita and Miyazawa many years ago. This force is shown to produce a repulsive interaction between valence neutrons after averaging effects from the third nucleon in the core. The same three-body force is responsible for neutron stars. By including such effects of the three-body force, one can predict the correct drip line of oxygen isotopes, for instance. Thus, the landscape of atomic nuclei varies in going from stable to exotic nuclei due to particular nuclear forces, leading to a paradigm shift [85].

The effects of nuclear forces on the shell structure can be studied in terms of monopole component or interaction of a given two body interaction, $\hat{V}$ We first define the monopole matrix element of an interaction, $\hat{V}$, as:

$$U_m = \frac{\sum_{k,\bar{k}\langle jk\bar{j}\bar{k}|\hat{V}||jk\bar{j}|\bar{k}\rangle}}{\sum_{k\bar{k}} 1} \qquad (4.12.1)$$

Where j and $\bar{j}$ denote single-particle orbits with k and $\bar{k}$ being their magnetic substate, respectively, and$\cdot|\hat{V}|$ is the antisymmetrized two-body matrix element. Equation (4.12.1) implies an averaging over all possible

orientations of two interacting particles in the orbits j and, $\bar{j}$ while the antisymmetrization (Pauli principle) is taken into account.

The monopole component of $\hat{V}$ is written, for $j \neq \bar{j}$ as:

$$\hat{U}_m : j.\bar{j} = U_m : j.\bar{j}\,\hat{n}\,j\,\hat{n}\,\bar{j} \qquad (4.12.2)$$

Where $\hat{n}\,j\,\hat{n}\,\bar{j}$ is the number operator of orbit j ($\bar{j}$). The monopole interaction, denoted $\hat{V}_{\mathrm{M}}$, is defined as the operator consisting of $\hat{U}_m : j.\bar{j}$ for all possible pairs of j and j- for $j \neq \bar{j}$ and slightly more complicated terms for all pairs of j = j- (see footnote 1).

As we mentioned, the monopole component of the interaction V is nothing but the average of effects of V, and it depends only on the number operators of these orbits. Its initial idea was introduced by Bansal and French [86].

while its relevance to the effective shell-model interaction was discussed by Poves and Zuker [87].

The importance of the monopole interaction for exotic nuclei originates in its linearity. As the orbit $\bar{j}$ is occupied, the single-particle energy (SPE), E_j of an orbit j is shifted by (see footnote 1),

$$\Delta E_j = U_m : j.\bar{j}\,\hat{n}\,\bar{j} \qquad (4.12.3)$$

For $j = \bar{j}$ for identical nucleons, slightly different forms are used.

spin–isospin interaction was considered, which was a central force with spin dependence:

$$V_c = (\vec{\tau_1}.\vec{\tau_2})(\vec{s_1}.\vec{s_2})c(r) \qquad (4.12.4)$$

Where $\vec{\tau_{1,2}}$ $(\vec{s_{1,2}})$ denotes the isospin (spin) of nucleons 1 and 2, and the symbol (·) means a scalar product. Here, $c(r)$ is a function of the relative distance, r. For the long-range limit of the central force [88].

The tensor force due to one-pion exchange is written as:

$$V_T = (\vec{\tau_1}.\vec{\tau_2})(|\vec{s_1}\,\vec{s_2}|).\gamma^{(2)} f(r) \qquad (4.12.5)$$

$f(r)$ is a function of the relative distance, r. Equation (4.12.5) is equivalent to the usual expression containing the S_{12} function. Because the spins $\vec{s_1}$ and $\vec{s_2}$ are dipole operators and are coupled to rank 2, the total spin $\vec{s} = \vec{s_1} + \vec{s_2}$ of two interacting nucleons must be S = 1. This plays a crucial role in the shell evolution by the tensor force as pointed out later. If both of the bra and ket states of V_{T} have L = 0, with L being the relative orbital angular momentum, their matrix element vanishes because of the $Y^{(2)}$ coupling. These properties are used later also.

Their wave numbers are k_1 and k_2, while their coordinates are denoted by x_1 and x_2. The wave function, ψ consists of products of two plane waves.We take a system of a proton and a neutron in total isospin T = 0. The

antisymmetrization is imposed. Because of S = 1, the coordinate wave function must be symmetric as:

$$\psi\alpha e^{ik_1x_1}e^{ik_2x_2} + e^{ik_2x_1}e^{ik_1x_2} = e^{ikx}\{e^{ikx} + e^{-ikx}\} = 2e^{ikx}\cos(kx) \quad (4.12.6)$$

Where center-of-mass and relative momenta are defined, respectively, as

$$k, k = k_1 \pm k_2 \quad (4.12.7)$$

In addition, center-of-mass and relative coordinates are likewise as,

$$X, x = \frac{(x_1 \pm x_2)}{2} \quad (4.12.8)$$

From these equations, we see that the relative motion is expressed by the wave function:

$$\emptyset(\mathrm{x})\alpha\cos(kx) \quad (4.12.9)$$

And the center-of-mass motion has a wave number *K*.

For the orbits *j* and j^-, the following identity has been derived for the tensor force in [40],

$$2(j_> + 1)U^T_{m:j>j^-} + (2j_c + 1)U^T_{m:j_kj} \quad (4.12.10)$$

Where T = 0 and 1, and j^- is either $j^- >$ or $j^- <$. Note that this identity is in the isospin formalism

The same property holds for a spin–spin central interaction. If only exchange terms remain, the spin-coordinate part of the T = 0 and 1 matrix elements are just opposite. Combining this with$(\overrightarrow{\tau_1}.\overrightarrow{\tau_2})$) in equation (4.12.5), one obtains:

$$U^{T=0}_{m:j>j^-} = 3xU^{T=m}_{m:j>j^-} \; for \; j \neq \overline{J} \quad (4.12.11)$$

Thus, the proton–neutron tensor monopole interaction is twice as strong as the T = 1 interaction.

The tensor force is due to pion (π_) exchange, but the rho meson (p_) contributes also. In the following, we use the (π +p) meson exchange potential [89]. The coupling constants are taken from [90].

In order to incorporate these features, we introduce a central Gaussian interaction as:

$$V_c = \sum_{S.T} f_{S.T}\rho_{S.T}\exp(-\left(\frac{r}{\mu}\right)^2) \quad (4.12.12)$$

Where *S* (*T)* means spin (isospin), *P* denotes the projection operator onto the channels (*S, T)*, and *f, r* and μ stand for the strength, inter nucleon distance and Gaussian parameter.

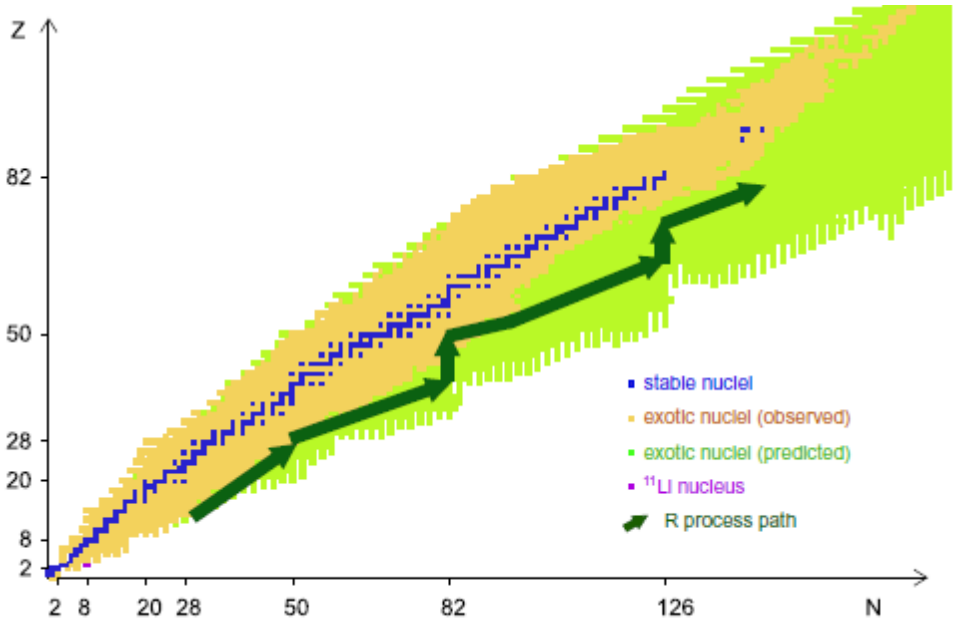

Figure (3.14) nuclear chart. Each nucleus is expressed by a box with the neutron number (*N*) and the proton number (*Z*).

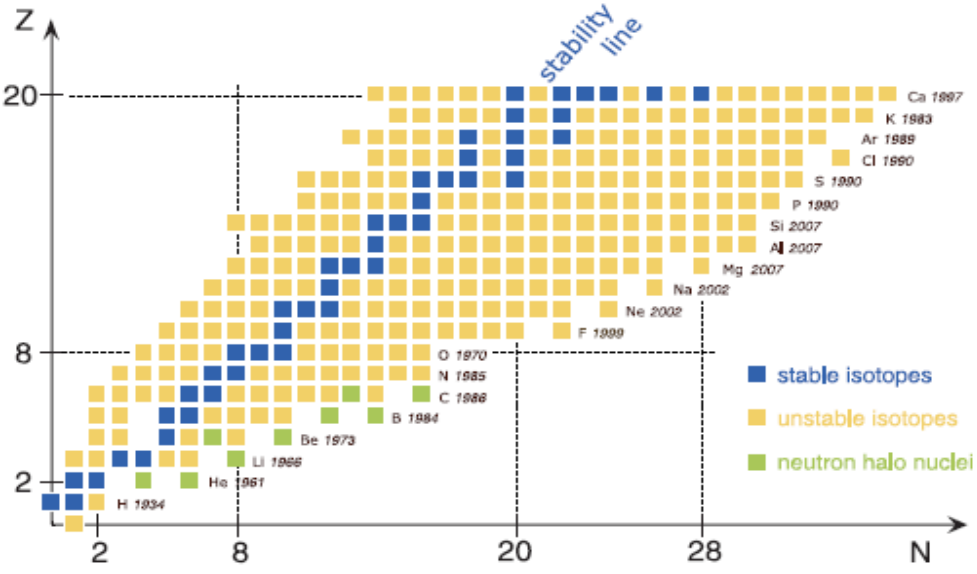

Figure (3.15) Left-lower part of the nuclear chart. A nucleus is expressed by a box located at its neutron number (*N*) and proton number (*Z*). The year of discovery of most neutron-rich isotope is shown at far right as well as the name of the element.

4.13 Investigation of The Existence of New Nuclear Magic Number in Even-Even O Isotopes Using Shell Model and Hartree–Fock Bogoliubov Method

In the present work, the features of some excited states in some even–even $^{14\text{-}26}$O isotopes have been investigated. The aim is to predict the evaluated existence of magic numbers in these isotopes using shell model and Hartree-Fock Bogoliubov method based on SLy4, SkC, SkD Skyrme parameterizations. In particular, root mean square radius, binding energies, one and two neutron separation energies, pairing gaps, transition probabilities, excitation energies, energy levels, transition densities and quadrupole deformation parameters have been investigated. The results are compared with the available experimental data.

From the research that has been carried out, it is possible to conclude that the SM with HF method is probably the best method for the investigation magicity of neutron rich nuclei. In particular, in the region far from stability, the HF method is probably the best model for anticipating the total binding energies and single-particle energies of the closed-shell nuclei. This work demonstrated connecting HF and large-basis SM calculations and used it for the system of valence neutrons in the *sd* and *p-sd* shell model spaces and HFB method on the evolution of quadrupole deformation. The calculated results for 18-26O isotopes are promising. The obtained results reproduced nicely the available experimental data, which based on the binding energies, one- and two-neutron separation energies, rms radii, low laying excitation energies, pairing gaps, transition probabilities, as well as quadrupole deformation, we reproduced the classic magic numbers and confirmed the existence of N=16 is a new one in the oxygen isotopes. The findings suggest that this approach could also be associate many more excited levels with the experiment, especially in the nuclear island of inversion region and near the proton and neutron driplines [91].

Theory and Methodology:

4.13.1 Shell Model Method

The many-particles reduced matrix elements of the electric multipole transition operator $\hat{T}$ for an n particles model space wave function of multi polarity λ can be expressed as the sum of the product of the elements of the one-body density matrix (*OBDM*) times reduced single-particle matrix elements, and is given by [92]:

$$\langle f \left\| \hat{T}^{\lambda} \right\| i \rangle = \langle n\omega_f j_f \left\| \hat{T}^{\lambda} \right\| n\omega_i j_i \rangle = \sum_{k_\alpha k_\beta} OBDM(f, i, k_\alpha, k_{\beta,} \lambda) \langle k_\alpha \left\| \hat{T}^{\lambda} \right\| k_\beta \rangle \quad (4.13.1)$$

Where k_i and k_f are the single particles states for the initial and final model space states $(n\omega_i j_{ii})$ and $(n\omega_f j_f)$, respectively. The ω indices distinguish the various basis states with the same J value. The OBDM in the proton-neutron formalism is given by [93]:

$$OBDM(f,i,k_\alpha,t_z,k_{\beta,}\,t_z,\lambda) = \langle \frac{n\omega_f j_f \left\| \left[a^{+}_{k_\alpha :,t_z} \otimes a^{\sim}_{k_{\beta,}\,t_z} \right]^{\lambda} \right\| n\omega_i j_i}{\sqrt{2\lambda+1}} \rangle \qquad (4.13.2)$$

Where *tz* =1/2 for neutron and *tz* = -1/2 for proton. Two different shell model spaces have been used in our work. The first one is the *sd* model space, which consists of the active shells 1*d*5/2, 2*s*1/2, and 1*d*3/2 above the inert ^{16}O nucleus core which remains closed. That model space interactions are USDA, USDB and USDE. While the other one is the *p-sd* model space, which consists of the active shells *1p3/2*, 1*p*1/2, 1*d*5/2, 1*d*3/2, and 2*s*1/2 above the inert ^{4}He nucleus core which remains closed with PSDMK interaction.

4.13.2 Hartree–Fock Bogoliubov Method

In HFB method, a two-body Hamiltonian of a system of fermions can be expressed in terms of a set of annihilation and creation operators (c, c†) [96].

$$\widehat{H} = \sum_{ij} t_{ij} C_i^{\wedge +} C^{\wedge} + \frac{1}{4} \sum_{ijkl} U^{-}_{ijkl} C_i^{\wedge +} C_j^{\wedge +} C_l^{\wedge} C_k^{\wedge} \qquad (4.13.3)$$

With the first term corresponding to the kinetic energy,

$U^{-}_{ijkl} = \langle ij|V|k\rangle$, are anti-symmetrized two body interaction matrix-elements. The Skyrme interaction for nuclear structure calculations, which is the central potential, was developed from the idea that the energy functional could be expressed in terms of a zero-range expansion, which lead to a simple derivation of the HF equations that the exchange terms have the same mathematical structure as the direct terms. Thus, when solving the equations, this approximation greatly reduces the number of integrations over single-particle states. The Skyrme effective interaction which leads to a two-body density-dependent interaction that models the strong force in the particle-hole channel and contains central, spin-orbit and tensor contributions in coordinate space and called the standard analytical form, is given by [94]

$$\begin{aligned} V_{sky}(\overrightarrow{r_1},\overrightarrow{r_2}) &= t_\circ(1 + x_\circ p_\sigma^{\wedge})\delta(\overrightarrow{r_1} - \overrightarrow{r_2}) \\ &= \frac{1}{2} t_1 (1 + x_1 p_\sigma^{\wedge})[k^{\wedge t^2}\delta(\overrightarrow{r_1} - \overrightarrow{r_2}) + \delta(\overrightarrow{r_1} - \overrightarrow{r_2})k_2^{\wedge} \\ &= t_2(1 + x_2 p_\sigma^{\wedge})[k^{\wedge -}\delta(\overrightarrow{r_1} - \overrightarrow{r_2})k^{\wedge} + \frac{1}{6} t_3 (1 + x_3 p_\sigma^{\wedge})\delta(\overrightarrow{r_1} - \\ \overrightarrow{r_2})p^{\alpha}\left(\frac{\overrightarrow{r_1}+\overrightarrow{r_2}}{2}\right) &+ i\omega_o(\overrightarrow{\sigma_1} + \overrightarrow{\sigma_2})\hat{k}\delta(\overrightarrow{r_1} - \overrightarrow{r_2})\hat{k} \qquad (4.13.4) \end{aligned}$$

Where W_0, t_n and x_n are the free parameters describing the strengths of the different interaction terms which are fitted to nuclear structure data. The t_0 term indicates a zero-range central potential, and the t_1 and t_2 terms are non-local, because these depend on the gradient of the densities and have both central and exchange components with the range of the potential associated with$\frac{t_o}{t_1}$ [95]. The term consisting of W_0 indicates the spin-orbit part of the nucleon-nucleon interaction and an effective density dependent three-body interaction is represented by the t_3 term. K, k' are the relative momentum operators with k acting on the right, while k' is the operator acting on the left [95]. In order to estimate the HF equations, we have to estimate the expectation value of the HF Hamiltonian in a Slater determinant *HF* It is given by:

$$E = \langle \phi_{HF} \left| \widehat{H} \right| \phi_{HF} \rangle$$

$$\sum_{i=1} \langle \phi \left| \widehat{T} \right| \phi_1 \rangle + \sum_{ij} \langle \phi_{ij} | V(i,j) | \phi_{ij} \rangle \qquad (4.13.5)$$

Where T is the kinetic energy operator and *V(i,j)* is the nucleon nucleon interaction. The full expression for the expectation value of the HF equation with the Skyrme force after substituting the Skyrme interaction terms into the full energy expression is [94]:

$$E = \frac{\hbar^2}{2m}\left(\tau_n + \tau_p\right) + \frac{1}{4}\, t_o\left[p(\bar{r})^2(2 + x_o) - (2x_o + i)(p_n(\bar{r})^2 + p_p(\bar{r})^2\right] +$$
$$\frac{1}{24} t_3 \rho^{\eta} \left[(2 + x_3)p^2 - (2x_3 + \eta\left({p_p}^2 + {p_p}^2\right) + \frac{1}{8}\, [t_1(2 + x_1) +$$
$$t_2(2 + x_2)]\tau_p\right] - \frac{1}{32}[3t_1(2x_1 + 1) - t_2(2x_2 + 1)]x\left[(\nabla p_n)^2 + \left(\nabla p_p\right)^2\right] +$$
$$\frac{1}{2}\omega_o\left[\vec{j}.\overrightarrow{\nabla p} + \overrightarrow{jp}.\overrightarrow{\nabla p_p} + \overrightarrow{J_n J_n}\right] + \frac{1}{16}[t_1 x_{1+} t_2 x_2]j^2 - (t_1 - t_2)(\overrightarrow{J_p^2} + \overrightarrow{J_n^2}) \qquad (4.13.6)$$

The Hamiltonian in Eq. (4.13.3) can be expressed in terms of the generalized quasiparticle operators as [96].

$$\widehat{H} = H^o + \sum_{k_1 k_2} H^{11}_{k_1 k_2}\, \beta^+_{k_1}\beta^+_{k_2} + \sum_{k_1 k_2}\left(H^{20}_{k_1 k_2}\beta^+_{k_1}\beta^+_{k_2} + h.c.\right)$$
$$+ \sum_{k_1 k_2 k_3 k_4}\left(H^{40}_{k_1 k_2 k_3 k_4}\beta^+_{k_1}\beta^+_{k_2}\beta^+_{k_3}\beta^+_{k_4} + h.c.\right)$$
$$+ \sum_{k_1 k_2 k_3 k_4}\left(H^{31}_{k_1 k_2 k_3 k_4}\beta^+_{k_1}\beta^+_{k_2}\beta^+_{k_3}\beta^+_{k_4} + h.c.\right)$$
$$+ \frac{1}{4}\sum_{k_1 k_2 k_3 k_4}\left(H^{22}_{k_1 k_2 k_3 k_4}\beta^+_{k_1}\beta^+_{k_2}\beta^+_{k_3}\beta^+_{k_4} + h.c.\right) \qquad (4.13.7)$$

Thus, the HFB equations can be written in matrix form since it is a variational theory that treats in an unified fashion MF and pairing correlations, as:

$$\begin{bmatrix} h - \mu & \Delta \\ -\Delta^* & -h^* + \mu \end{bmatrix}\begin{bmatrix} u_k \\ u_k \end{bmatrix} = E_k \begin{bmatrix} u_k \\ u_k \end{bmatrix} \qquad (4.13.8)$$

where E_k are the quasiparticle energies, μ is the chemical potential, h and Δ are the HF Hamiltonian and the pairing potential, respectively, and the u_k and v_k are the upper and lower components of the quasiparticle wave functions.

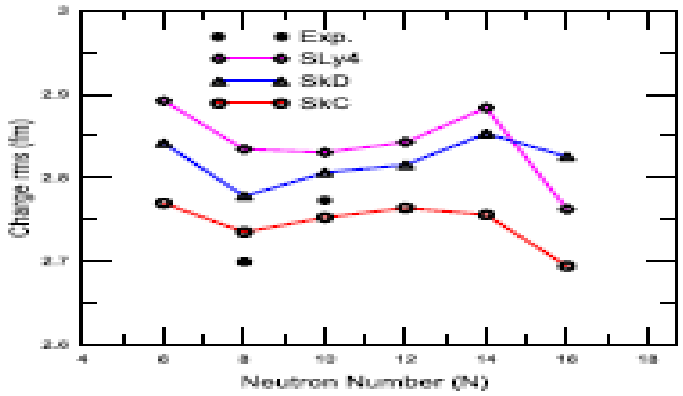

Figure(4.16) Proton, neutron, charge and mass root mean square radius for even- even $^{14\text{-}24}$O isotopes plotted as a function of neutron number (N) obtained from HFB calculations with SLy4, SkC and SkD parameterizations represented in pink, red and blue lines, respectively. The black circle is the experimental data of charge rms .

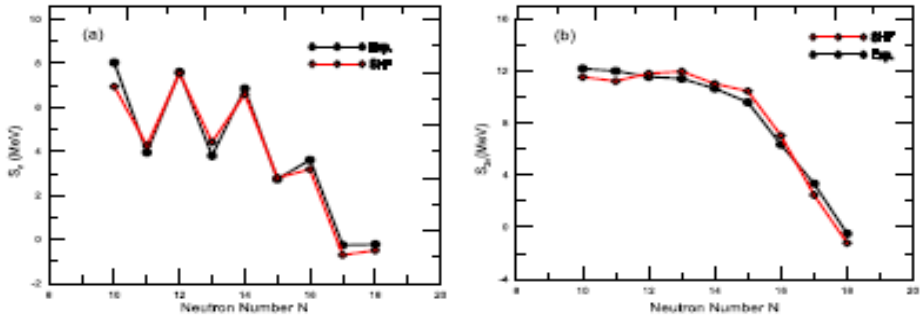

Figure (4.17): (a) single and (b) two-neutron separation energies as a function of neutron number (N) for the oxygen isotopes. Black circles are the experimental values taken from [21] and red squares obtained using SM with Skyrme interactions

Chapter Five

5. 1 Introduction

This chapter is concerned with the theoretical model based on potential dependent special relativity to explain the origin of magic number. This was achieved by using modified Klein – Gordon equation.

5.2 Energy Conservation for Potential Dependent special Relativity and string Quantum Energy with Imaginary Energy

It is well known that the suitable quantity, which simplify the equation of motion, is the lagrangian L, which is defined b

$$L = T - V = \frac{1}{2}mv^2 - V \qquad (5.2.1)$$

With T, V, m, v stands for kinetic energy, potential energy mass and velocity. The lagrangian and the equation of motion are related to the action I, which is extremum, reflecting the tendency of the system to select a path that enable it to give minimum or extract maximum energy from the surrounding via changing the generalized coordinates due to the change of trajectories at affixed space – time point. The state of physical systems can also be simplified by extracting from the action integrand quantities that are invariant under space and time transition like momentum and energy E which is given by:

$$E=T+V \qquad (5.2.2)$$

Which the Newtonian expression for energy using GSR energy mass relation (see equation) (3.5.20)

$$E = mc^2 = \frac{m_o c^2}{\sqrt{1+\frac{2\emptyset}{c^2}-\frac{v^2}{c^2}}} = m_o c^2 \left(1 + \frac{2\emptyset}{c^2} - \frac{v^2}{c^2}\right)^{-1/2} \qquad (5.2.3)$$

For a weak field and macroscopic world:

$$\frac{2\emptyset}{c^2} < 1 \quad , \frac{v^2}{c^2} < 1 \qquad (5.2.4)$$

Using the identity:

$$(1+x)^n = 1+nx \qquad (5.2.5)$$

For small x.

Setting:

$$x = \frac{2\emptyset - v^2}{c} \qquad (5.2.6)$$

In equation (3) then using (5) yields:

$$E = m_o c^2 \left(1 - \frac{\emptyset}{c^2} + \frac{1}{2}\frac{v^2}{c^2}\right) = -m_o \emptyset + \frac{1}{2} m_o v^2 + m_o c^2$$

$$E = T - V + m_o c^2 \qquad (5.2.7)$$

With kinetic energy T and potential energy V given by:

$$T = \frac{1}{2} m_o v^2 \ , \qquad V = m_o \emptyset \qquad (5.2.8)$$

But according to Newtonian and classical mechanics, that energy in equation (5.2.7) is the lagrangian:

$$L = T - V \qquad (5.2.9)$$

Hence:

$$E = L \qquad (5.2.10)$$

Where see equation (3.5.18)

$$E = \frac{m_o c^2}{\sqrt{g_{\circ\circ} - \frac{v^2}{c^2}}} = \frac{m_o c^2}{\sqrt{\frac{g_{\circ\circ} m^2 c^4 - m^2 v^2 c^2}{m^2 c^4}}} \qquad (5.2.11)$$

$$E = \frac{m_o c^2}{\sqrt{\frac{g_{\circ\circ} E^2 - P^2 c^2}{E^2}}} = \frac{m_o c^2 E}{\sqrt{g_{\circ\circ} E^2 - P^2 C^2}}$$

$$\left(\sqrt{g_{\circ\circ} E^2 - P^2 c^2}\right)^2 = m_o^2 c^4$$

$$E^{\sim 2} = g_{\circ\circ} E^2 = P^2 c^2 + m_o^2 c^4 \qquad (5.2.12)$$

$$E^2 = g_{oo}^{-1} = (P^2 c^2 + m_o^2 c^4) \qquad (5.2.13)$$

Thus, the energy conservation requires:

$$E = \text{constant} \qquad (5.2.14)$$

$$g_{oo}^{-1}(P^2 c^2 + m_o^2 c^4) = \text{constant} \qquad (5.2.15)$$

One can also look at the conservation 0f energy using space-time language. In view of equation (5.2.12) for a particle at rest in free space:

$$v = 0\,, \qquad p = 0, g_{\circ\circ} = 1, \quad \tilde{E} = \widetilde{E_o} = E_o \tag{5.2.16}$$

In this case, equation (5.2.12) reduces to:

$$\tilde{E} = \widetilde{E_o} = E = E_o = m_o c^2$$

$$\widetilde{E_o} = E_o = m_o c^2 \tag{5.2.17}$$

The energy can written using complex notation as [see equation (5.2.12)]

$$m_o^2 c^4 = \widetilde{E_o^2} = \widetilde{E^2} - P^2 c^2 = \tilde{E}^2 + (ipc)^2 \tag{5.2.18}$$

$$m_o^2 c^4 = \widetilde{E^2} + E_4^2 \tag{5.2.19}$$

Where:

$$E_4 = ipc \tag{5.2.20}$$

One can write (5.2.18) in the form:

$$\widetilde{E} = \widetilde{E_o} + i\tilde{E}_4 \tag{5.2.21}$$

Where the subscript stands for a complex quantity, thus a cording to the vector notion, one can written equation (5.2.21) in the form:

$$E^{\sim} = \widetilde{E_1}\hat{e_1} + \widetilde{E_2}\hat{e_2} + \widetilde{E_3}\hat{e_3} + \widetilde{E_4}\hat{e_4} \tag{5.2.22}$$

$$\widetilde{E_1} = E_x, \ \widetilde{E_2} = E_y, \ \widetilde{E_3} = E_z, \ \widetilde{E_4} = ipc \tag{5.2.23}$$

$$\widetilde{E^2} = m_o^2 c^4 = \widetilde{E_1} + \widetilde{E_2} + \widetilde{E_3} + \widetilde{E_4}$$

$$E_x^2 + E_y^2 + E_z^2 + i^2 p^2 c^2 = E^2 - p^2 c^2 \tag{5.2.24}$$

This means that the square of the components of the energy in the four-space time dimension is conserved, provided that:

$$\tilde{E} = (\widetilde{E_1}, \widetilde{E_2}, \widetilde{E_3}, \widetilde{E_4}) = (\widetilde{E_\iota}) = \widetilde{E}_\iota \tag{5.2.25}$$

One can re write equation (5.2.18), in a complex form [see equation (5.2.12)].

$$\tilde{E} = g_{\circ\circ} E = p^2 c^2 + m_o^2 c^4 \tag{5.2.26}$$

By suggesting:

$$E_c = \tilde{E} = g_{\circ\circ}E \qquad (5.2.27)$$

$$E_r = pc, \quad E_i = m_o c^2 \qquad (5.2.28)$$

Thus, the complex energy representation is given by:

$$E_c = E_r + iE_i \qquad (5.2.29)$$

Thus:

$$|E_c|^2 = \widetilde{E^2} = E_r^2 + E_i^2 = p^2c^2 + m_o^2c^4 \qquad (5.2.30)$$

Comparing the vector and the complex representation looks more convenient with additional time component.

$$\widetilde{E_4} = ipc$$

Compared to the convention three-dimensional one. Generalized Potential dependent Weak Field Quantum

Klein Gordon equation

The g p s r energy momentum relation in a weak field is given by equation (5.2.7).

$$E = \frac{1}{2}m_o v^2 - V + m_\circ c^2 = \frac{p^2}{2m} - V + + m_\circ c^2 \qquad (5.2.31)$$

Using the wave function:

$$\psi = Ae^{\frac{i}{\hbar}(px-Et)} \qquad (5.2.32)$$

Clearly:

$$\frac{\partial\psi}{\partial t} = \frac{-E}{i\hbar}\psi, \qquad \frac{\partial^2\psi}{\partial t^2} = -\frac{E}{\hbar}\psi$$

$$\nabla\psi = \frac{i}{\hbar}p\psi \ , \qquad \nabla^2\psi = -\frac{p^2}{\hbar^2}\psi$$

$$i\hbar\frac{\partial\psi}{\partial t} = E\psi, \qquad -\hbar^2 \ \frac{\partial^2\psi}{\partial t^2} = E^2\psi$$

$$\frac{\hbar}{i}\nabla\psi = p\psi, \qquad -\hbar^2 \ \nabla^2\psi = p^2\psi \qquad (5.2.33)$$

Multiplying both sides of (5.2.31) by ψ and using equation (5.2.33) given:

$$E\psi = \frac{p^2}{2m}\psi - V\psi + m_o c^2\psi$$

$$i\hbar\frac{\partial\psi}{\partial t} = -\frac{\hbar^2}{2m}\nabla^2\psi - V\psi + m_o c^2\psi \qquad (5.2.34)$$

This equation resembles ordinary Schrodinger equation with V replaced by $m_o c^2 - V$

$$V \to m_o c^2 - V \qquad (5.2.35)$$

The Schrodinger equation, r dependent part, for spherically symmetric potential is given by:

$$\frac{\hbar^2}{2m}\ddot{u} - V(r)u + Eu = c\frac{u}{r^2} \qquad (5.2.36)$$

To study behavior of the nucleons, one consider nucleons as oscillators. Where for harmonic oscillator, the potential taken the form:

$$V(r) = \frac{1}{2}k_o r^2 \qquad (5.2.37)$$

Rearranging equation (5.2.36) and setting for Schrodinger equation

$$k^2 = \frac{2mE}{\hbar^2}$$

$$c_2 = \frac{m}{\hbar^2}k_{o,} \qquad c_1 = \frac{2mc}{\hbar^2} = \qquad \frac{2ml(l+1)\hbar^2}{2m\hbar^2} = l(l+1) \qquad (5.2.38)$$

Or using the gsr potential lagrangian Schrodinger equation (5.2 34), and in view of equation (5.2.35).equation (5.2.36) become

$$\frac{\hbar^2}{2m}\ddot{u} + V(r)u + (E - m_o c^2)u = \frac{\mathrm{cu}}{r^2} \qquad (5.2.39)$$

Using equation (37) equation (39) becomes:

$$\ddot{u} + \frac{m}{\hbar^2}k_o r^2 + \frac{2m}{\hbar^2}(E - m_o c^2)u = \frac{2m}{\hbar^2}\frac{c}{r^2}\,u \qquad (5.2.40)$$

Taking and setting:

$$c_2 = \frac{m}{\hbar^2}k_{o,} \qquad k^2 = \frac{2mE}{\hbar^2}(E - m_o c^2), c_1 = l(l+1) \quad (5.2.41)$$

Equation (5.2.36) becomes:

$$\ddot{u} - c_2 r^2 u + k^2 u - \frac{c_1}{r^2}u = 0 \qquad (5.2.42)$$

This equation can be simplified by defining the variable y to satisfy:

$$y = \propto r$$

$$u^{"} = \frac{d^2u}{dy^2} = \frac{\ddot{u}}{\alpha^2} \qquad (5.2.43)$$

Inserting (5.2.43) in (5.2.42) given:

$$u^{"} - \frac{c_2}{\alpha^4} y^2 u + \frac{k^2}{\alpha^2} u - \frac{c_1}{y^2} u = 0 \qquad (5.2.44)$$

The simplification can be a achieved by choosing $\propto$ to satisfy:

$$\propto^4 = c_2 \ ,$$

$$\lambda = \frac{k^2}{\alpha^2} = \frac{2m}{\hbar^2 \alpha^2}(E - m_o c^2) \qquad (5.2.45)$$

Thus inserting equation (5.2.45) in equation (5.2.44) given:

$$u^{"} + (\lambda - y^2)u - \frac{c_1}{y^2} u = 0 \qquad (5.2.46)$$

This equation can be solved by taking u to be in the form:

$$u = He^{-\frac{1}{2}y^2} \qquad (5.2.47)$$

$$\bar{u} = (\bar{H} - yH)e^{-\frac{1}{2}y^2}$$

$$u^{"} = \left(H^{"} - H - yH^{-}\right)e^{-\frac{y^2}{2}} - y(H^{-} - yH)e^{\frac{y^2}{2}}$$

$$u^{"} = \left(H^{"} - 2yH^{/} + y^2H - H\right)e^{-\frac{y^2}{2}} \qquad (5.2.48)$$

Inserting equation (48) in equation (46) given:

$$H^{"} - 2yH^{/} + y^2H - H + \lambda H - y^2H - \frac{c_1}{y^2} H = 0 \qquad (5.2.49)$$

If one consider (L=0), thus according to equation (5.2.38).

$$c_1 = 0 \qquad (5.2.50)$$

Thus, equation (5.2.49) becomes:

$$H^{"} - 2yH^{/} + (\lambda - 1)H - \frac{c_1}{y^2} H = 0 \qquad (5.2.51)$$

Let:

$$H = \sum_s a_s y^s \ \ , \ H^{/} = \sum_s a_s y^{s-1}$$

$$H^{"} = \sum_s s(s-1)a_s\, y^{s-2} \qquad (5.2.52)$$

Substituting equation (5.2.52) in equation (5.2.5.51) given:

$$\sum_s s(s-1)a_s\, y^{s-1} - 2\sum sa_s\, y^s + (\lambda - 1)\sum a_s\, y^s - c_1 \sum_s a_s y^{s-2} = 0 \qquad (5.2.53)$$

Replacing s-2 by s in the first term gives:

$$\sum(s+2)(s+1)a_{s+2}y^s \sum_s[\lambda - 1 - 2s]a_s y^s = 0 \qquad (5.2.54)$$

Equation the powers of y^s on both sides:

$$[(s+1)(s+2)]a_{s+2} - [\lambda - 1 - 2s]a_s = 0 \qquad (5.2.55)$$

$$a_{s+2} = \frac{[2s+1-\lambda]}{(s+1)(s+2)}\, a_s \qquad (5.2.56)$$

Since the wave function is finite, there for H should be a finite series with finite terms. This requires to terminate H, such that the last term is (s=n). This means that

$$a_n \neq 0 \quad , \; a_n + 1 = 0 \quad , \; a_{n+2} = 0, a_{n+3} = 0 \ldots \qquad (5.2.57)$$

$taking$ (s=n) in equation (5.2.56) yields

$$0 = a_{n+2} = \frac{[2n+1-\lambda]a_n}{(n+1)(n+2)} \qquad (5.2.58)$$

This requires:

$$\lambda = 2n + 1 \qquad (5.2.59)$$

To find the energy E, one uses equations (5.2.45) and (5.2.41) to get:

$$\propto^2 = (c_2)^{\frac{1}{2}} = \left(\frac{-mk_o}{\hbar^2}\right)^{\frac{1}{2}} - = \left(\frac{-m^2\omega^2}{\hbar^2}\right)^{\frac{1}{2}} = \frac{m\omega}{\hbar}\, i \qquad (5.2.60)$$

There fore

$$\lambda = \frac{2m}{\hbar^2 \propto^2}(E - m_o c^2) = \frac{2}{\hbar\omega i} = (E - m_o c^2) \qquad (5.2.61)$$

$$\frac{2(E - m_o c^2)}{\hbar\omega i} = (2n + 1)$$

$$E - m_o c^2 = (n + \frac{1}{2})\hbar\omega i$$

$$E = m_o c^2 + (n + \frac{1}{2})\hbar\omega i \qquad (5, 2.62)$$

$$m_o c^2 = E - i(n + \frac{1}{2})\hbar\omega \qquad (5.2.63)$$

This resembles the representation of four-space time relativistic energy in equation (5.2.22) and (5.2.23) with

$$\widetilde{E_1} = E_x = E,\ \widetilde{E_4} = ipc = -i(n + \tfrac{1}{2})\hbar\omega \qquad (5.2.64)$$

$$\tilde{E} = \widetilde{E_1}\widehat{e_1} + \widetilde{E_4}\widehat{e_4} = E\widehat{e_1} - \left(n + \frac{1}{2}\hbar\omega\right) i\widehat{e_4} \qquad (5.2.65)$$

Thus, the real energy has given according to equation (5.2.24) to be

$$\widetilde{E^2} = E_1^2 + i^2(-\left(n + \frac{1}{2}\hbar\omega\right)^2 \qquad (5.2.66)$$

$$\widetilde{E^2} = \left|\widetilde{E^2}\right|^2 = E_1^2 + \left(n + \frac{1}{2}\right)^2 \hbar^2\omega^2$$

$$\widetilde{E^2} = \left|\widetilde{E^2}\right|^2 = E^2 + \left(n + \frac{1}{2}\right)^2 \hbar^2\omega^2 \qquad (5.2.67)$$

Where

$$|\widetilde{E}| = m_o c^2 \qquad (5.2.68)$$

Thus

$$m_o^2 c^4 = E^2 + \left(n + \frac{1}{2}\right)^2 \hbar^2\omega^2 \qquad (5.2.69)$$

Here $m_o c^2$ is real

Since at rest p=0, v=0, $E = mc^2 = \frac{m_o c^2}{\sqrt{1-\frac{v^2}{c^2}}} = m_o c^2$

$$\widetilde{E_4} = ipc = 0 = -i((n + \tfrac{1}{2})\hbar\omega \qquad (5.2.70)$$

Which requires

$$\omega = 0 \qquad (5.2.71)$$

Thus a direct substitution of (5.2.70) and (5.2.71) in (5.2.63) gives

$$m_o c^2 = m_o c^2 - 0 \qquad (5.2.72)$$

Thus according to equation (5.2.69):

$$E^2 = [m_o^2c^4 - \left(n + \frac{1}{2}\right)^2\ \hbar^2\omega^2 \qquad (5.2.73)$$

For small rest mass

$$m_o = 0 \qquad (5.2.74)$$

$$E = i(n + \tfrac{1}{2})\hbar\omega \qquad (5.2.75)$$

Thus according to equation (5.2.75)

And according to the representation (23) the energy results mainly from the kinetic momentum quantized part. It also shows that the momentum is the relativistic energy momentum relation:

$$E^2 = m_o^2c^4 + p^2c^2 \qquad (5.2.76)$$

Can be written in the complex form:

$$E = m_oc^2 + ipc \qquad (5.2.77)$$

Such that

$$E^2 = |E|^2 = m_o^2c^4 + p^2c^2 \qquad (5.2.78)$$

In view of equation (5.2.62)

$$E = m_oc^2 + (n + \tfrac{1}{2})\hbar\omega i \qquad (5.2.79)$$

$$E^2 = |E|^2 = m_o^2c^4 + \left(n + \frac{1}{2}\right)^2\ \hbar^2\omega^2 \qquad (5.2.80)$$

For small rest mass ($m_o = 0$), equation (5.2.77) gives

$$E = ipc \qquad (5.2.81)$$

Comparing equations (75) and (81)

$$E_4 = pc = (n + \tfrac{1}{2})\hbar\omega \qquad (5.2.82)$$

Which stands for the time energy component [see equation (5.2.64)], while E represents the spatial components (E_x, E_yE_z) as equation (5.2.64)indicates , where [see equation(5.2.69)]

$$E^2 = E_x^2 + E_y^2 + E_z^2 \qquad (5.2.83)$$

With

$$\underline{E} = E_x e_1^{\wedge}, + E_y e_2^{\wedge} + E_z e_3^{\wedge}) \qquad (5.2.84)$$

Thus according to equation (5.2.69), as far as $m_o c^2$ is a constant , the fourth dimensional energy including time coordinate is conserved according to equations (5.2.62),(5.2.63),(5.2.69) and (5.2.82).

It is also very important to note that when the rest mass part is very small equation (5.2.81) gives

$$E = (n + \tfrac{1}{2})\hbar\omega \qquad (5.2.85)$$

Which is the ordinary expression for the harmonic oscillator. Neglecting the rest mass term.

5.3 Using Potential Dependent Klein Gordon Equation to Find Magic Quantum Number

Consider a particle moving with repulsive electric field a way from afield source. This resembles the case of motion of an electron away from a negatively charged capacitor , where its field is uniform .In this case the final speed v can be written in terms of the initial speed v_0 and the acceleration a, beside displacement x in the from

$$v^2 = v_o^2 + 2ax \qquad (5.3.1)$$

However, the force per unit mass is defined

$$F = -\frac{\partial \phi}{\partial x} = a \qquad (5.3.2)$$

Thus:

$$\phi = \int d\phi = -\int a dx$$

For uniform acceleration

$$\phi = -\text{ax} \qquad (5.3.3)$$

Thus equation ( ) gives

$$v^2 = v_o^2 + 2ax = v_o^2 - 2\phi$$

$$v_o^2 = v^2 + 2\phi \qquad (5.3.4)$$

Using the ordinary SR mass formula and inserting equation (5.3.4) gives

$$E = mc^2 = \frac{m_o c^2}{\sqrt{1-\frac{v_o^2}{c^2}}} = \frac{m_o c^2}{\sqrt{1-\frac{(v^2+2\phi)}{c^2}}} \qquad (5.3.5)$$

$$E = \frac{m_o c^2}{\sqrt{\frac{m^2c^4-m^2v^2c^2-2m^2\phi c^2}{m^2c^4}}}$$

$$E = \frac{m_o c^2 E}{\sqrt{E^2-P^2C^2-2VE}}$$

$$E^2 - P^2C^2 - 2EV = m_o^2c^4$$

$$E^2 = P^2C^2 + 2EV + m_o^2c^4 \qquad (5.3.6)$$

Where the potential V is related to the potential per unit mass ϕ according to the relation.

$$V = m\phi \qquad (5.3.7)$$

$$\psi = Ae^{\frac{i}{\hbar}(px-Et)} \qquad (5.3.8)$$

$$i\hbar\frac{\partial\psi}{\partial t} = E\psi$$

$$-\hbar^2\frac{\partial^2\psi}{\partial t^2} = E^2\psi$$

$$\frac{\hbar}{i}\nabla\psi = \frac{\hbar}{i}\frac{\partial\psi}{\partial x} = p\psi$$

$$-\hbar^2\nabla^2\psi = p^2\psi \qquad (5.3.9)$$

Multiplying both sides of (5.3.6) by ψ gives:

$$E^2\psi = P^2C^2\psi + 2VE\psi + m_o^2c^4\psi \qquad (5.3.10)$$

A direct substitution of equation (5.3.9) gives

$$-\hbar^2\frac{\partial^2\psi}{\partial t^2} = -C^2\hbar^2\nabla^2\psi + 2i\hbar V\frac{\partial\psi}{\partial t} + m_o^2c^4\psi \qquad (5.3.11)$$

To simplify the equation consider the solution:

$$\psi(r,t) = \psi = e^{-i\omega t}\phi(r)$$

$$\frac{\partial\psi}{\partial t} = -i\omega_o\psi \qquad \frac{\partial^2\psi}{\partial t^2} = -\omega_o^2\psi$$

$$\nabla^2\psi = e^{-i\omega_o t}\nabla^2\phi \qquad (5.3.12)$$

Inserting equation (5.3.12) in (5.3.11) gives:

$$\hbar^2\omega_o^2\, e^{-i\omega_o t}\psi = [-C^2\hbar^2\nabla^2\phi + 2\left(\hbar\omega V\frac{\partial\psi}{\partial t} + m_o^2c^4\right)\phi]e^{-i\omega_o t}$$

(5.3.13)

Let

$$\hbar\omega_o = E \qquad (5.3.14)$$

To get:

$$-C^2\hbar^2\nabla^2\phi + 2EV\phi + m_o^2c^4\phi = E^2\phi$$

$$\nabla^2\phi + \frac{E^2\phi}{C^2\hbar^2} - \frac{2EV\phi}{C^2\hbar^2} - \frac{m_o^2c^4\phi}{C^2\hbar^2} = 0 \qquad (5.3.15)$$

For simplicity, let us consider

$$\frac{E^2 - m_o^2c^4}{C^2\hbar^2} = \frac{p^2c^2}{C^2\hbar^2} = \frac{p^2}{\hbar^2} = \frac{(\hbar K)^2}{\hbar^2} = K^2$$

$$C_o = \frac{2E}{C^2\hbar^2} \qquad (5.3.16)$$

To get

$$\nabla^2\phi - C_oV\phi + K^2\phi = 0 \qquad (5.3.17)$$

In spherical coordinate

$$\nabla^2\phi = [\frac{1}{r^2}\frac{\partial}{\partial r}\left(r^2\frac{\partial\phi}{\partial r}\right) + \frac{1}{r^2 sin\theta}\frac{\partial}{\partial\theta}\left(sin\theta\frac{\partial\phi}{\partial\theta}\right) + \frac{1}{r^2 sin\theta^{-2}}\frac{\partial^2\phi}{\partial\phi^2}] \quad (5.3.18)$$

Inserting (5.3.18) in (5.3.17) and writing $\phi(r,\theta,\phi)$

In the form

$$\phi(r,\theta,\phi) = R(r)Y(\theta,\phi) \qquad (5.3.19)$$

Yields

$$= \frac{1}{r^2}[\frac{y}{yR}\frac{\partial}{\partial r}\left(r^2\frac{\partial R}{\partial r}\right) + \frac{R}{Rysin\theta}\frac{\partial}{\partial\theta}\left(sin\theta\frac{\partial y}{\partial}\right) + \frac{R}{Rysin^2}\frac{\partial^2 y}{\partial\phi^2} - c_oV + K^2 = 0$$
(5.3.20)

$$\frac{1}{R}\frac{\partial}{\partial r}\left(r^2\frac{\partial R}{\partial r}\right) - c_o r^2 V + k^2 r^2 = -\frac{1}{ysin\theta}\frac{\partial}{\partial\theta}\left(sin\theta\frac{\partial y}{\partial\theta}\right) - \frac{1}{ysin\theta^2}\frac{\partial^2 y}{\partial\phi^2} = C_2$$

(5.3.21)

$$C_2 = \mathcal{L}(\mathcal{L}+1) \qquad (5.3.22)$$

$$\frac{1}{R}\frac{\partial}{\partial r}\left(r^2\frac{\partial R}{\partial r}\right) + k^2 r^2 - c_o r^2 V = C_2 \qquad (5.3.23)$$

For simplicity let

$$u = rR \qquad \frac{dR}{dr} = \frac{1}{r}\frac{du}{dr} - \frac{u}{r^2} \qquad (5.3.24)$$

$$\frac{\partial}{\partial r}\left(r^2\frac{\partial R}{\partial r}\right) = \frac{\partial}{\partial r}\left(r^2\left(\frac{1}{r}\frac{du}{dr} - \frac{u}{r^2}\right)\right) = \frac{\partial}{\partial r}\left(r\frac{\partial u}{\partial r} - u\right) = r\frac{\partial^2 u}{\partial r^2} + \frac{\partial u}{\partial r} - \frac{\partial u}{\partial r} = \frac{r\partial^2 u}{\partial r^r}$$

(5.3.26)

$$r\frac{\partial^2 u}{\partial r^2} + (k^2 r^2 - c_o r^2 V)\frac{u}{r} = C_2\frac{u}{r}$$

$$r\frac{\partial^2 u}{\partial r^2} + (k^2 - c_o V) ru = C_2\frac{u}{r} \qquad (5.3.26)$$

$$\frac{\partial^2 u}{\partial r^2} + \left(k^2 - c_o V - \frac{C^2}{r^2}\right)u = 0 \qquad (5.3.27)$$

$$u^{//} + \left(k^2 - c_o V - \frac{C^2}{r^2}\right)u = 0 \qquad (5.3.28)$$

For a harmonic oscillator oscillating in a radial direction:

$$V = \frac{1}{2}k_o r^2 \qquad (5.3.29)$$

Equation (5.3.28) becomes

$$u^{//} + \left(k^2 - \frac{c_o k_o}{2}r^2 - \frac{C^2}{r^2}\right)u = 0 \qquad (5.3.30)$$

Further simplification can be made by defining

$$y = \alpha r$$

$$u^{"} = \frac{d^2 u}{dr^2} = \alpha^2\frac{d^2 u}{dy^2} = \alpha^2\ddot{u} \qquad (5.3.31)$$

$$\alpha^2\ddot{u} + \left(k^2 - \frac{c_o k_o}{2\alpha^2}y^2 - \frac{C^2}{y^2}\right)u = 0$$

$$\ddot{u} + \left(\frac{k^2}{\alpha^2} - \frac{c_o k_o}{2\alpha^4} y^2 - \frac{C^2}{y^2}\right) u = 0 \qquad (5.3.32)$$

α Can be adjusted to be such that

$$\frac{c_o k_o}{2\alpha^4} = 1 \qquad (5.3.33)$$

In view of equation (5.3.16) and the definition of k_o

$$\alpha^4 = \frac{c_o k_o}{2} = \frac{E}{C^2\hbar^2} k_o = \frac{mc^2(m\omega^2)}{C^2\hbar^2}$$

$$\alpha^2 = \frac{m\omega}{\hbar} \qquad (5.3.34)$$

Defining [see equation (16) and (34)

$$\lambda = C_3 = \frac{K^2}{\alpha^2} = \frac{(E^2 - m_o^2 c^4)}{c^2\hbar^2 m\omega}\hbar \qquad (5.3.35)$$

$$u = He^{-\frac{y^2}{2}}\bar{u} = u = u^{/} = \left(H^{-}e^{-\frac{y^2}{2}} - yHe^{-\frac{y^2}{2}}\right)$$

$$u^{"} = \ddot{u} = \left(H^{"} - yH^{/} - H - yH^{/} + y^2 H\right)e^{-\frac{y^2}{2}} = \left(H^{"} - 2yH^{/} + (y^2 - 1)He^{-\frac{y^2}{2}}\right. \qquad (5.3.36)$$

A direct insertion of equation (5.3.36) and equation (5.3.3) and (5.3.35) in equation (5.3.32) yields

$$\ddot{H} - 2y\dot{H} + (y^2 - 1)H + \left(\dot{C}_3 - y^2 - \frac{c^2}{y^2}\right) H = 0$$

$$\ddot{H} - 2y\dot{H} + (\lambda - 1)\dot{H} - \frac{c^2}{y^2} H = 0 \qquad (5.3.37)$$

$$H = \sum_s a_s y^s \quad , \ \dot{H} = \sum_s s a_s y^{s-1} \ , \ \ddot{H} = \sum_s s(s-1)\ a_s y^{s-2} \qquad (5.3.38)$$

$$\sum_s s(s-1)\ a_s y^{s-2} - 2\sum_s a_s y^s + \sum_s (\lambda - 1) a_s y^s - c_2 \sum_s a_s y^{s-2} = 0 \qquad (5.3.39)$$

To make all term raised to the power s, one can replace sbysts in the first and last terms on the left hand side of equation (5.3.39), to get $[\sum_s s(-1)(s+1)a_{s+2}y^s + (\lambda - 2s - 1)a_s y^s - \sum c_2\, a_{s+2}y^s = 0$

(5.3.40)

Equating the coefficients of equal powers

$[(s+2)(s+1) - c_2]a_{s+2} + (\lambda - 2s - 1)a_s = 0$ (5.3.41)

Since the wave function ψ, u are finite. Thus the series must be finite, such that the last term is (s=n).

There fore

$a_n \neq 0\,, \quad a_{n+1} = 0 \qquad a_{n+2} = 0$ (5.3.42)

From equation (41)

$a_{s+2} = \frac{(2s+1-\lambda)a_s}{(s+1)(s+2)-c_2}$ (5.3.43)

Setting (s=n)

$0 = a_{n+2} = \frac{(2n+1-\lambda)a_n}{(n+1)(n+2)-c_2}$ (5.3.44)

Since $a_n \neq 0$, it follows that

$\lambda = 2n + 1$ (5.3.45)

In view of equation (5.3.35)

$\lambda = \frac{(E-(\frac{m_o^2 c^4}{E})}{\hbar\omega}$ (5.3.46)

Thus in view of equations (5.3.45, 5.3. 46)

$E - \frac{m_o^2\ C^4}{E} = (2n+1)\hbar\omega$ (5.3.47)

For very small rest mass or very large energy resulting from the nuclear potential is given by

$E_n = E = (2N+1)\hbar\omega$ (5.3.48)

This describes the effect of the nuclear electric field on nucleons energies.

Another additional energy is effect of the agnatic field. This can be achieved by using perturbation theory. To do this, one can find the nuclear magnetic flux nuclear magnetic moment μ , which is define in term of the current i and area A to be:

$$\mu = iA = i(\pi r^2) = \frac{-e}{2m}\,\underline{L} \qquad (5.3.49)$$

Thus

$$i = \frac{\mu}{\pi r^2} \qquad (5.3.50)$$

But the magnetic flux density B can be found due to a circulation of current i in a circular path of the radius r, in a medium having magnetic permeability μ_o . Thus, B has given by:

$$B = \frac{\mu_o \mu}{2\pi r^3} = \frac{\mu_o e}{4\pi m r^3}\,L \qquad (5.3.51)$$

The Interaction potential between nucleon spin, $\mu_{s,}$ and nuclear magnetic field is given by:

$$V_m = -\mu_s . B = -\frac{e}{m}\,S.B \qquad (5.3.52)$$

$$V_m = \frac{\mu_o e^2}{4\pi m r^3}\,S.L = \frac{\mu_o^2 e^2}{4\pi m r^3}\,L.S = V.(r)L.S \qquad (5.3.53)$$

There for the a additional magnetic moment gained by the nucleons is given by

$$E_s = \int \bar{u}_i\, V_m u_j dr = \left(\int \bar{u}_i\, V_o(r) u_j d\right) L.S = V_o ijL.S = V_s L.S \quad (5.3.54)$$

Where

$$V_o == \frac{\mu_o^2 e^2}{4\pi m r^3}\,, \qquad V_s = V_o ij \qquad (5.3.55)$$

But the total orbital angular momentum is given by

J=L+S (5.3.56)

There for

$$\underline{j}.\underline{j} = \left(\underline{L} + \underline{S}\right)\left(\underline{L} + \underline{S}\right) = \underline{L}.\underline{L} + \underline{S}.\underline{S} = 2\underline{L}.\underline{S} = L^2 + S^2 + 2L.S$$

$$\underline{L}.\underline{S} = \frac{1}{2}(j^2 - L^s - s^2) = \frac{\hbar^2}{2}(j(j+1) - l(l+1) - s(s+1)$$

$= \frac{\hbar^2}{2}[j^2 + j - l^2 - l - s^2 - s)$ (5.3.56)

There fore

J=L+s (5.3.57)

$\underline{L}.\underline{S} = \frac{\hbar^2}{2}[l^2 + 2ls + s^2 + s - l^2 - l - s^2 - s) = \frac{\hbar^2}{2}[2ls]$

$\underline{L}.\underline{S} = \hbar^2 ls$ (5.3.58)

Hence

$L.S = \frac{\hbar^2}{2}L, \qquad s = \frac{1}{2}, \qquad j = l + \frac{1}{2}$

$.S = \frac{\hbar^2}{2}L, \quad s = -\frac{1}{2}, \qquad j = l - \frac{1}{2}$ (5.3.59)

Thus from equation (5.3.48), (5.3.50) and (5.3.59), the total energy is given

$E = E_n + E_s = (2n + 1)\hbar\omega \pm \frac{\hbar^2 V_s}{2}L$ (5.3.60)

The magic number can be explained using this expression as shown by M. GOppert Mayer and by D Haxel J.Jensen and H.suess.

L=n, n-2, n-4… n-2i , i=0, 1, 2, 3 (5.3.61)

Table (5.3) explained magic number can be using this expression as shown by M. GOppert Mayer and by D Haxel J.Jensen and H.suess.

n =0	1	2	3	4	5	6
L= 0	1	0. 2	1.3	0.2.4	1.3.5	0.2.4.6

n=0 (n_x, n_y, n_z)

(0, 0, 0) proton

Neuton

$n= n_x+ n_y+ n_z$

n =1 (n_x, n_y, n_z)

(1,0,0), (0,1,0), (0,0,1)

$$3\begin{bmatrix}(1,0,0)\ \ldots\ldots\ldots\ldots\ldots\ldots\ \begin{matrix}p\\n\end{matrix}\\(0,1,0)\ \ldots\ldots\ldots\ldots\ldots\ldots\ \begin{matrix}p\\n\end{matrix}\\(0,0,1)\ \ldots\ldots\ldots\ldots\ldots\ldots\ \begin{matrix}p\\n\end{matrix}\end{bmatrix}6$$

n=2 $n=n_x+n_y+n_z$

$$6\begin{bmatrix}(1,1,0)\ \ldots\ldots\ldots\ldots\ldots\ \begin{matrix}p\\n\end{matrix}\\(1,0,1)\ \ldots\ldots\ldots\ldots\ldots\ \begin{matrix}p\\n\end{matrix}\\(0,1,1)\ \ldots\ldots\ldots\ldots\ \begin{matrix}p\\n\end{matrix}\\(2,0,0)\ \ldots\ldots\ldots\ldots\ \begin{matrix}p\\n\end{matrix}\\(0,2,0)\ \ldots\ldots\ldots\ldots\ \begin{matrix}p\\n\end{matrix}\\(0,0,2)\ \ldots\ldots\ldots\ldots\ldots\ \begin{matrix}p\\n\end{matrix}\end{bmatrix}12$$

n=3 $n=n_x+n_y+n_z$

$$10\begin{bmatrix}(1,1,1)\ \ldots\ldots\ldots\ldots\ldots\ \begin{matrix}p\\n\end{matrix}\\(2,1,0)\ \ldots\ldots\ldots\ldots\ \begin{matrix}p\\n\end{matrix}\\(2,0,1)\ \ldots\ldots\ldots\ldots\ \begin{matrix}p\\n\end{matrix}\\(2,0,1)\ \ldots\ldots\ldots\ldots\ \begin{matrix}p\\n\end{matrix}\\(1,2,0)\ \ldots\ldots\ldots\ \begin{matrix}p\\n\end{matrix}\\(0,2,1)\ \ldots\ldots\ldots\ \begin{matrix}p\\n\end{matrix}\\(1,0,2)\ \ldots\ldots\ldots\ \begin{matrix}p\\n\end{matrix}\\(3,0,0)\ \ldots\ldots\ldots\ \begin{matrix}p\\n\end{matrix}\\(0,3,0)\ \ldots\ldots\ldots\ \begin{matrix}p\\n\end{matrix}\\(0,0,3)\ \ldots\ldots\ldots\ \begin{matrix}p\\n\end{matrix}\end{bmatrix}20$$

$$j = L + S\,, \qquad L - \frac{1}{2}$$

$S = \frac{1}{2}\,, S = -\frac{1}{2}\,, \quad j = L + \frac{1}{2}\,, L - \frac{1}{2}$

Splitting

$$s(L = 0): j = \frac{1}{2} \qquad 2j + 1$$

$$p(L = 1) : j = 1 + \frac{1}{2} = \frac{3}{2} \qquad 2j + 1 = 4$$

$$j = 1 - \frac{1}{2} = \frac{1}{2} \qquad 2j + 1 = 2$$

$$d(l = 2) = j = 2 + \frac{1}{2} = \frac{5}{2} \qquad 2j + 1 = 6$$

$$j = 2 - \frac{1}{2} = \frac{3}{2} \qquad 2j + 1 = 4$$

$$F(L = 3) = j = 3 + \frac{1}{2} = \frac{7}{2} \qquad 2j + 1 = 8$$

$$j = 3 - \frac{1}{2} = \frac{5}{2} \qquad 2j + 1 = 6$$

$$g(L = 4) = j = 4 + \frac{1}{2} = \frac{9}{2} \qquad 2j + 1 = 10$$

$$j = 4 - \frac{1}{2} = \frac{7}{2} \qquad 2j + 1 = 8$$

$$h(j = 5): j = 5 + \frac{1}{2} = \frac{11}{2} \qquad 2j + 1 = 12$$

$$j = 5 - \frac{1}{2} = \frac{9}{2} \qquad 2j + 1 = 10$$

5.4 Conclusion

The conservation of energy in potential dependent special relativity has been found using 4- dimensional representation with the time part recognizing the momentum. In version, the square of momentum multiplied by the square of the free speed of light subtracted from the curved space energy is invariant and constant everywhere. The quantum equation derived from this equation in a weak field limit shows that the momentum is quantized and the energy reduced to that of Schrodinger harmonic oscillator where neglecting the rest mass term.

In addition, the proposed model shows the possibility of using potential dependent Klein-Gordon equation to find the magic number. This shows that, this equation can describe fermions as well as bosons.

5.5 Recommendation

1. The complex energy representation can be extend to include other physics quantities like the momentum.

2. The energy of potential dependent SR can be extend to include temperature and pressure.

3. The relativistic quantum model need also examined for new physical phenomena like super conductivity.

Reference

[1] Eisberg, Robert M., Quantum Physics of atoms and Molecules, Mc graw Hill, USA, 1974.

[2] Simeon, and,et al, J. Scie. of. . Inst., Vol.22, Number34, may2012.

[3] Semat , Introduction to Atomic and Nuclear Physics, Pearson Education, Inc., publishing as Addison. wesley, New yourk, 2012.

[4] Raymond A. serway, Emerity and James, physics for scientists and Engineers, Raymond A. Serway and johnw. Jewett,Jr. LondonUK,2012.

[5] Ahmed. M. S. Hamid,and, etal Inter. J. of End ScienceManagement,Hamid,6(2):April ,2016.

[6] sawan. A.Elhouri, int.J.of Research sc. and Management, Ahmed eta.3 (4): April, 2016.

[7] Lutfi.M.A.ALgadir,etal, int. J of Eng, Sci, And Research Tecn, Algadir 5(2) february,2016.

[8] DanielV. Schroeder, An Introduction to Thermal Physics, Addison Wsley longman, New York, 2000.

[9] Melissinos, Eisberg & Resnick, Experiments in Modern Physics, Raymond A.Serway and johnw. Jewett,Jr. LondonUK, 1992.

[10] Hugh D.Yyong, University Physics with Modern Physics, Pearson Education, Inc., publishing as Addison. wesley, New yourk, 2012.

[11] Melission,Esiberg and Resnic, Experiment in Modern Physics, Addison Wsley longman, New York,1992.

[12] M.Diar,etal, In. J.Of. innov.Sci.Eng and tech, vol.3 I(4), April 2016.

[13] M.Dirar etal,Int.J.of. Eng. Scie, and Management, Abdalla, 6(1), Jan. March 2016.

[14] Hashim.M. Ali,etal, Int.J. Of Scie.Eng, and App. Sci, v.2 I (5), May2016.

[15] Taylor, John R. *Classical Mechanics*. USA, Edwards Brothers, Inc.: University Science Books 2005.
[16] Kleppner and R. Kolenkow, *An Introduction to Mechanics.* United Kingdom, Cambridge: Cambridge University Press. 2014
[17] Stephen Gasiorowicz, *Quantum physics.* John Wileky and sons (US) 2003.
[18] Semat,H *Introduction to Atomic and Nuclear Physics*, Pearson Education Inc:Fletcher & Son Ltd, Norwich, New York, 1985.
[19] Haj H.Diab, M.Hashim, M.Dirar and A.KhalafAllah, String Model Solution for Linearized GSR Quantum Theory, International Journal of Multidisciplinary Research (IJMR), 2018.
[20] Abdelkareem Gesmallah Khogli, Mubarak Dirar Abdallah, Musa Ibrahim Babiker Hussain & Sawsan Ahmed Elhouri Ahmed, Energy-Momentum Relation and Eigen Equations In a Curved Space Time, International Journal of Recent Engineering Research and Development (IJRERD), Volume 04 – Issue 05, May 2019.
[21] Hasbalrsoual. G Ismail Hamza, Mubarak Dirar Abdallh-and Amal.M.Abass, Derivation of the Lorentz transformation in Generalized Special Relativity, Journal of applied Science, Vol(1),Issue(1), June2020.
[22] Mohammed Saeed Dawood Aamir, Mubarak Dirar Abdallah, Ibrahim Hassan Hassan& Sawsan Ahmed Elhouri Ahmed, Generation of Elementary Particles inside Black Holes at Planck Time, International Journal of Innovative Science, Engineering & Technology, Vol. 5 Issue 1, January 2018.
[23] Nuha Abdelrahman Khalid, Mubarak Dirar Abdallah, Zoalnoon Ahmed Abeid Allah, & Sawsan Ahmed Elhouri Ahmed, Lorenz Transformation For Free Space And Fields Using Maxwell's Equations And Newton's Laws, Global Journal Of Engineering Science and Researches, March 2018.
[24] Mubarak Dirar Abdallah, Nuha Abdelrahman Khalid, Zoalnoon Ahmed Abeid Allah and Sawsan Ahmed Elhouri Ahmed, Maxwell Equation And Lorentz Transformation Inacurved Space For Fields And Free Space On The Basis Of Maxwell's Equations, Global Journal Of Engineering Science And Researches, 2018.
[25] Abeer Mohammed Khairy Ahmed, Mashair Ahmed Mohammed Yousif, Zainab Mustapha Kurawa, Zoalnoon Ahmed Abeid Allah Saad, Suhair Salih Makawy, Mohammed Idriss Mohammed, Mubarak Dirar Abd-Alla, Sami Abdalla Elbadawi Mohamed, Determination of Photon and Elementary Particles Rest Masses Using Maxwell's Equations and

Generalized Potential Dependent Special Relativity, Natural Science, vol12, (No,8) 2020,

[26] Francis W. Sears, Mark W. Zemansky, Hugh D. Yong, University Physics, Canada, Pearson Education, 1987.

[27] John R. Taylor, Chris D. Zairats, MicaelA. Dubsn, Modern Physics for Scientist and Engineers, Colorado: prentice Hall (2004).

[28] Eugened D. Commis, *Quantum Mechanics an Experimentalist's Approach*, United States of America. Cambridge University Press 2014.

[29] David J. Griffith, Introduction to Quantum Mechanics, Untied state of America: Pearson Prentice Hall, 2005

[30] Dennis Morris, Quantum Mechanics: An introduction, New Delhi, Mercury Learning & Information, 2016

[31] Roger G Newton, Quantum Physics A Text for Graduate Students, New York: Springer 2002

[32] Serway. Jewett, Physics for Scientist and Engineer with Modern Physics, UK, London: Cengage Learning, 2018.

[33] Fatma O. M., Mubarak D. A. , Ahmed A. E., Musa I. B., Sawsan Ahmed Elhouri Ahmed, *Quantum Equation for Generalized Special Relativistic Linear Hamiltonian*, *International Journal of Recent Engineering Research and Development (IJRERD),* Vol 04 , July 2019 ,PP. 31-35.

[34] N.E.A. Ahmed, M. Dirar, A.A.Mohamed, Innovative Science, Engineering and Technology, Volume2, Isuue10, ct, (2015).

[35] Fatma O. M. , Mubarak D. A. ,Ahmed, A.E., Musa ,I. B. H., Sawsan A. E. A., *Time Independent Generalized Special Relativity Quantum Equation and Travelling Wave Solution*, International Journal of Recent Engineering Research and Development (IJRERD), Volume 04 , July 2019 , PP. 36-39.

[36] Serway. Jewett, Physics for Scientist and Engineer with Modern Physics, Raymond A. Serway and johnw. Jewett,Jr. LondonUK,2014.

[37] James. D. Bjorken, Sidney, D, Drell, Quantum Mechanics, first Edition, 1998.

[38] Jean- Louis Basdvant, James Rich, Michel Spiro, Fundamentals in Nuclear Physics, France, EFD-JET, 2005.

[39] HughD. Young ,RogerA, Freedman, A.Lewis Ford, University of Physics With Modern physics,Sanfrancisco,perarson Education,2012.

[40] B.R.Matin,Nuclear and Particle physics, New Delhi, Themson Press(Indi) 2006.

[41] James. D. Bjorken, Sidney, D, Drell, Quantum Mechanics, first Edition, 1998.

[42] Kennths. Krane, Introductory Nuclear Physics, Canada, Simultone usly, 1998.

[43] Rebert Eisberg Rebert Resnic, Quantum Physics of Atoms Molecules, Sold, Nuclei, and Particle, New Delhi, Jone Wiley and Sons,1974.

[44] Ay Balantsev and Alexander Studenikin, J. of. Phy. Seri718 (06257), may 2016.

[45] Serway. Jewelt, Physics for Scientists and Engineers with Modern Physics,

[46] Nouredin Zeltili, Quantum Mecchanics Concept and Application, New York, John Wiley and Sons, 1988.

[47]N and C.J.Joachain, Quantum Mechanics,United Kingdom,pearson Education,2000.

[48] Mubarak Dirar Abd-alla, Introduction to Quantum Mechanic, Sudan, 2003.

[49] W.Edward Gettys, Frederic J, Skove, Physics and Physic Classicaland Modern, United States of America, McGraw Hill, 1989.

[50] Matthias Burkardt, James J. Kelly, Advancein Nuclear Physic, New York,KluwerAcademic, 2002.

[51] Y.B. Band,Y.Arishai, Quantum Mechanics with Applications to Nano technology and Information Science, Indi, Raj Kamal Electric Prees,2013
[52] Adamu A.*, Ngadda Y. H. Determination of Nuclear Potential Radii and Its Parameter from Finite – Size Nuclear Model, International Journal of Theoretical and Mathematical Physics ,V0; 7(1) 2017, 10-59.

[53] J. L. Basdevant, J. Rich, and M. Spiro, Fundamentals in Nuclear physics: from nuclear structure to cosmology, (Springer Science and Business Media, Inc., New York, USA, 2005) 11.
[54] E. Tel, S. Okuducu, G. Tanir, N. N. Akti and M. H. Bolukdemir, Calculation of Radii and Density of 7–19B Isotopes using Effective Skyrme Force, Commun. Theor. Phys. Vol. 49 No. 3 (2008) pp. 696 – 702.
[55] C. Merino, I. S. Novikov, and Yu. M. Shabelski, Nuclear Radii Calculations in Various Theoretical Approaches for Nucleus-Nucleus Interactions, arXiv: 0907.1697v1 [nucl-th] 10 Jul 2009.
[56] S. K. Kenneth, Introductory Nuclear Physics, (John Wiley & Sons, New York, 1988) 12.
[57] J. J. Sakurai, Modern Quantum Mechanics, (Addison Wesley Publishing Company Inc., California, 1994) 304.
[58] A. Palffy, Nuclear effects in atomic transitions, arXiv: 1106.3218v1 [physics.atom-ph] 16 Jun 2011.
[59] L. Yung-Kuo, Problems and Solutions on Atomic, Nuclear and Particle Physics, (World Scientific Publishing Co. Pte. Ltd. Singapore, 2000) 61.
[60] I. Milstein, O. P. Sushkov, and I. S. Terekhov, Finite nuclear size effect on Lamb shift of $s1/2$, $p1/2$, and $p3/2$ atomic states, arXiv: physics/0309018v1 [physics.atom-ph] 2 Sep 2003.
[61] D. Andreas, M. Reiher, and J. Hinze, A Comparative Study of Finite Nucleus Models for low-lying States of few-electron high-Z Atoms, Chemical Physics Letters 320, 2000, 457 - 468.
[62]. A. Adamu and Y. H. Ngadda, The Effect of Finite Size Nuclear Potential on 1s2s2p Energy States of Light and Heavy Nuclei, J – NAMP. Vol. 28, No. 2, (2015) pp 351 357.
[63] A. Adamu and Y. H. Ngadda, The Nuclear Finite–Size Corrections to Energies of n = 1, n = 2 and n = 3 States of Hydrogen Atom, J – NAMP. Vol. 30, (2015) pp 133 – 137.
[64]. S. N. Ghoshal, Nuclear Physics, (S Chand and company limited, Ram Nagar, New Delhi, (2007) 406 .407, 424.
[65]. Harvinder Kaur1, M. S. Mehta, Nuclei at or Near Drip-Lines, Journal of Nuclear and Particle Physics, Vo: 4(1), 2014, 25-30.
[66]. R. Machleidt, The meson theory of nuclear forces and nuclear structure, Adv. Nucl. Phys. 19, 189 (1989).
[67]. S. K. Patra and C. R. Praharaj One neutron removal reaction using relativistic mean field densities, Phys. Rev. C 44, 2552 (1991).

[68]. M. Del Estal, M. Centelles, X. Vi\~nas and Patra S. K., Versatility of field theory motivated nuclear effective Lagrangian approach, Phys. Rev. C 63, 024314 (2001).

[69].D. G. Madland and J. R. Nix, New model of the average neutron and proton pairing gaps, Nucl. Phys. A 476, 1 (1988).

[70]. Min Long, George C. Jordan IV, Daniel R. van Rossum, Benedikt Diemer, Carlo Graziani, Richard Kessler, Bradley Meyer, Paul Rich, and Don Q. Lamb, Three-Dimensional Simulations Of Pure Deflagration Models For Thermonuclear Supernovae, the Astrophysical Journal, 789:103, July2014, (22pp).

[71] Kabiru Muhammed1, M. Y. Onimisi1, S. A. Jonah, Investigation of the Shell Effect on Neutron Induced Cross Section of Actinides, Journal of Nuclear and Particle Physics, 1(1), 2011, 10.5923.

[72] Hesham M. M. Mansour1, Khaled S. A. Hassaneen, Nuclear and Neutron Matter Properties Using BHF Approximation, Journal of Nuclear and Particle Physics, 2(2) , 2012 DOI: 10.5923.

[73] Khaled S. A. Hassaneen, H. M. Abo-Elsebaa, E. A. Sultan, and H.M.M. Mansour,Annals of Physics 326 (2011) 566.

[74] J.P. Jeukenne, A. Leijeune and C. Mahaux, Phys. Reports 25, (1976) 83.

[75] W. Ulmer1,*, E. Matsinos, A Calculation Method of Nuclear Cross-Sections of Proton Beams by the Collective Model and the Extended Nuclear-Shell Theory with Applications to Radiotherapy and Technical Problems , Journal of Nuclear and Particle Physics, 2(3), 2012, 42-56 DOI: 10.5923.

[76]. (Andreyev *et al* 2018 *Rep. Prog. Phys*. 81 016301).

[77] Schunck and Robledo 2016 *Rep. Prog. Phys*. 79 116301)

[78] (Möller and Randrup 2015 *Phys. Rev*. C 91 044316).

[79] (Schmidt *et al* 2016 *Nucl. Data Sheets* 131 107)

[80] Karl-Heinz Schmidt , and Beatriz Jurado, Review on the progress in nuclear fission—experimental methods and theoretical descriptions, Reports on Progress in Physics, Volume 81, Number 10 September 2018 •

[81] J. Phys. G: Nuclear. Part. Phys., 45: 075106 (2018)],

[82] Hong-Ming Liu , You-Tian Zou (, Xiao Pan (), Xiao-Jun Bao and Xiao-Hua Li ,' Systematic study of the α decay preformation factors of the nuclei around the $Z = 82$, $N = 126$ shell closures within the generalized liquid drop model. Chinese Physical Society and the Institute of High Energy Physics of the Chinese Academy of Sciences and the Institute of Modern Physics of the Chinese Academy of Sciences and IOP, Chinese Physics C, Volume 44, Number 9,2020.

[83] Tasleem Ahmad Siddiqui, Abdul Quddus, Shakeb Ahmad, and S K Patra , A search for neutron magicity in the isotopic series of $Z = 122$, 128 super heavy nuclei, Journal of Physics G: Nuclear and Particle Physics, Volume 47, Number 11, September 2020.

[84] Rituparna Kanungo, A new view of nuclear shells, Physica. Scripta, Vo, (2013), January 2013, 014002 (14) pp.

[85] Takaharu Otsuka, Exotic nuclei and nuclear forces, Phys. Scr. T152 (2013), January 2013, 014007 (18pp).
[86] Bansal R K and French J B 1964 *Phys. Lett.* 11 145
[87] Poves A and Zuker A 1981 *Phys. Rep.* 70 235
[88] Otsuka T *et al* 2001 *Phys. Rev. Lett.* 87 082502
[89] Otsuka T, Suzuki T, Fujimoto R, Grawe H and Akaishi Y 2005 *Phys. Rev. Lett.* 95 232502

[90] Osterfeld F 1992 *Rev. Mod. Phys.* 64 491.

[91] Redhab A Allawi and Ali A Alzubadi, Investigation of the existence of new nuclear magic number in even-even O isotopes using shell model and Hartree–Fock Bogoliubov method, Materials Science and Engineering 757 October (2020) 012016.
[92] B. A. Brown, Lecture Notes in Nuclear Structure Physics, National Superconducting Cyclotron ,Laboratory and Department of Physics and Astronomy, Michigan State University, E. Lansing, MI 48824, 2005.
[93] S. Burrello "Effective interactions and pairing correlations: from nuclei to compact stars" anno accademico (2016).
[94] E. Chabanat, P. Bonche, P. Hansel, J. Meyer, and R. Schaeffer, Nucl. Phys. A 627 (1997) 710.
[95] J. Stone and P. -G. Reinhard, Prog. Part. Nucl. Phys. 58 (2007) 587.
[96] J. Kvasil "Nuclear Structure and Nuclear Processes"(Prague: Institute of Particle and Nuclear.